NASA TECHNICAL NOTE

NASA TN D-8173

NASA TN D-8173

TECH LIBRARY KAFB, NM
0133786

EXHAUST EMISSION CALIBRATION OF TWO J-58 AFTERBURNING TURBOJET ENGINES AT SIMULATED HIGH-ALTITUDE, SUPERSONIC FLIGHT CONDITIONS

LOAN COPY: RETURN TO
AFWL TECHNICAL LIBRARY
KIRTLAND AFB, N. M.

James D. Holdeman

Lewis Research Center
Cleveland, Ohio 44135

NATIONAL AERONAUTICS AND SPACE ADMINISTRATION • WASHINGTON, D. C. • FEBRUARY 1976

TECH LIBRARY KAFB, NM

0133786

1. Report No. NASA TN D-8173	2. Government Accession No.	3. Recipient's Catalog No.
4. Title and Subtitle EXHAUST EMISSION CALIBRATION OF TWO J-58 AFTERBURNING TURBOJET ENGINES AT SIMULATED HIGH-ALTITUDE, SUPERSONIC FLIGHT CONDITIONS		5. Report Date February 1976
		6. Performing Organization Code
7. Author(s) James D. Holdeman		8. Performing Organization Report No. E-8490
9. Performing Organization Name and Address Lewis Research Center, National Aeronautics and Space Administration, Cleveland, Ohio 44135		10. Work Unit No. 505-03
		11. Contract or Grant No.
12. Sponsoring Agency Name and Address National Aeronautics and Space Administration, Washington, D.C. 20546		13. Type of Report and Period Covered Technical Note
		14. Sponsoring Agency Code

15. Supplementary Notes

16. Abstract

Emissions of total oxides of nitrogen, nitric oxide, unburned hydrocarbons, carbon monoxide, and carbon dioxide from two J-58 afterburning turbojet engines at simulated high-altitude flight conditions are reported. Test conditions included flight speeds from Mach 2 to 3 at altitudes from 16.0 to 23.5 km. For each flight condition exhaust measurements were made for four or five power levels, from maximum power without afterburning through maximum afterburning. The data show that exhaust emissions vary with flight speed, altitude, power level, and radial position across the exhaust. Oxides of nitrogen emissions decreased with increasing altitude and increased with increasing flight speed. Oxides of nitrogen emission indices with afterburning were less than half the value without afterburning. Carbon monoxide and hydrocarbon emissions increased with increasing altitude and decreased with increasing flight speed. Emissions of these species were substantially higher with afterburning than without.

17. Key Words (Suggested by Author(s)) Exhaust gases; Afterburning; J-58 engine; Turbojet engines; Simulated supersonic flight; Air pollution; Combustion products	18. Distribution Statement Unclassified - unlimited; STAR Category 07 (rev.)

19. Security Classif. (of this report)	20. Security Classif. (of this page)	21. No. of Pages	22. Price*
Unclassified	Unclassified	73	$4.25

* For sale by the National Technical Information Service, Springfield, Virginia 22161

CONTENTS

	Page
SUMMARY	1
INTRODUCTION	2
APPARATUS	3
Engine	3
Facility	3
Gas Sample Probe and Transport System	3
Gas Analysis Instrumentation	4
Test Conditions and Procedure	5
RESULTS AND DISCUSSION	7
Profile Data	7
Integrated Average Emissions	9
Oxides of nitrogen emissions	9
Correlation for oxides of nitrogen emissions	11
Ratio of nitric oxide to total oxides of nitrogen	12
Carbon monoxide emissions	12
Unburned hydrocarbon emissions	14
SUMMARY OF RESULTS	15
REFERENCES	17
APPENDIXES	
A - CONCENTRATION PROFILES	34
B - EXPERIMENTAL DATA	45

EXHAUST EMISSION CALIBRATION OF TWO J-58 AFTERBURNING TURBOJET ENGINES AT SIMULATED HIGH-ALTITUDE, SUPERSONIC FLIGHT CONDITIONS

by James D. Holdeman

Lewis Research Center

SUMMARY

Emissions of total oxides of nitrogen (NO_x), nitric oxide (NO), unburned hydrocarbons (HC), carbon monoxide (CO), and carbon dioxide (CO_2) from two J-58 afterburning turbojet engines at simulated high-altitude flight conditions are reported. Test conditions included flight speeds from Mach 2 to 3 at altitudes from 16.0 to 23.5 kilometers. For each flight condition emission measurements were made for four or five engine power levels from maximum power without afterburning (military power) through maximum afterburning. These measurements were made using a single-point gas sample probe traversed across the horizontal diameter of the exhaust. The local emissions data were mass weighted and area integrated to obtain average emissions.

The data show that emissions vary with flight speed, altitude, power level, and radial position across the exhaust. Oxides of nitrogen emissions decreased with increasing altitude at constant flight speed and increased with increasing flight speed at constant altitude. The NO_x emission indices for military power were correlated in terms or primary combustor conditions. The NO_x emission indices, both with and without afterburning, have been correlated with flight speed, altitude, and power level. Carbon monoxide and unburned hydrocarbon emissions increased with increasing altitude at constant flight speed and decreased with increasing flight speed at constant altitude. Both carbon monoxide and hydrocarbon emissions were substantially higher with afterburning than without afterburning. The exhaust concentrations of the oxides of nitrogen were similar for the two J-58 engines at the same test conditions. The exhaust concentrations of carbon monoxide and hydrocarbons at afterburning power levels were quite different for the two engines at the same test conditions.

INTRODUCTION

Testing of two J-58 afterburning turbojet engines was conducted in an altitude facility to determine their oxides of nitrogen, unburned hydrocarbons, carbon monoxide, and carbon dioxide emissions at simulated supersonic, high-altitude flight conditions.

Emission measurements from aircraft turbine engines, and in particular afterburning engines, at high-altitude supersonic flight conditions are needed to answer questions about the environmental impact of the supersonic transport. Previous studies dealing with aircraft jet-engine emissions at altitude conditions are reported in references 1 to 6. In these, various engines and flight conditions have been examined. The J-93 tests (ref. 5), conducted at the Arnold Engineering and Development Center as part of the Climatic Impact Assessment Program, are the most closely related to the present investigation in terms of the size of the engine tested and flight conditions examined.

The purpose of the present investigation is to provide an emissions calibration for the J-58 engines for subsequent use in the NASA Stratosphere Jet Wake Experiment (discussed in ref. 7). In this program, sampling of exhaust constituents will be made in the wake of a YF-12 aircraft, powered by two J-58 engines, during supersonic, stratospheric flight. The emissions calibration tests will provide the initial conditions for assessing the dispersion and dilution of exhaust products in the stratosphere and for evaluating jet-wake dispersion models such as that given in reference 8. In addition, these tests will add to the general knowledge about emissions from afterburning turbojet engines at high-altitude conditions. Although emission levels for the J-58 engine may not necessarily be representative of emissions from engines designed for present or future commercial supersonic aircraft, the trends should be similar.

The present investigation was conducted in the propulsion systems laboratory at the Lewis Research Center. Some of the data from the first engine tested (herein designated as engine A) for Mach 2.0, 2.4, and 2.8 at 19.8 kilometers have been reported previously (refs. 9 and 10). Test conditions for the second engine (engine B) were Mach 2.0 at 16.0, 17.9, and 19.8 kilometers; Mach 2.4 at 19.8 kilometers; Mach 2.8 at 19.8, 22.0, and 23.5 kilometers; and Mach 3.0 at 19.8 kilometers. At each flight condition data traverses across the horizontal diameter of the exhaust were made for four or five engine power levels from maximum power without after-

burning (military power) through maximum afterburning. Results from tests on both engines are reported here. The engine A results are included both for completeness and for comparision with engine B results.

APPARATUS

Engine

The J-58 engine is an afterburning turbojet designed for operation at flight speeds in excess of Mach 2 at stratospheric altitudes. The two J-58 engines tested in this program will be installed in the NASA YF-12 aircraft for the flight tests in the NASA Stratospheric Jet Wake Experiment.

Facility

The engines were tested in the propulsion systems laboratory at the Lewis Research Center. This altitude chamber facility and associated air handling equipment provided conditioned inlet airflow and appropriate exhaust pressure to accurately simulate the conditions at the engine inlet and exhaust corresponding to the selected supersonic flight conditions. All tests were run using JP-7 fuel, which was heated to 395 K before it entered the engine to simulate the condition on the aircraft during supersonic flight. The atomic hydrogen-carbon ratio of this fuel is 2.0. Specifications for JP-7 are similar to JP-5, except that JP-7 is lower in aromatics and has greater thermal stability.

Gas Sample Probe and Transport System

A single-point, traversing, water-cooled gas sample probe was used to obtain emission measurements. The probe and its traversing mechanism are shown mounted behind the engine in figure 1(a). The traversing mechanism was capable of translating the probe ± 60 centimeters horizontally and ± 20 centimeters vertically from the engine centerline. A photograph and a schematic of the sensor area of the probe are shown in figures 1(b) and (c). A total-pressure sensor was mounted 2.5 centimeters above the sample probe, and three unshielded iridium/iridium-rhodium thermocouples were mounted 2.5 and 5 centimeters below and 5 centimeters

above the gas sample probe. The gas sample sensor had an inside diameter of 0.717 centimeters. The probe tip extended 1.9 centimeters forward of the rake body. This section was water-cooled for a distance of 8 centimeters downstream from the tip, both for sample conditioning and probe integrity. Following this section, the sample line increased to 0.818 centimeter inside diameter. For afterburning conditions a second water-cooled heat exchanger on the next 30 centimeters of line was used to provide additional quenching of the sample.

A line drawing of the gas analysis system is shown in figure 2(a). Approximately 10 meters of 0.95-centimeter stainless-steel line was used to transport the sample to the analyzers. To prevent condensation of water and to minimize adsorbtion-desorbtion effects of hydrocarbon compounds, the line was heated with steam at 428 K. Four heated metal bellows pumps (two pumps in series in each of two parallel legs) were used to supply sufficient gas sample pressure (17 N/cm^2) to operate the analytical instruments. The gas sample line residence time was less than 2 seconds for all test conditions.

Gas Analysis Instrumentation

The exhaust-gas analysis system (fig. 2(b)) consists of four commercially available instruments, along with associated peripheral equipment necessary for sample conditioning and instrument calibration. In addition to the visual readout at the console, electrical inputs are provided to the facility computer for on-line analysis and data evaluation.

The hydrocarbon (HC) content of the exhaust gas was measured on a wet basis, using a Beckman Instruments Model 402 Hydrocarbon Analyzer. The instrument is of the flame ionization detector type. Both carbon monoxide (CO) and carbon dioxide (CO_2) were measured dry, using analyzers of the nondispersive infrared (NDIR) type. These instruments were Beckman Instruments Model 315B. The concentration of the oxides of nitrogen (NO_x) was measured on a dry basis using a Thermo Electron Corporation Model 10A Chemiluminescence Analyzer. This instrument includes a thermal converter to reduce nitrogen dioxide (NO_2) to nitric oxide (NO). Data for engine A were obtained as total NO_x ($NO + NO_2$). For the engine B tests a second (nominally identical) NO_x analyzer was used to obtain NO data. Since both NO_x analyzers could be operated with or without their converters, frequent checks were made to insure that they were reading the same when in the same mode.

Test Conditions and Procedure

The flight conditions simulated in the tests conducted on the J-58 engines are given in table I. These conditions, in addition to being representative of cruise operation of supersonic transport aircraft, were selected to provide parametric variation of flight conditions and combustor and afterburner inlet conditions. Flight speed variation at an altitude of 19.8 kilometers is given by test conditions 3, 4, 5, and 8. This altitude would be a typical cruise altitude for advanced or second-generation SST aircraft and is the nominal altitude selected for the YF-12 flight experiments. For these conditions combustor-inlet temperature and pressure and afterburner-inlet pressure increase with increasing flight speed.

Conditions 1, 2, and 3 give a variation of altitude at a constant flight speed of Mach 2.0. For these conditions the combustor-inlet temperature is constant. Combustor-inlet pressure and afterburner-inlet pressure decrease with increasing altitude. Conditions 5, 6, and 7 also give an altitude variation at constant flight speed, in these cases for Mach 2.8.

The third parametric variation is given by conditions 2, 4, and 6. The altitudes for conditions 2 and 6 were chosen so that the combustor-inlet pressure and afterburner pressure for these conditions would be equal to the corresponding pressures for condition 4. Thus, the parameter varied in conditions 2, 4, and 6 is the combustor-inlet temperature, which increases from condition 2 to 6.

For each condition the engine inlet air was conditioned to correspond in both temperature and pressure to the values at the engine face during flight. Also, for each condition tests were made at four or five engine power levels, including military power (maximum power without afterburning), minimum afterburning, maximum afterburning, and either one or two intermediate afterburning power levels. The altitude chamber pressure for each flight condition was selected to insure that the flow was sonic at the engine primary exhaust nozzle. Note that the altitude chamber pressure does not need to be equal to the ambient static pressure for the simulated altitude because the internal performance of the engine is correctly simulated for all external static pressures low enough to choke the nozzle. When installed on the aircraft the engine exhaust passes through a secondary ejector nozzle and leaves the tailpipe at supersonic velocity.

Engine B was tested at all eight flight conditions (table I) for five power levels

at each condition. Exhaust constituents measured were CO_2, CO, HC, NO, and NO_x. Engine A was tested at conditions 3, 4, and 5 for four of the power levels at each condition. Constituents measured for these tests were CO_2, CO, HC, and NO_x.

Emission traverses were made at the plane of the primary nozzle (actually, the probe was 6.7 cm from the exit plane when the engine was cold with the nozzle wide open). Data were obtained at 5-centimeter (nominal) intervals across the horizontal exhaust diameter, resulting in approximately 20 data points per traverse. These small increments were necessary to document the steep gradients in emissions and temperature found in afterburning operation. The interval was increased to approximately 7.5 centimeter for military power tests, since emissions and temperature gradients at this condition were much less than for afterburning conditions. The time required for each traverse varied from 30 to 45 minutes. Complete surveys (five power levels at each flight condition) required four to five hours of continuous engine operation.

At the Mach 2.0 condition for engine A, limited data were obtained up to 20 centimeters above and below the engine centerline on the vertical diameter. These data showed variations similar to those on the horizontal diameter.

All gas analysis instruments were checked for zero and span before each traverse. Because the console allows rapid selection of zero, span, or sample modes, these frequent checks could be made during power level changes while the engine was running.

The concentrations which were measured on a dry basis (NO_x, NO, CO, and CO_2) are reported on a wet basis, correcting for water vapor, including both inlet-air humidity and water vapor from combustion. The relations used are given in reference 11. The NO and NO_x data have been corrected to zero ambient humidity by multiplying the measured (wet basis) data by exp (19H), where H is the humidity of the engine inlet air expressed in grams water per gram of dry air, (ref. 12).

The local concentration data were mass weighted and area integrated to obtain average concentrations. In this procedure the exhaust was assumed to be sonic at the average total pressure, and the static pressure was calculated. The static pressure was assumed to be constant across the exhaust. The exhaust nozzle radius (R8) was calculated from the measured engine airflow and the average exhaust temperature and pressure. Average concentrations were obtained from the local measurements of total temperature, total pressure, and species concentration using a

trapezoidal integration.

For each power level at each test condition, the measured values of CO, CO_2, and HC were used to compute an emissions based fuel-air ratio (FAR8) using the relations given in reference 11. These values are compared with the metered fuel-air ratio (FAHI) in figure 3. Although all data points fall within the ±15 percent tolerance allowed in reference 11, the emission-based fuel-air ratios were consistently slightly higher than the metered fuel-air ratios for the engine B tests, and they were consistently slightly lower than the metered fuel-air ratios for the engine A tests. In figures showing the variation of average emissions with power level, the metered fuel-air ratios have been used for the engine B tests, and the emission based fuel-air ratios have been used for the engine A tests.

Emission indices (g pollutant/kg fuel) were calculated from the average concentration of each constituent and the average concentrations of CO, CO_2, and HC using relations given in reference 11. These emission indices are designated EI FAR8. Emission indices were also calculated from the average concentration of each constituent and the metered fuel-air ratio. These emission indices are designated EI FAHI. For each constituent the ratio EI FAR8/EI FAHI is approximately proportional to FAHI/FAR8.

RESULTS AND DISCUSSION

Profile Data

A typical set of profile data are shown in figure 4. These engine A data are for test condition 4 (Mach 2.4, 19.8 km). The CO and NO_x concentrations are given as parts per million by volume (ppmv), and the HC concentrations are given as parts per million carbon by volume (ppmC). The horizontal axes in the figures are the radial distance from the engine centerline nondimensionalized by the calculated nozzle exit radius (R8) for each test. This radius varies with flight condition and engine power level.

The total-temperature distribution across the nozzle diameter at each power level for condition 4, engine A, is shown in figure 4(a). At military power (nonafterburning) the temperature is quite uniform across the exhaust plane, but for afterburning power significant temperature gradients exist across the diameter. The data shown have been corrected for radiation errors by the method given in refer-

ence 13, using radiation constants appropriate to the type of wire and the probe geometry used in this investigation.

The local fuel-air ratios calculated from the gas sample measurements for condition 4, engine A, are shown in figure 3(b). The similarity of the fuel-air ratio and temperature profiles and the increase in the average temperature with increasing power level is expected, since increasing the fuel-air ratio increases the temperature for all fuel-air ratios less than stoichiometric. The corresponding oxides of nitrogen concentration profiles are shown in figure 4(c). Although the NO_x concentration profiles and the temperature and fuel-air ratio profiles show a similar shape, the NO_x concentration increases only slightly with increasing power in afterburning. For all afterburning conditions the NO_x concentrations at midradius (downstream of and in line with the afterburner flame holders) were greater than at the same radius at military power. However, the NO_x concentrations on the engine centerline were less in afterburning than at military power.

The carbon monoxide and unburned hydrocarbon concentration profiles are shown in figures 4(d), and (e). For this flight condition and this engine, concentrations of CO and HC for minimum and intermediate afterburning conditions are substantially higher in the center of the exhaust than at the intermediate to maximum radial locations. At maximum afterburning hydrocarbon concentrations in the center have decreased substantially, although a center peak is still evident. Carbon monoxide also still shows a center peak; however, the striking feature of the CO data at maximum afterburning is the appearance of twin regions of high concentration downstream of the afterburner flame holders. Examination of the fuel-air ratio profiles in figure 4(b) shows that the local fuel-air ratio is near stoichiometric at these locations, thus the high CO levels represent an approach to equilibrium CO rather than combustion inefficiency. The CO and HC emissions at military power are low ($CO < 32$ ppmv, $HC < 11$ ppmC) and uniform across the exhaust. To avoid congestion on the figures, these are not shown.

Although the profile data shown in figure 4 are typical, significant differences in distribution do occur for different engines, flight speeds, and altitudes. For this reason, emission profiles for all conditions tested are included in appendix A.

With respect to the NO_x concentration profiles, most conditions exhibit the character shown in figure 4(c); that is, the NO_x concentration downstream of, and in line with the flame holders for afterburning conditions was greater than at the same

radius for military power, but near the engine centerline the NO_x concentration in afterburning was less than at military power. Exceptions to this pattern occurred for afterburning conditions whenever the hydrocarbon concentration and the carbon monoxide concentration in the center region were very low. For these conditions the NO_x concentration was greater than at the corresponding military power condition at all radii.

In general, the high carbon monoxide and hydrocarbon concentrations in the center region decreased both in peak concentration and radial extent with increasing power level, decreasing altitude, or increasing flight speed. The twin peaks in the CO distribution at maximum afterburning were stronger or weaker than shown in figure 4(d), depending on the relation of the local fuel-air ratio to stoichiometric conditions.

A complete tabulation of the experimental data obtained in this investigation is included in appendix B.

Integrated Average Emissions

The effect of each of the three types of parametric variations on the average emissions is discussed in the following paragraphs. The average emissions data are shown in figures 5 to 8 and 12 to 19 both as emission indices in parts (a) of the figures and as average concentrations in parts (b). Although either parameter can be readily calculated from the other for a known fuel-air ratio, the data are shown both ways in recognition of the fact that the emission indices are more relevant to the combustion researcher and that the average concentrations are more directly applicable to the flight experiment and to chemical kinetics and fluid dynamic modeling of the jet-wake flow field. The engine fuel-air ratio is the axis of abscissas on these figures. Fuel-air ratios less than 0.02 are at military power (no afterburning); fuel-air ratios greater than 0.02 are for afterburning conditions.

Oxides of nitrogen emissions. - The variation of the oxides of nitrogen emissions with altitude and fuel-air ratio at Mach 2.0 is shown in figure 5. In the concentration curves (fig. 5(b)) it is evident that the NO_x concentration at minimum afterburning is very nearly equal to the concentration at military power for each altitude. With increasing power level in afterburning, the average NO_x concentration increases slightly. Since the fuel-air ratio at minimum afterburning is slightly more

than double the value at military power, the emission index at minimum afterburning is less than half the value at military power for each altitude. The NO_x emission index appears to decrease slightly in going from minimum to maximum afterburning. (The solid curves shown here and in figs. 6 to 8 result from the NO_x correlation discussed in the next section.) A comparison of the three altitude conditions shows that the NO_x emissions decrease with increasing altitude. This is expected because the formation of the oxides of nitrogen during combustion is pressure dependent and the combustor and afterburner pressures decrease with increasing altitude. For all of these conditions the combustor-inlet and afterburner-inlet temperatures are constant because engine inlet temperature and rotational speed are constant.

The variation of the oxides of nitrogen emissions with altitude and power level at Mach 2.8 are shown in figure 6. The effect of fuel-air ratio and altitude are similar to the effects shown in figure 5, except that the concentrations and emission indices are higher because the combustor-inlet temperature is higher.

The variation of the NO_x emissions with flight speed and power level at an altitude of 19.8 kilometers is shown in figure 7. For each flight condition the average NO_x concentrations at minimum afterburning and military power are nearly equal, but the emission index at minimum afterburning is less than half the value at military power. The increase in NO_x concentration from minimum to maximum afterburning is less rapid than the increase in fuel-air ratio, causing the emission index to decrease slightly in this region.

Since the oxides of nitrogen emissions are mainly dependent on the primary combustor conditions and since increasing flight speed at constant altitude causes both combustor temperature and pressure to rise, the NO_x emissions increase substantially with increasing flight speed. Oxides of nitrogen emissions for both engines A and B are shown in figure 6. The average NO_x emissions are nearly equal for the two engines at the same flight conditions. Because the NO_x data in reference 10 (engine A) were not corrected to zero ambient humidity, values in that reference are from 5 to 15 percent lower than the values shown here.

The effect of variation of primary combustor-inlet temperature on NO_x emissions is shown in figure 8. The increase in NO_x emissions from Mach 2.0 to 2.8 shown here is less than in figure 7 because, for the conditions shown in figure 8, the combustor-inlet and afterburner pressures are constant.

For the range of flight conditions tested, the average concentration of the oxides of nitrogen at military power (no afterburning), varied from 80 to 170 ppmv, corres-

ponding to emission indices from 8 to 21. The average concentrations of NO_x at minimum afterburning were approximately equal to the concentrations at military power, but increased by about 50 percent from minimum to maximum afterburning. Since the fuel-air ratio in afterburning was from 2 to 4 times that at military power, the NO_x emission indices for afterburning conditions were less than half the emission indices without afterburning.

Correlation for oxides of nitrogen emissions. - The effects of combustor parameters on the formation of the oxides of nitrogen from a nonafterburning turbofan engine were correlated in reference 6 using the form

$$NO_xEI \sim \frac{e^{2\theta}\,\delta^{0.5}\,(f/a)^{1.5}}{M_3} \tag{1}$$

where

θ combustor-inlet total temperature normalized by standard sea level temperature

δ combustor-inlet total pressure normalized by standard sea level pressure

f/a combustor fuel-air ratio (which is a measure of exit temperature)

M_3 combustor-inlet Mach number

The results from the J-58 tests at military power can also be sucessfully correlated with this form as shown in figure 9. This correlation shows that the effects of combustor-inlet temperature, combustor-inlet pressure, fuel-air ratio, and combustor-inlet Mach number found in reference 6 for a small turbofan engine with a reverse flow combustor, are also appropriate to the J-58, which is a large, axial-flow turbojet engine.

For any given engine type the combustor conditions may be directly related to flight speed, altitude, and power level. The J-58 NO_x data were correlated with these flight parameters using the form

$$NO_xEI = 2.53\, e^{M}\left(\frac{p_{amb}}{p_{std}}\right)^{0.3}\,[1 - 0.57\,(AB)] \tag{2}$$

where

M flight Mach number

p_{amb} static pressure at flight altitude

p_{std} standard sea level static pressure

AB = 0 for nonafterburning conditions, = 1 for afterburning conditions

This correlation is shown in figure 10. The calculated emission indices agree with the data within ± 15 percent. The solid lines shown in parts (a) of figures 5 to 8 are the NO_x emission indices calculated with this correlation. The emission index data decrease slightly with increasing afterburning, but because of the form chosen for equation (2), the correlation emission indices are independent of afterburning power level. No doubt the agreement could be improved with a more complicated power level form in equation (2), but the introduction of the fuel-air ratio as a correlating parameter does not seem justified in view of the satisfactory agreement obtained with the step function. The average concentrations calculated from the emission indices obtained with equation (2) are shown in parts (b) of figures 5 to 8. These are in good agreement with the data. It should be noted that the correlation in equation (2) is appropriate for J-58 engines only. Comparison of data from other types of engines must be performed using a correlation form such as given by equation (1). Of course, the afterburning step function in equation (2) could also be applied to the correlation form in equation (1) to extend this form to afterburning conditions.

Ratio of nitric oxide to total oxides of nitrogen. - For the tests on engine B, two (nominally) identical NO_x analyzers were used to obtain data for NO and NO_x ($NO + NO_2$). Because both instruments could be operated with or without their thermal converters (to reduce NO_2 to NO), these instruments were frequently cross checked to ensure that they were reading the same when in the same operating mode. The nitric oxide fraction of the total oxides of nitrogen is shown in figure 11. At military power the $NO-NO_x$ ratio was everywhere greater than 0.95. At low afterburning power, the ratio was between 0.8 and 0.95, but the ratio of NO to NO_x appeared to increase slightly with increasing power level in afterburning. These data are in agreement with the results of references 3, 5, and 6.

Carbon monoxide emissions. - The variation of carbon monoxide emissions with altitude and power level for Mach 2.0 is shown in figure 12. For these conditions

the combustor-inlet temperature and the afterburner-inlet temperature are constant. The increase in CO emissions with altitude are due to decreasing combustion efficiency as both the primary combustor and afterburner pressures decrease with increasing altitude. In figure 12(b), the marked increase in CO concentration in going from military power to afterburning is evident. Since the increase in CO concentration is proportionately larger than the increase in fuel-air ratio, the emission indices also increase substantially.

The variation of carbon monoxide emissions with altitude and power level at Mach 2.8 is shown in figure 13. The trends here are similar to those in figure 12 for Mach 2.0. The CO emissions increase less rapidly as maximum afterburning is approached at Mach 2.8 (fig. 13) than at Mach 2.0 (fig. 12) because the overall fuel-air ratio at maximum afterburning for Mach 2.8 is less than for Mach 2.0.

In figure 14, CO emissions for conditions with constant combustion pressure are given. The concentrations and emission indices at military power decrease for increasing flight speed, since the increasing combustor-inlet temperature increases combustion efficiency. At any given afterburning power level, the CO emissions for all the conditions differ only slightly because afterburner-inlet temperature and pressure are nearly constant for these conditions.

The variation of carbon monoxide emissions with flight speed and power level at 19.8 kilometers is shown in figure 15. The results for both engines A and B are shown, and it is evident that for afterburning power levels the CO emissions from engine A are consistantly higher than for engine B. Because the values of the exhaust nozzle radius at afterburning conditions for engine A, calculated using the present data reduction method, are up to 10 percent larger than the values used in reference 10, the average CO concentrations and emission indices for engine A (fig. 15) are up to 20 percent smaller than the values given in reference 10. For both engines, the decrease in CO emissions with increasing flight speed (fig. 15) is considerable. This increase in combustion efficiency occurs because afterburner pressure increases as flight speed increases. For intermediate afterburning at Mach 3.0 (engine B), the combustion efficiency is greater than 99.9 percent (a CO EI of 4.27 = 0.1 percent inefficiency).

For the range of flight conditions tested, the carbon monoxide emissions at military power were quite low, from 10 to 60 ppmv, which corresponds approximately to emission indices from 1 to 4. Carbon monoxide emission indices in afterburning modes were approximately an order of magnitude greater than at military power.

The CO emissions typically decreased slightly from minimum to intermediate afterburning, but increased nearly an order of magnitude from intermediate to maximum afterburning.

Unburned hydrocarbon emissions. - The variation of hydrocarbon emissions with altitude and power level at Mach 2.0 is shown in figure 16. At military power the HC concentrations in the exhaust are negligibly small (< 6 ppmC). The concentrations at minimum afterburning are more than two orders of magnitude greater than at military power. This is a consequence of the region of high unburned hydrocarbons which appears in the center region of the exhaust. (See fig. 4(e).) The peak concentration and radial extent of this region decrease with increasing power, and the average HC concentrations and emission indices decrease accordingly. The variation of hydrocarbon emissions with altitude is as expected, with emissions increasing with increasing altitude as afterburner pressure is decreasing.

The variation of hydrocarbon emissions with altitude and power level at Mach 2.8 is shown in figure 17. At each flight condition the hydrocarbon emissions increase substantially from military power to minimum afterburning, then decrease with increasing power in afterburning. The HC concentrations at maximum afterburning are nearly equal to the nonafterburning concentrations. Since the fuel-air ratio at maximum afterburning is about four times that at military power, the HC emission indices at maximum afterburning are about a quarter of the value at military power.

The variation of the hydrocarbon emissions with altitude for afterburning conditions at Mach 2.8 contains a bit of a surprise. Since the afterburner pressure decreases monotonically from condition 5 to condition 7, the hydrocarbon emissions would be expected to increase monotonically with increasing altitude, as was true at Mach 2.0 (fig. 16). However, at Mach 2.8, the highest hydrocarbon emissions occurred at the intermediate altitude condition. A check of the carbon monoxide and hydrocarbon profiles for these conditions (figs. A5 to A7) shows that both CO and HC profiles have higher concentrations in the center region for condition 6, than for conditions 5 and 7. Since the average hydrocarbon emissions in afterburning are almost exclusively determined by the concentrations in the center (hydrocarbon concentrations at intermediate to maximum radii are negligible), the effect on the average emissions is very pronounced.

The variation of the average hydrocarbon emissions at constant combustor and afterburner pressures is shown in figure 18. Unlike the CO emissions, which

were nearly equal for these three conditions, the afterburning HC emissions decrease with increasing flight speeds, with the most marked decrease evident between Mach 2.0 and 2.4 at intermediate afterburning power.

The variation of hydrocarbon emissions with flight speed and power level at 19.8 kilometers is shown in figure 19. Results for both engines A and B are shown, and it is evident that, at the same flight speeds and for nearly all afterburning power levels, the hydrocarbon emissions for engine A are substantially higher than for engine B. As with the CO emissions the integrated average HC emissions in afterburning are very sensitive to the radius of the integration. The average HC emissions in afterburning for engine A shown in figure 19 are up to 30 percent lower than the corresponding values given in reference 10, primarily because of differences in the values used for the exhaust nozzle radius.

For the range of flight conditions tested, the hydrocarbon emissions at military power were almost negligible ($<$ 8 ppmC, which corresponds to emission indices of less than 0.3). At minimum afterburning power levels, the average hydrocarbon emissions were appreciably greater than at military power, but varied over two orders of magnitude as a function of flight speed and altitude. The range of average concentrations was from 10 to 2000 ppmC, which corresponds approximately to emission indices from 0.2 to 20. At all flight conditions the hydrocarbon emissions decreased with increasing power from minimum to maximum afterburning. For almost all conditions the concentrations at maximum afterburning were of the same order of magnitude as the concentrations without afterburning.

SUMMARY OF RESULTS

Gaseous emissions from two J-58 afterburning turbojet engines were measured at simulated high-altitude supersonic-flight conditions. For each flight condition, detailed concentration profile measurements were made for four or five engine power levels from military (nonafterburning) through maximum afterburning. These measurements were made on the horizontal diameter at the engine primary exhaust nozzle, using a single-point traversing gas sample probe. The data show that emissions vary with flight speed, altitude, power level, and radial position. The principal results of this investigation are as follows:

1. With afterburning there are significant gradients in exhaust temperature, local fuel-air ratio, and species concentration across the exhaust plane. Traverse increments on the order of one tenth of the exhaust radius were required to document these gradients.

2. Emissions of the oxides of nitrogen (NO_x) decreased with increasing altitude at constant flight speed and increased with increasing flight speed at constant altitude.

3. The average exhaust concentrations of NO_x at minimum afterburning and military power were nearly equal. The NO_x concentrations increased by about 50 percent from minimum to maximum afterburning.

4. The oxides of nitrogen emission indices at military power varied from 8 to 21 over the range of altitudes and flight speeds tested. For each flight condition the NO_x emission indices in afterburning were approximately 43 percent of the value at military power.

5. The NO_x emission indices at military power were correlated in terms of the primary combustor-inlet parameters (temperature, pressure, and fuel-air ratio), with a form used previously for data from other engines.

6. The NO_x emission indices, both with and without afterburning, have been simply correlated with flight speed, altitude, and power level.

7. Emission of carbon monoxide (CO) increased with increasing altitude at constant flight speed and decreased with increasing flight speed at constant altitude.

8. The carbon monoxide emission indices at military power varied from 1 to 4 over the range of altitudes and flight speeds tested. The CO emission indices for minimum afterburning conditions were approximately an order of magnitude greater than at military power. The CO emissions typically decreased slightly from minimum to intermediate afterburning, but increased nearly an order of magnitude from intermediate to maximum afterburning.

9. Emissions of unburned hydrocarbons (HC) generally increased with increasing altitude at constant flight speed and decreased with increasing flight speed at constant altitude.

10. At military power unburned hydrocarbon emission indices were less than 0.3 for all test conditions. In afterburning conditions HC emissions were often substantially higher than at military power because of high hydrocarbon concentrations in the center of the exhaust. At minimum afterburning the HC emission indices

varied from 0.2 to 20 for the range of flight speeds and altitudes tested. At all flight conditions, HC emissions decreased with increasing power level in afterburning.

11. Data for test conditions that were run on both engines showed that the exhaust concentrations of CO and HC for the two engines were similar at military power, but quite different for afterburning conditions. The exhaust NO_x concentrations, which are primarily dependent on primary combustor conditions, were very similar for both engines at the same flight conditions.

Lewis Research Center,
National Aeronautics and Space Administration,
Cleveland, Ohio, October 30, 1975,
505-03.

REFERENCES

1. Diehl, Larry A.: Preliminary Investigation of Gaseous Emissions From Jet Engine Afterburners. NASA TM X-2323, 1971.

2. Palcza, J. Lawrence: Study of Altitude and Mach Number Effects on Exhaust Gas Emissions of an Afterburning Turbofan Engine. NAPTC-ATD-212; Naval Air Propulsion Test Center (AD-741249; FAA-RD-72-31), 1971.

3. Diehl, Larry A.: Measurement of Gaseous Emissions from an Afterburning Turbojet Engine at Simulated Altitude Conditions. NASA TM X-2726, 1973.

4. German, R. C.; High, M. D.; and Robinson, C. E.: Measurement of Exhaust Emissions from a 185-GE-5B Engine at Simulated High-Altitude Supersonic Free-Stream Flight Conditions. ARO-PWT-TR-73-49, ARO Inc. (AD-764-717; AEDC-TR-73-103; FAA-RD-73-92), 1973.

5. Davidson, D. L.; and Domal, A. F.: Emission Measurements of a J93 Turbojet Engine. ARO-ETF-TR-73-46, ARO, Inc. (AD-766648; AEDC-TR-73-132), 1973.

6. Diehl, Larry A.; and Biaglow, James A.: Measurement of Gaseous Emissions From a Turbofan Engine at Simulated Altitude Conditions. NASA TM X-3046, 1974.

7. Farlow, N. H.; Watson, V. R.; Hoshizaki, H.; Conti, R. J.; and Meyer, J. W.: Measurements of Supersonic Jet Aircraft Wakes in the Stratosphere. Second Intern. Conf. on the Environmental Impact of Aerospace Operations in the High Atmosphere, Am. Meteorology Soc., 1974, pp. 53-58.

8. Holdeman, J. D.: Dispersion and Dilution of Jet Aircraft Exhaust at High-Altitude Flight Conditions. J. of Aircraft, vol. 11, no. 8, Aug. 1974, pp. 483-487.

9. Holdeman, James D.: Gaseous Exhaust Emissions From a J-58 Engine at Simulated Supersonic Flight Conditions. NASA TM X-71532, 1974.

10. Holdeman, J. D.: Emission Calibration of a J-58 Afterburning Turbojet Engine at Simulated Supersonic, Stratospheric Flight Conditions. Second Intern. Conf. on the Environmental Impact of Aerospace Operations in the High Atmosphere, Am. Meteorology Soc., 1974, pp. 65-72. (Also NASA TM X-71571.)

11. Procedure for the Continuous Sampling and Measurement of Gaseous Emissions From Aircraft Turbine Engines. Aerospace Recommended Practice 1256, SAE, Oct. 1971.

12. Marchionna, Nicholas R.; Diehl, Larry A.; and Trout, Arthur M.: Effect of Inlet-Air Humidity, Temperature, Pressure, and Reference Mach Number on the Formation of Oxides of Nitrogen in a Gas Turbine Combustor. NASA TN D-7396, 1973.

13. Glawe, George E.; Simmons, Frederick S.; and Stickney, Truman M.: Radiation and Recovery Corrections and Time Constants of Several Chromel-Alumel Thermocouple Probes in High-Temperature, High-Velocity Gas Streams. NACA TN 3766, 1956.

TABLE I. - TEST CONDITIONS

Condition	Flight Mach number	Altitude, km
1	2.0	16.0
2	2.0	17.9
3	2.0	19.8
4	2.4	19.8
5	2.8	19.8
6	2.8	22.0
7	2.8	23.5
8	3.0	19.8

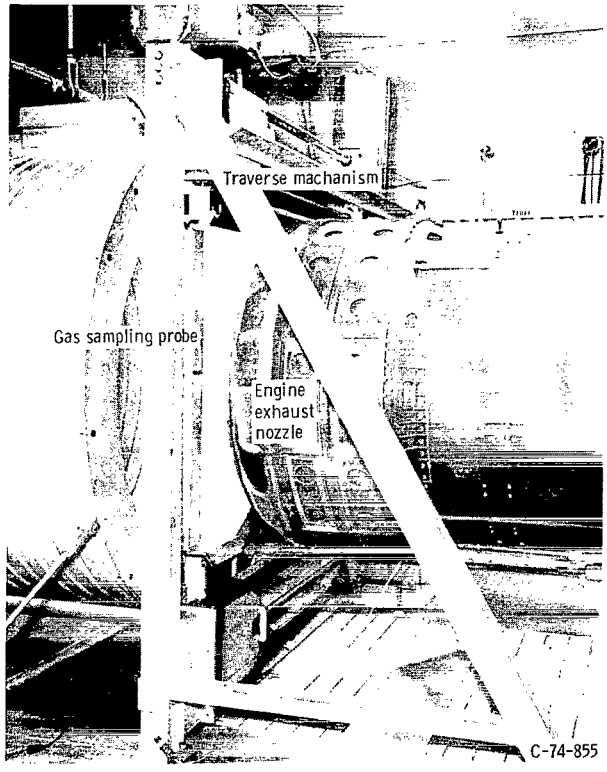

(a) Probe and traversing mechanism.

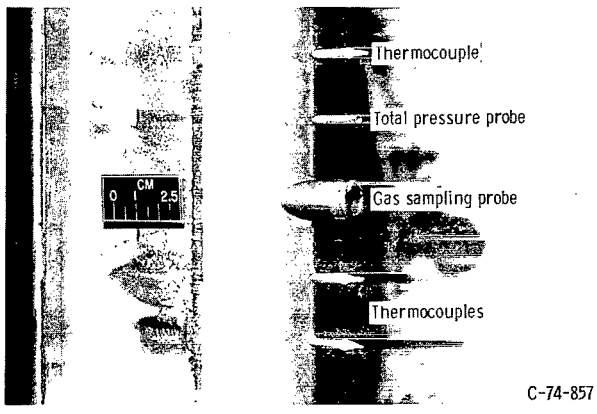

(b) Detail of sensor area.

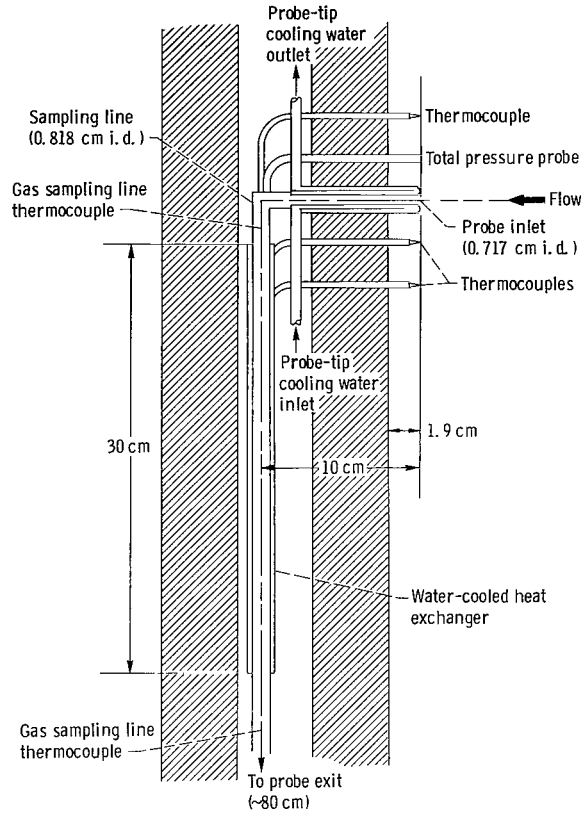

(c) Schematic of gas sample probe.

Figure 1. - Gas sampling probe.

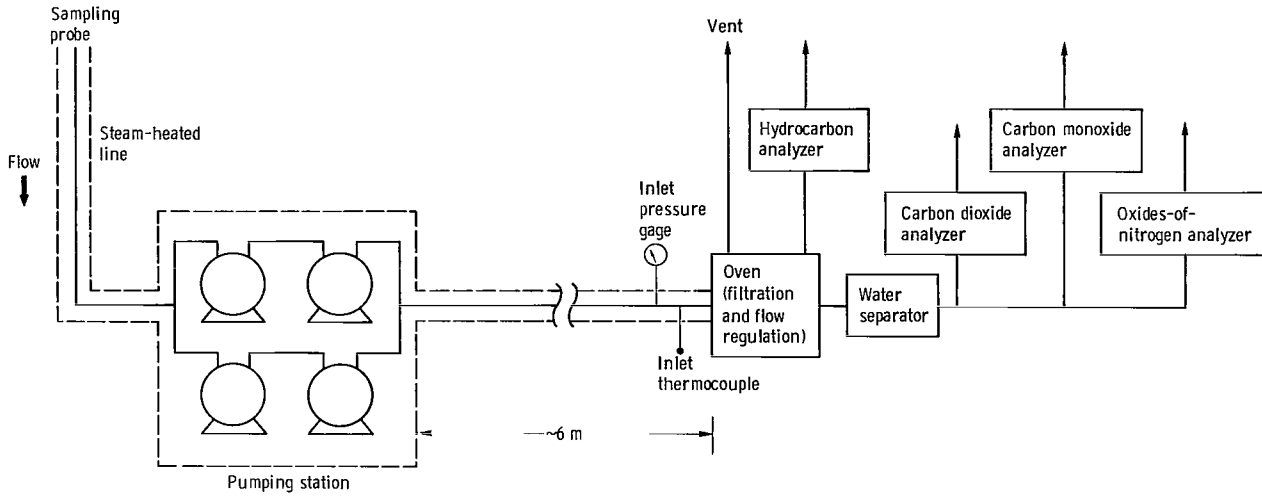

(a) Flow schematic.

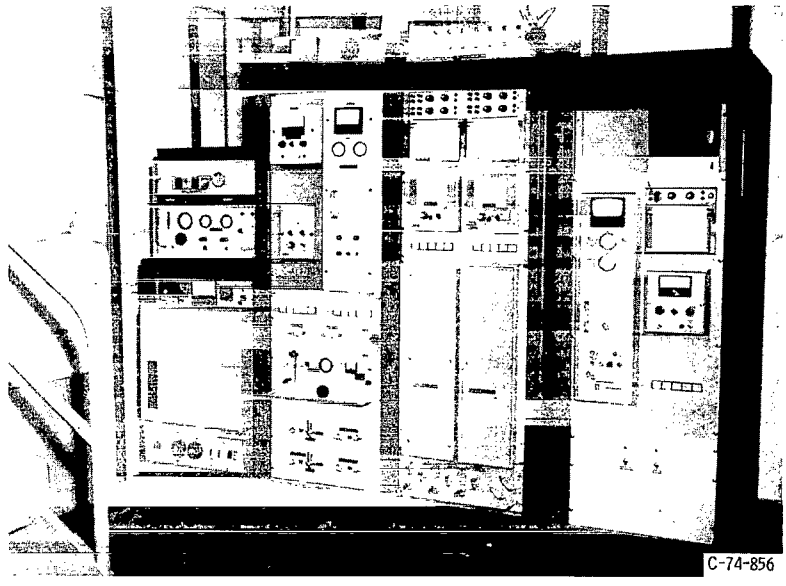

(b) Console.

Figure 2. - Gas analysis system.

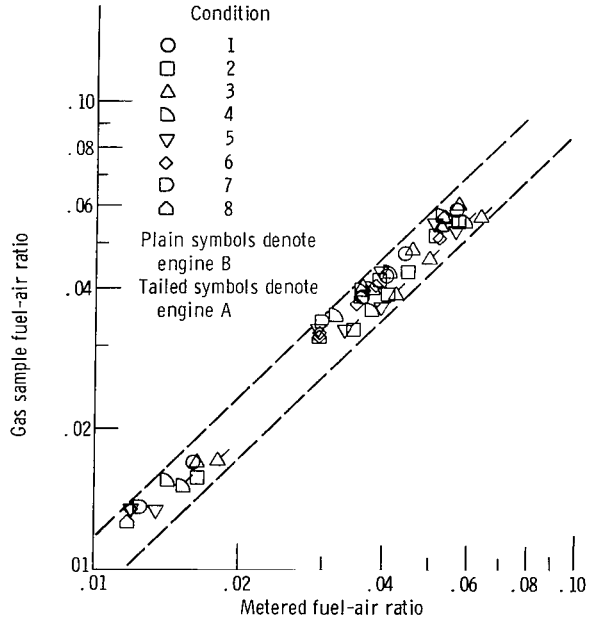

Figure 3. - Comparison of gas sample and metered fuel-air ratios.

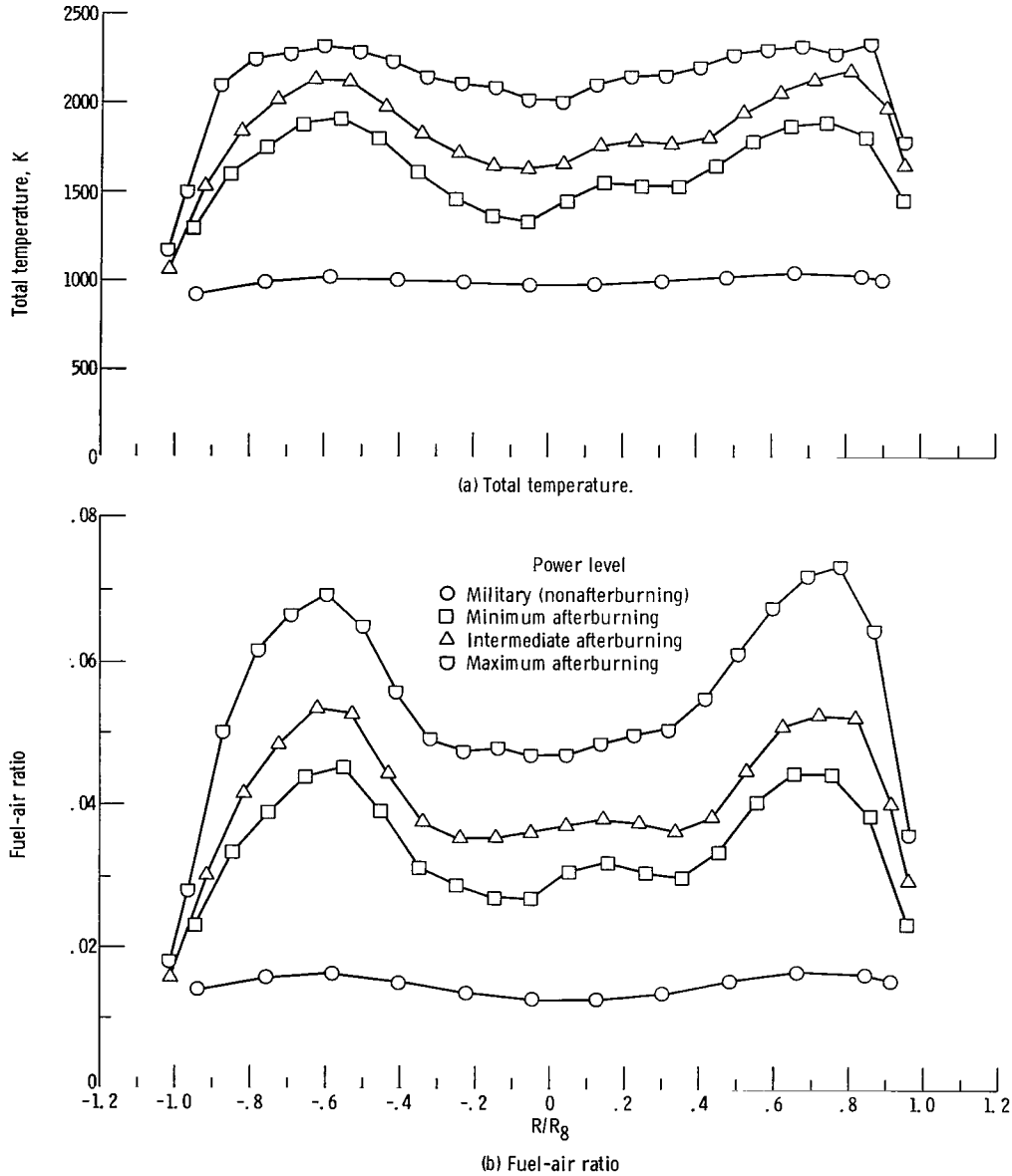

Figure 4. - Temperature, fuel-air ratio, and concentration profiles for condition 4 (Mach 2.4, 19.8 km); engine A.

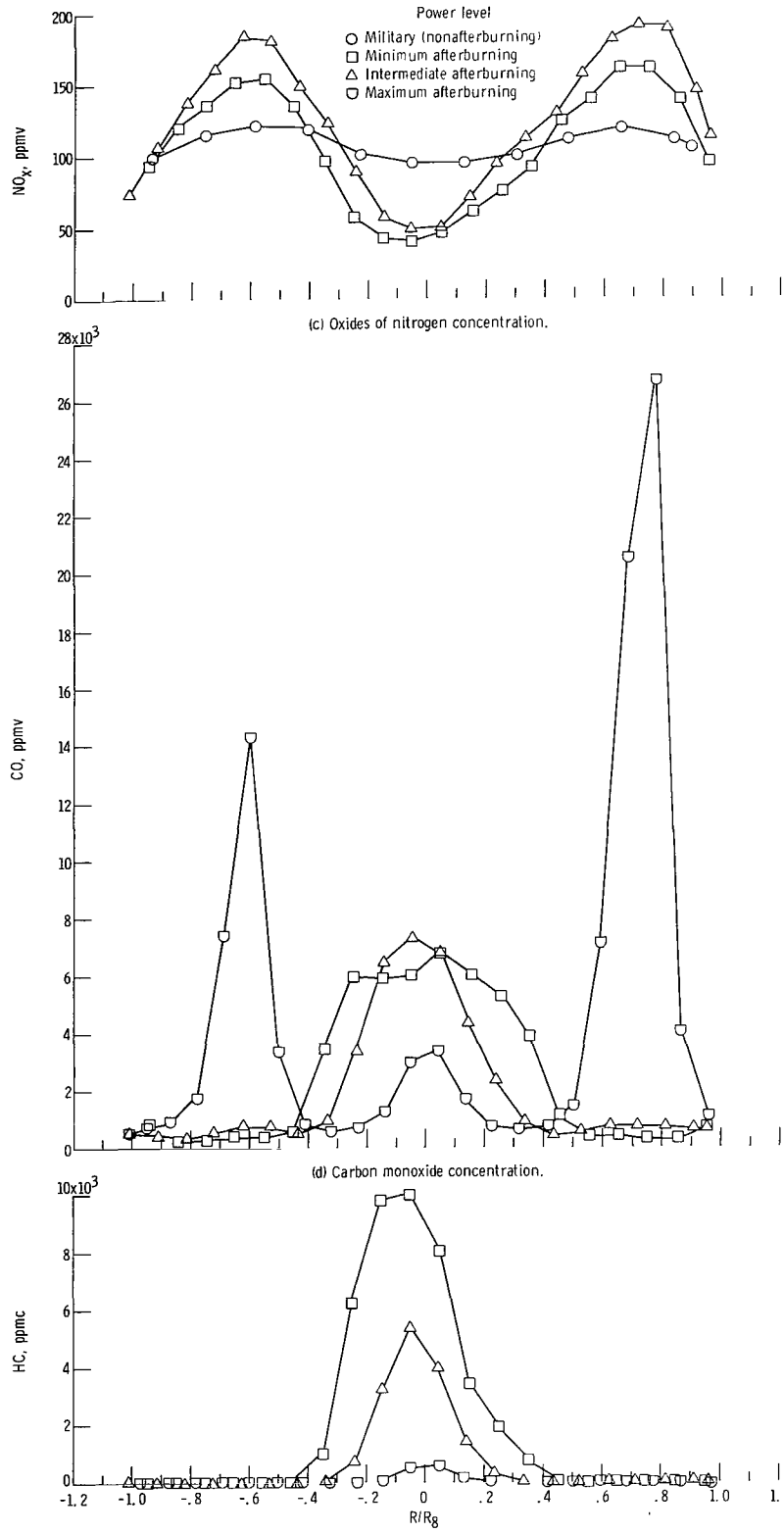

(e) Hydrocarbons concentration.

Figure 4. - Concluded.

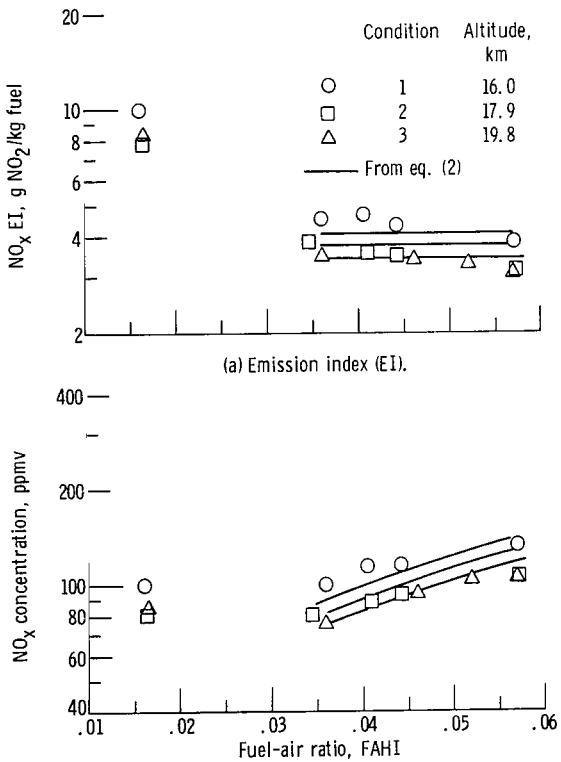

(a) Emission index (EI).

(b) Concentration.

Figure 5. - Variation of oxides of nitrogen emissions with altitude and power level at Mach 2.0 for engine B.

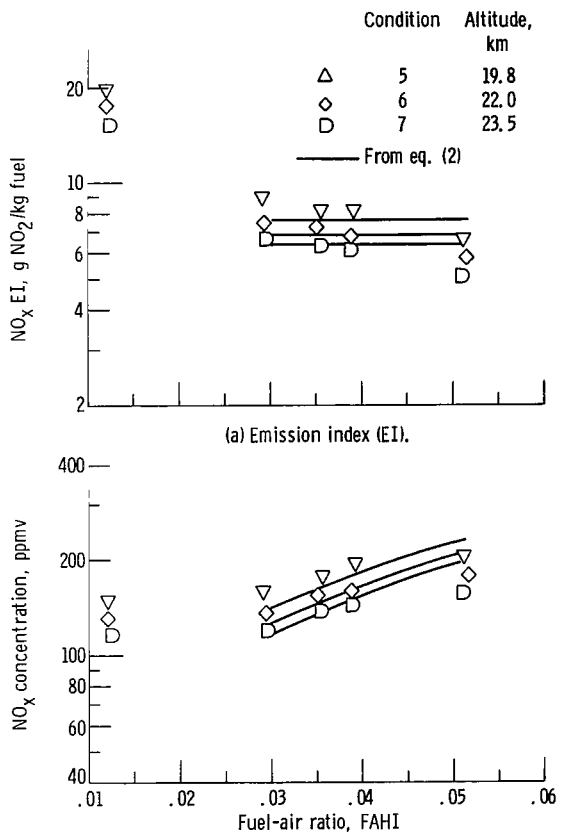

(a) Emission index (EI).

(b) Concentration.

Figure 6. - Variation of oxides of nitrogen emissions with altitude and power level at Mach 2.8 for engine B.

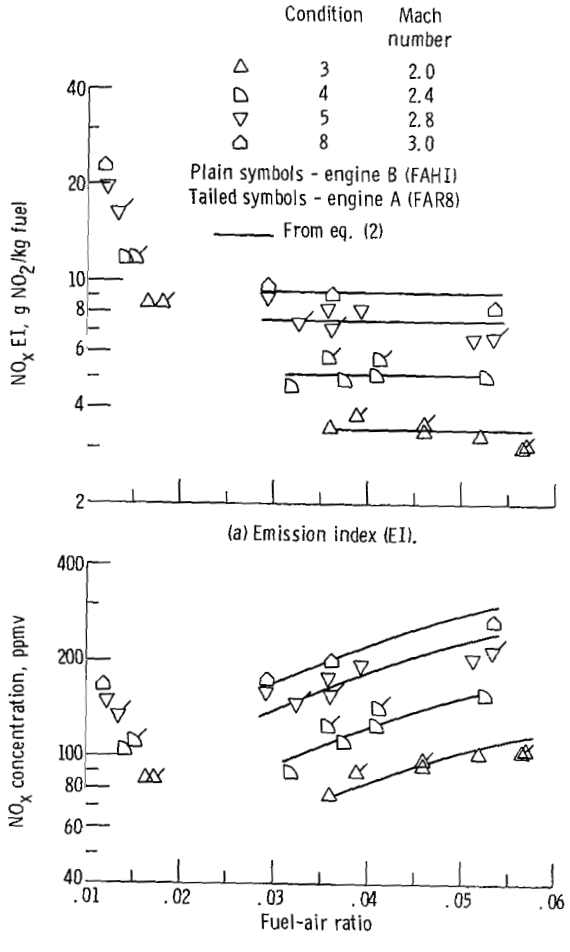

(b) Concentration.

Figure 7. - Variation of oxides of nitrogen emissions with flight speed and power level at 19.8 kilometers.

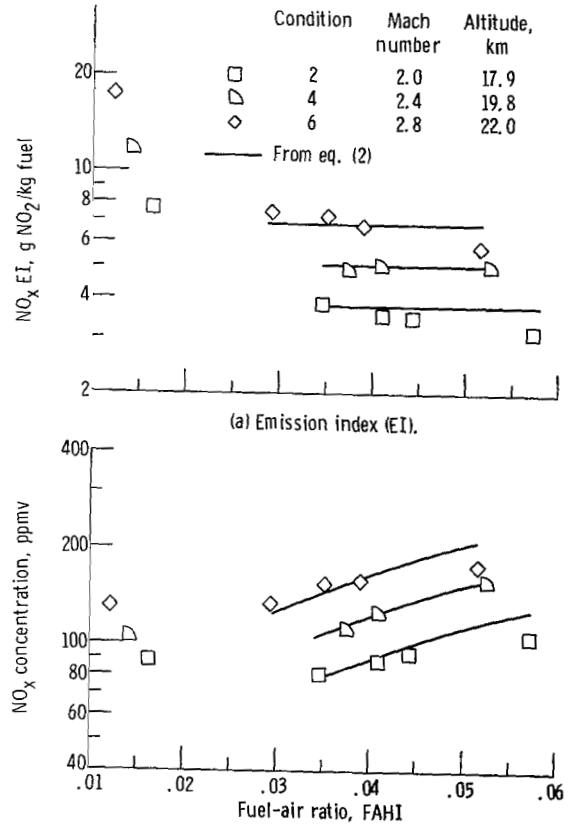

(b) Concentration.

Figure 8. - Oxides of nitrogen emissions at constant combustor pressure for engine B.

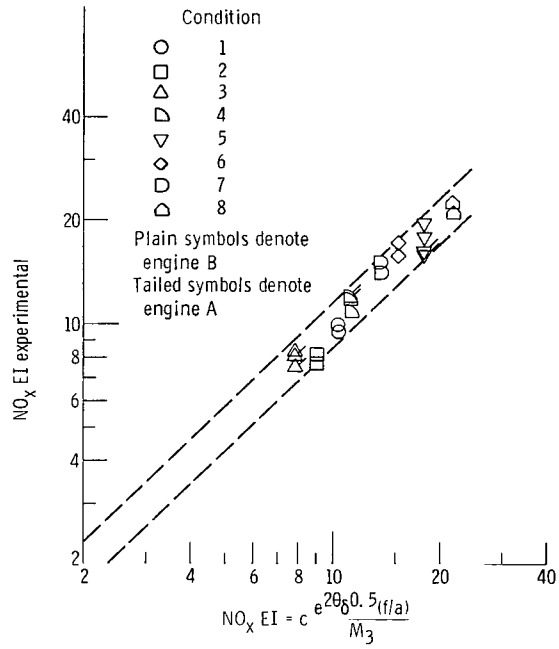

Figure 9. - Correlation of oxides of nitrogen emission index with combustor parameters; military power.

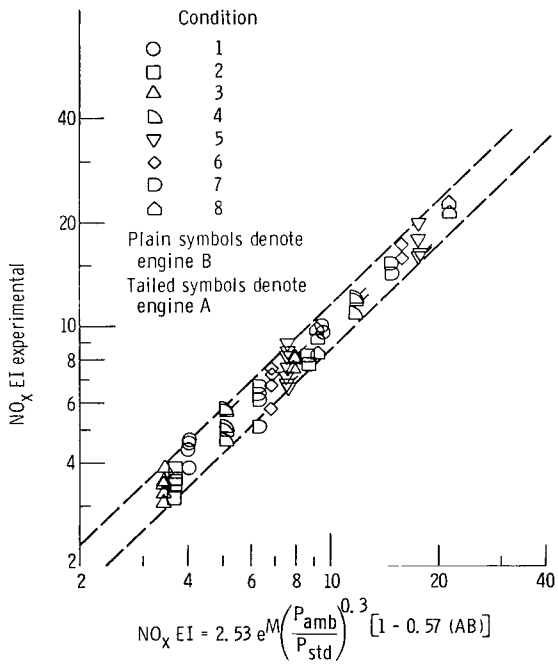

Figure 10. - Correlation of oxides of nitrogen emission index with flight parameters. (AB = 0 for military power; = 1 for afterburning.)

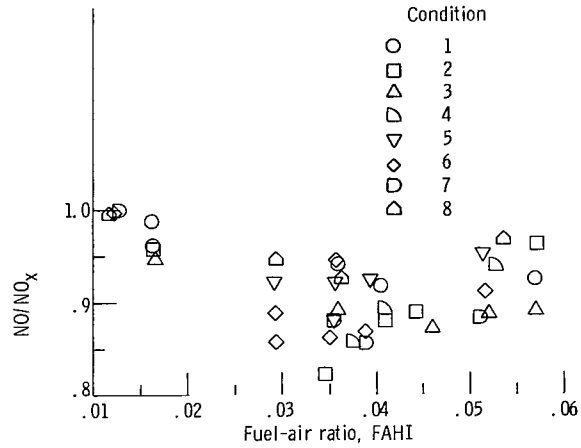

Figure 11. - Ratio of nitric oxide to total oxides of nitrogen.

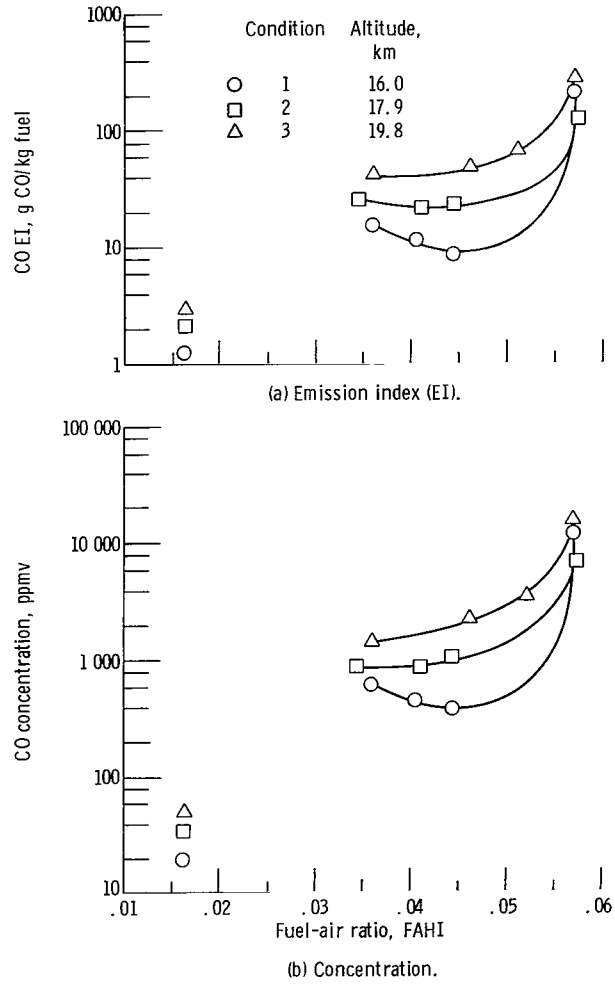

(a) Emission index (EI).

(b) Concentration.

Figure 12. - Variation of carbon monoxide emissions with altitude and power level at Mach 2.0 for engine B.

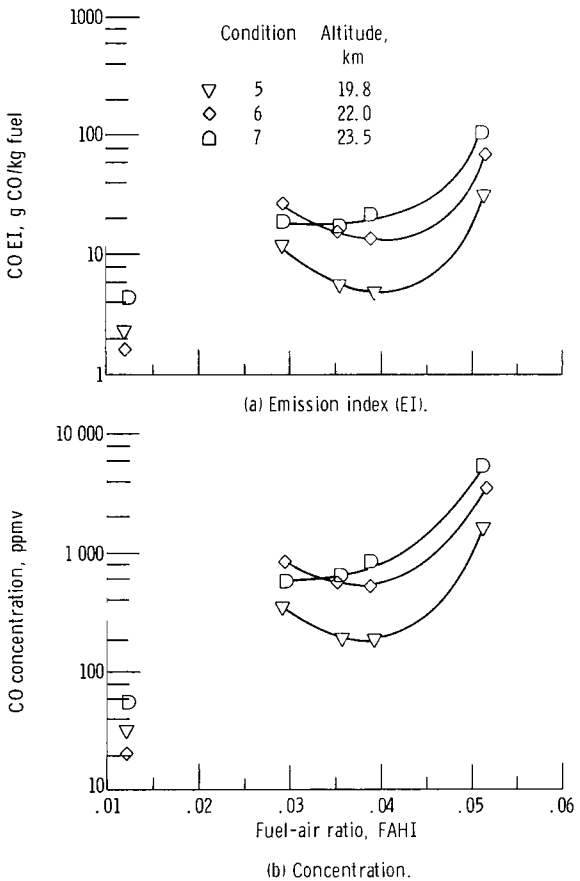

Figure 13. - Variation of carbon monoxide emissions with altitude and power level at Mach 2.8 for engine B.

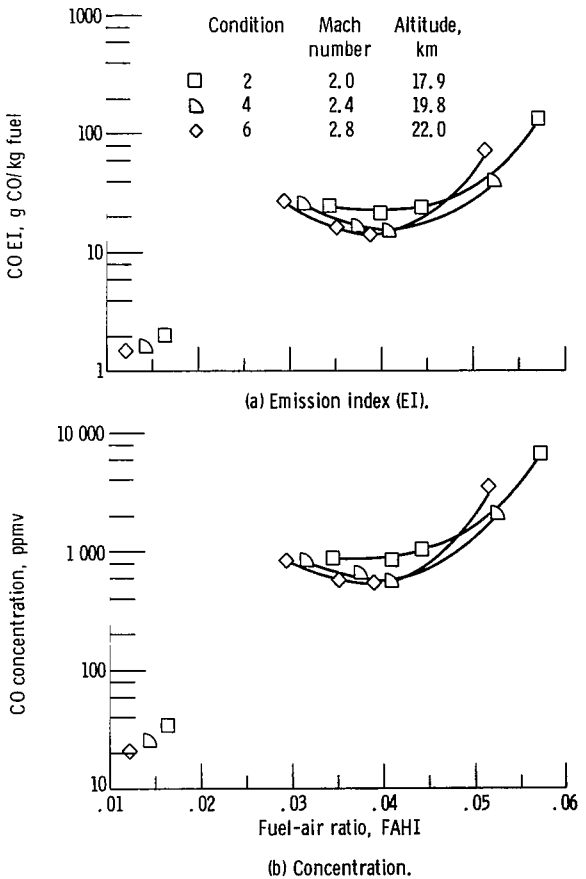

Figure 14. - Carbon monoxide emissions at constant combustion pressure for engine B.

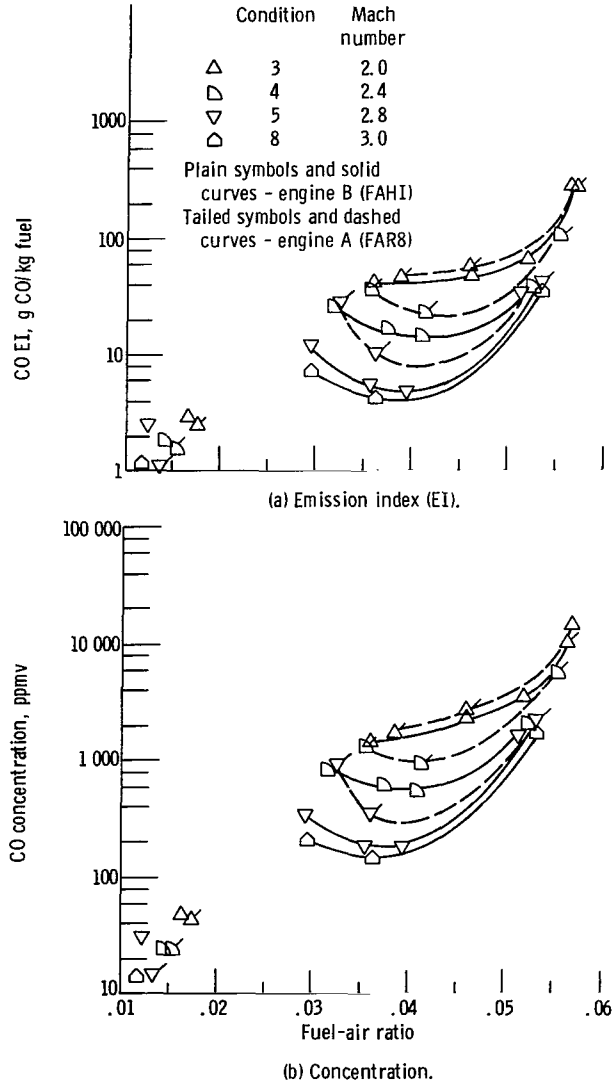

Figure 15. - Variation of carbon monoxide emissions with flight speed and power level at 19.8 kilometers.

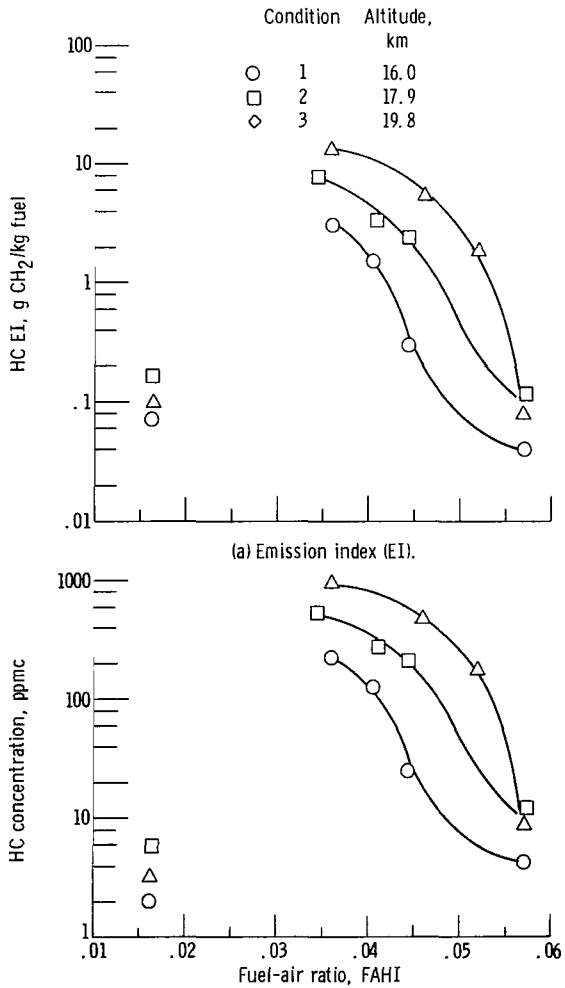

(a) Emission index (EI).

(b) Concentration.

Figure 16. - Variation of hydrocarbon emissions with altitude and power level at Mach 2.0 for engine B.

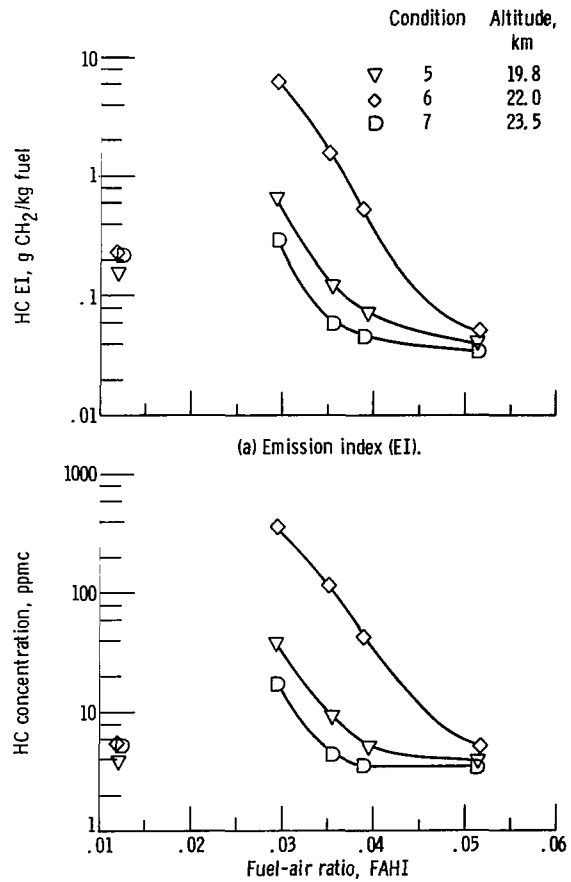

(a) Emission index (EI).

(b) Concentration.

Figure 17. - Variation of hydrocarbon emissions with altitude and power level at Mach 2.8 for engine B.

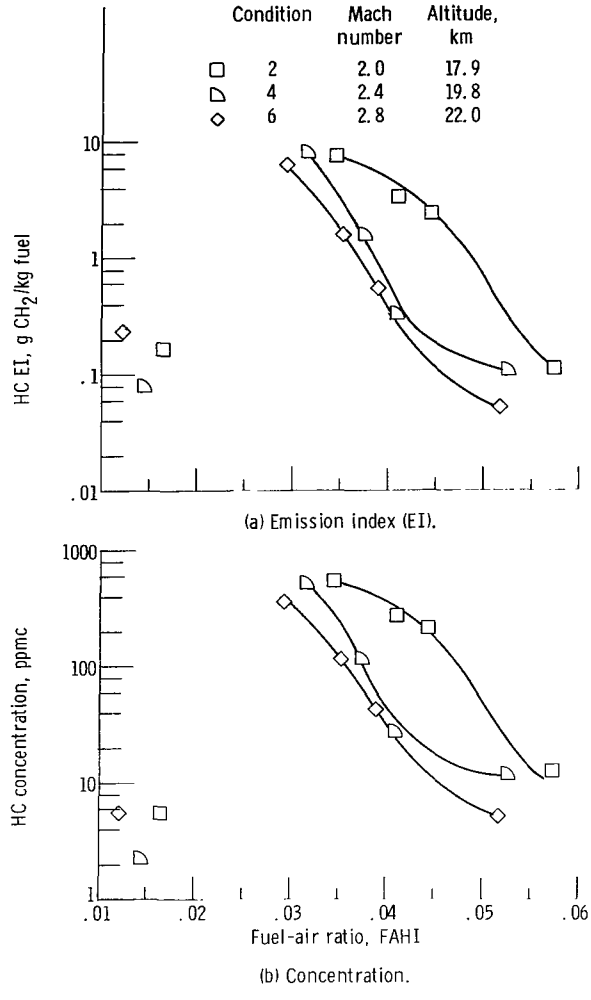

Figure 18. - Hydrocarbon emissions at constant combustion pressure for engine B.

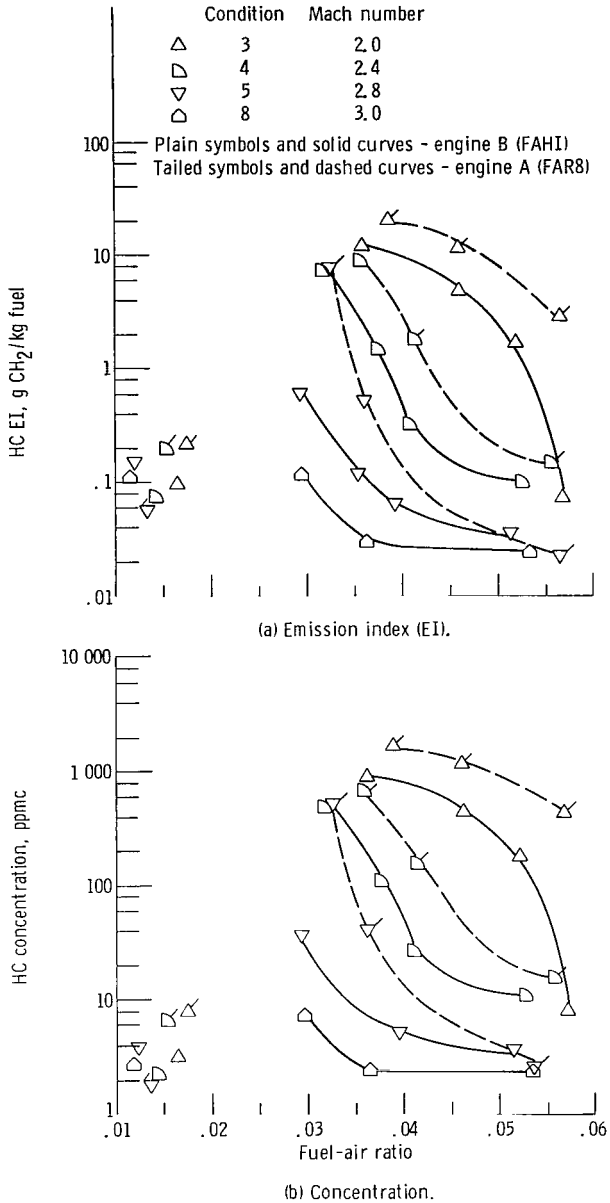

Figure 19. - Variation of hydrocarbon emissions with flight speed and power level at 19.8 kilometers.

APPENDIX A

CONCENTRATION PROFILES

Exhaust concentration profiles of the oxides of nitrogen (NO_x), carbon monoxide (CO), and unburned hydrocarbons (HC) for all test conditions (except condition 4, engine A) are shown in figures A-1 to A-10 in this appendix. The NO_x and CO concentrations are given as parts per million by volume (ppmv); HC concentrations are given as parts per million carbon by volume (ppmC). The axis of abscissas in these figures is the dimensionless radial distance from the engine centerline, R/R_8, where R_8 is the nozzle exit radius that varies with flight condition and power level. The engine power levels are identified in the figure keys; the fuel-air ratios corresponding to each power level at each condition are given in appendix B.

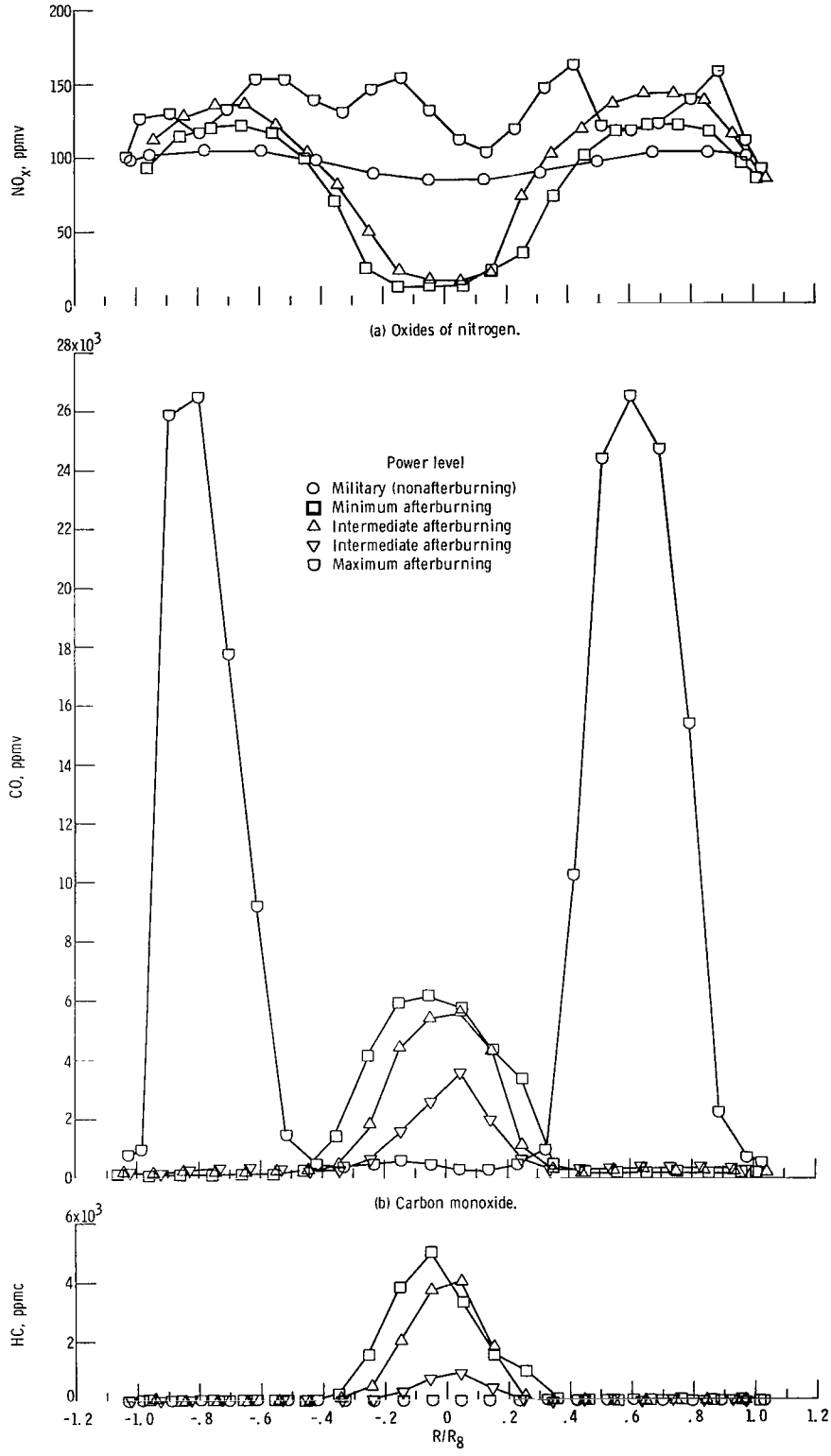

Figure A-1. - Concentration profiles for condition 1 (Mach 2.0, 16.0 km); engine B.

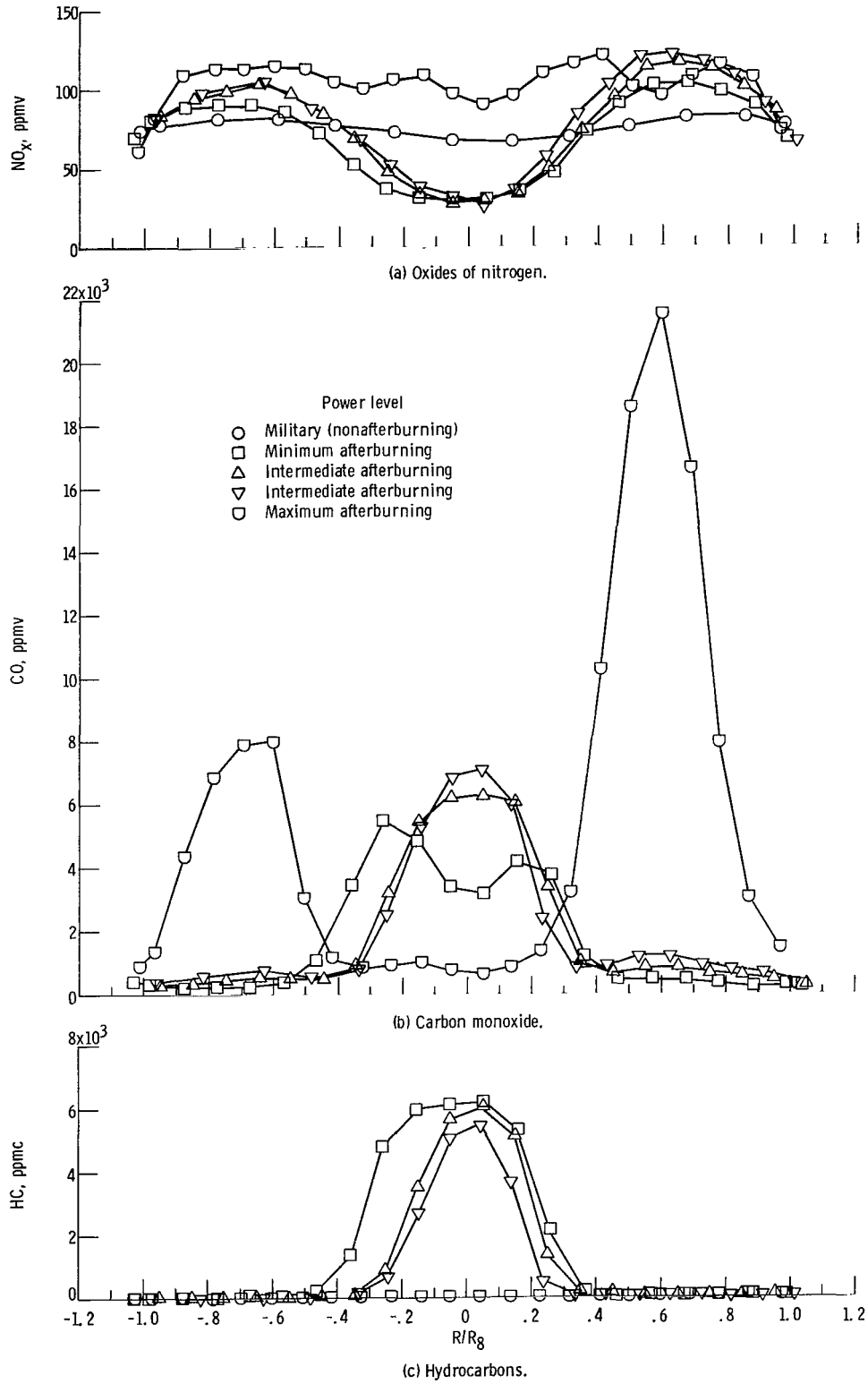

(c) Hydrocarbons.

Figure A-2. - Concentration profiles for condition 2 (Mach 2.0, 17.9 km); engine B.

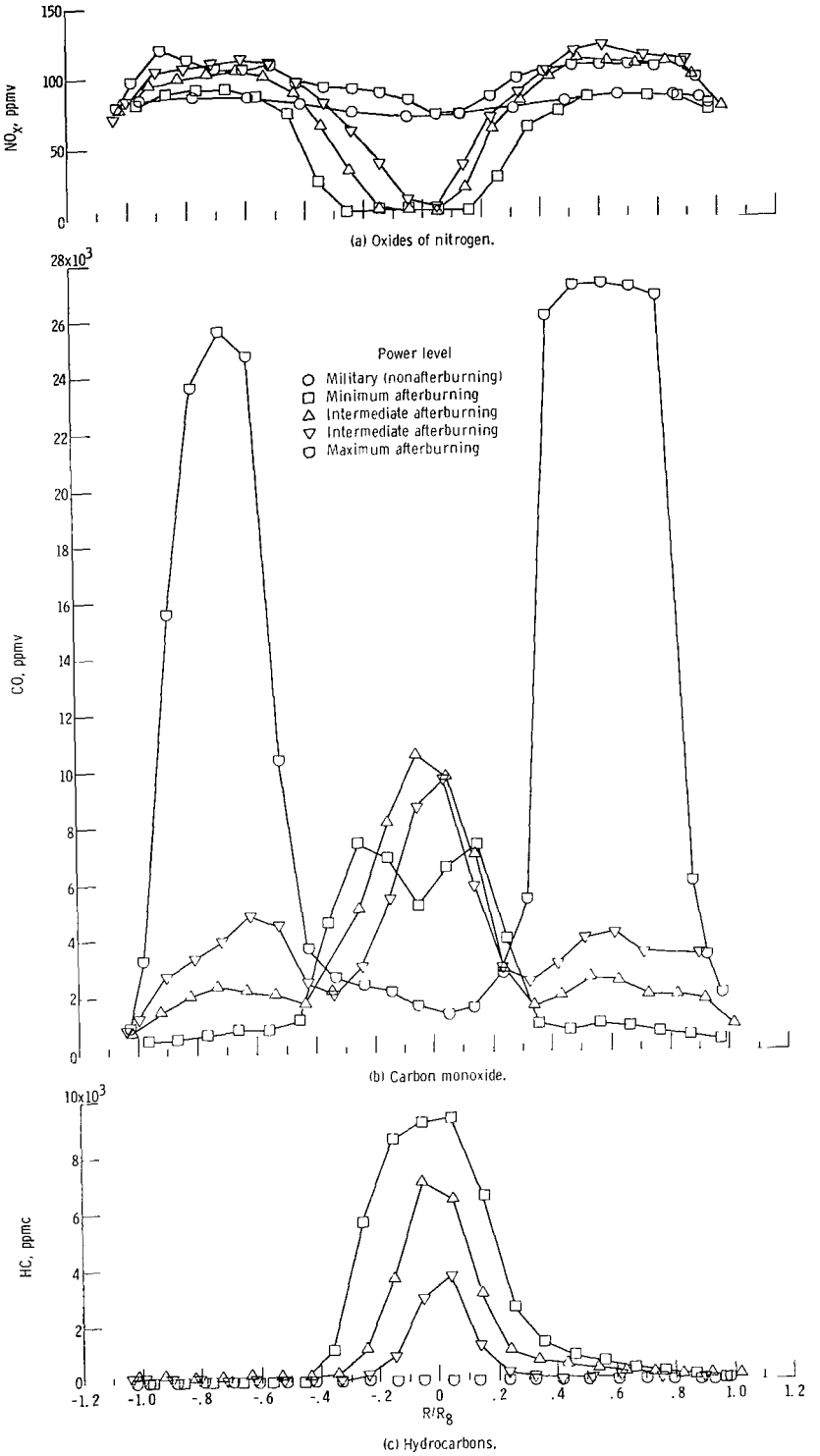

Figure A-3. - Concentration profiles for condition 3 (Mach 2.0, 19.8 km); engine B.

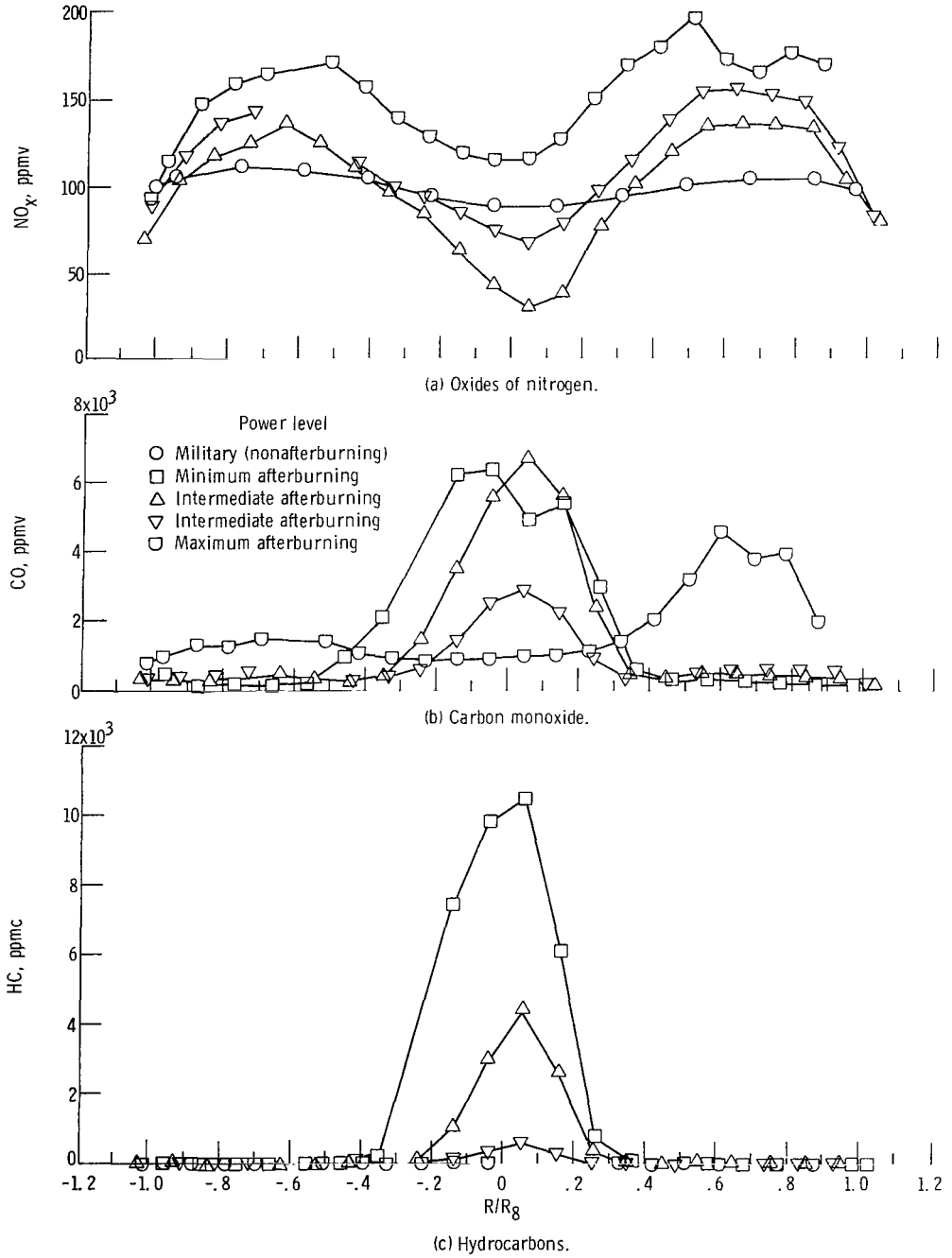

Figure A-4. - Concentration profiles for condition 4 (Mach 2.4, 19.8 km); engine B.

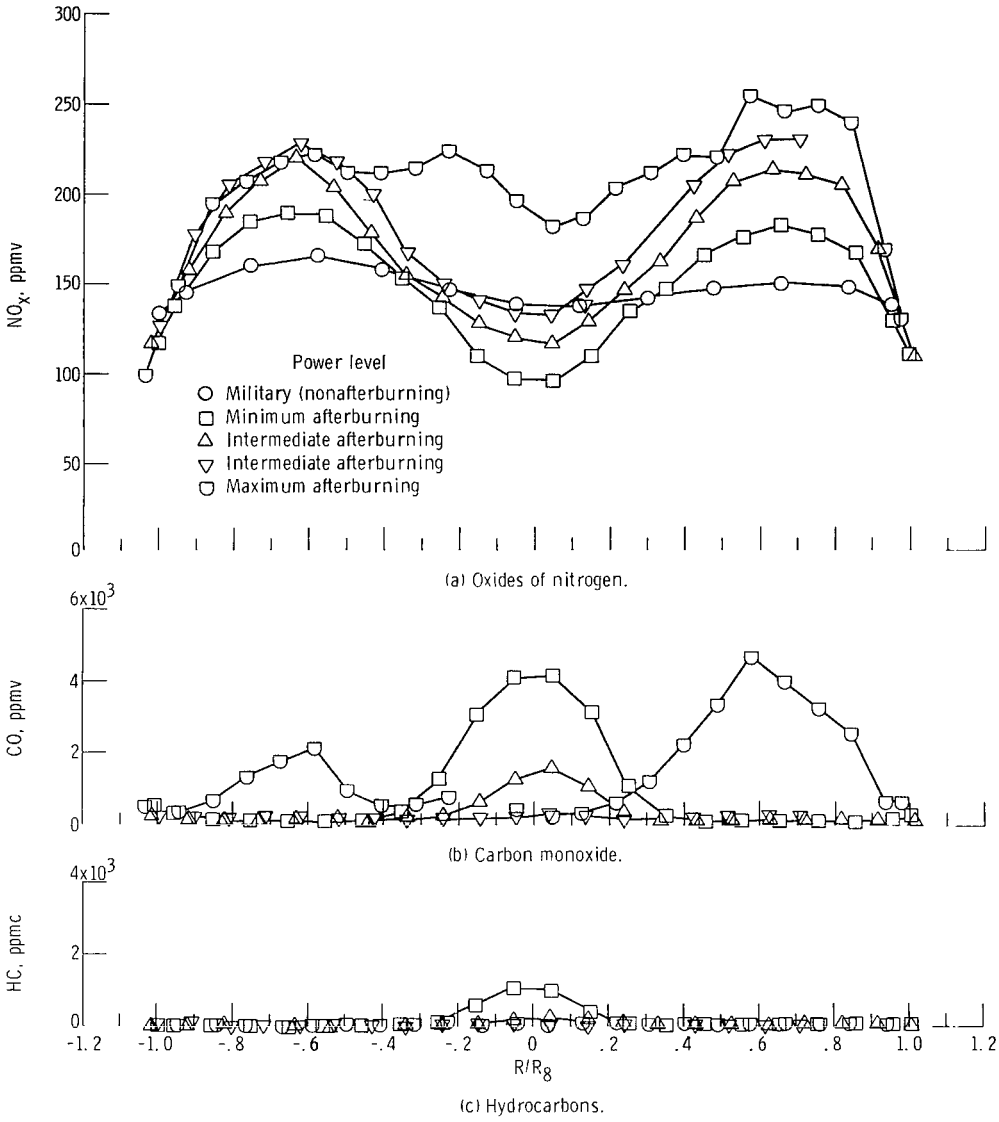

Figure A-5. - Concentration profiles for condition 5 (Mach 2.8, 19.8 km); engine B.

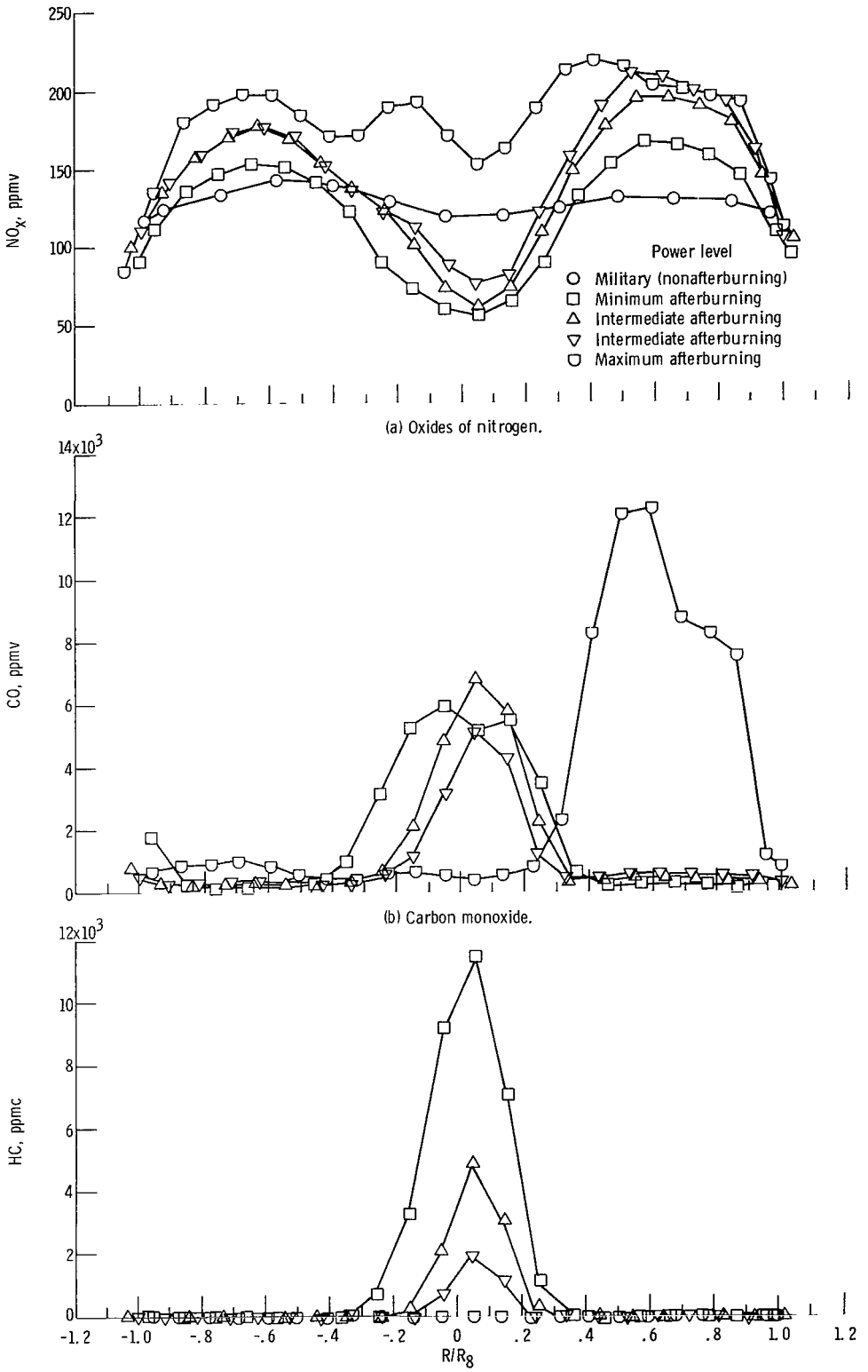

(c) Hydrocarbons.

Figure A-6. - Concentration profiles for condition 6 (Mach 2.8, 22.0 km); engine B.

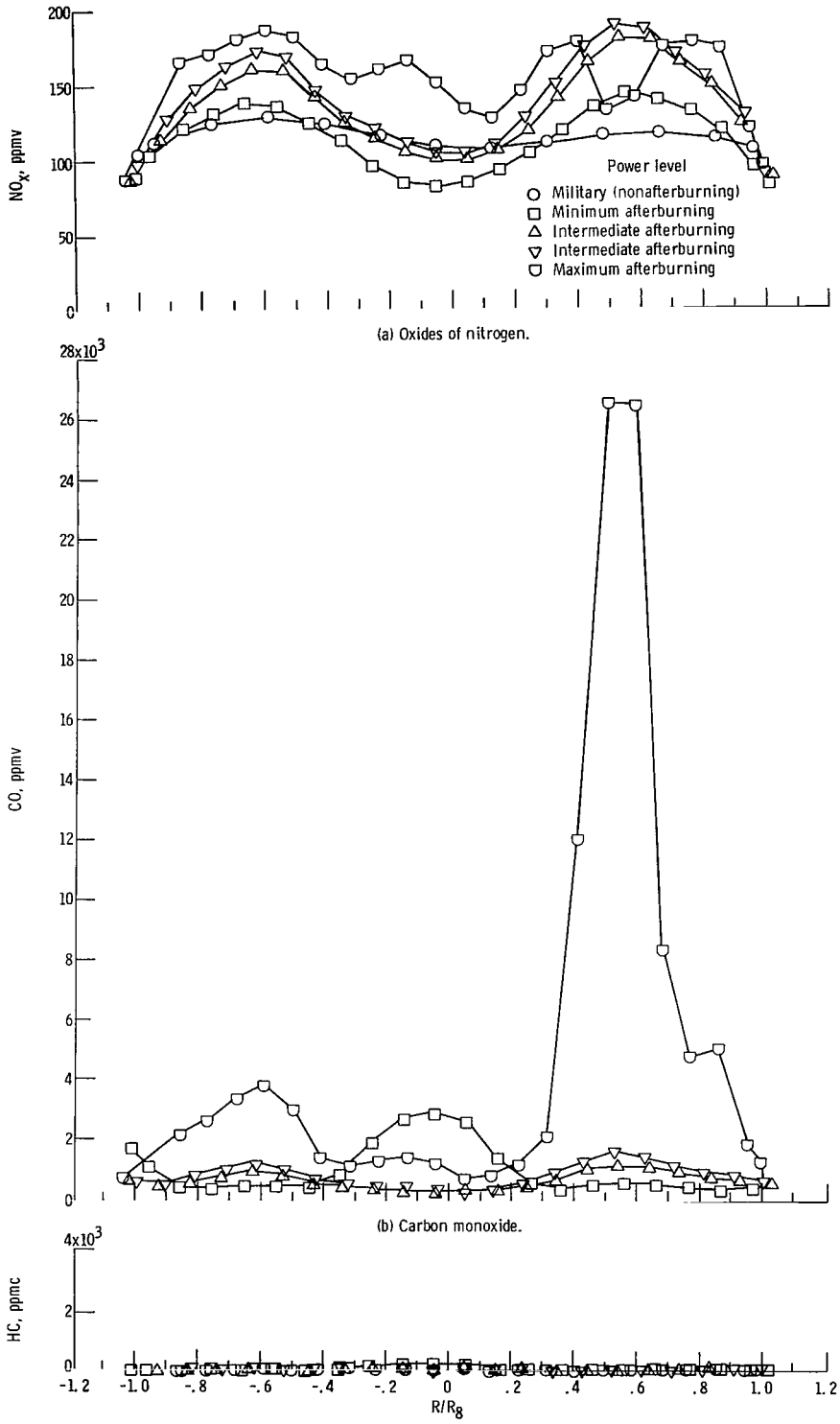

Figure A-7. - Concentration profiles for condition 7 (Mach 2.8, 23.5 km); engine B.

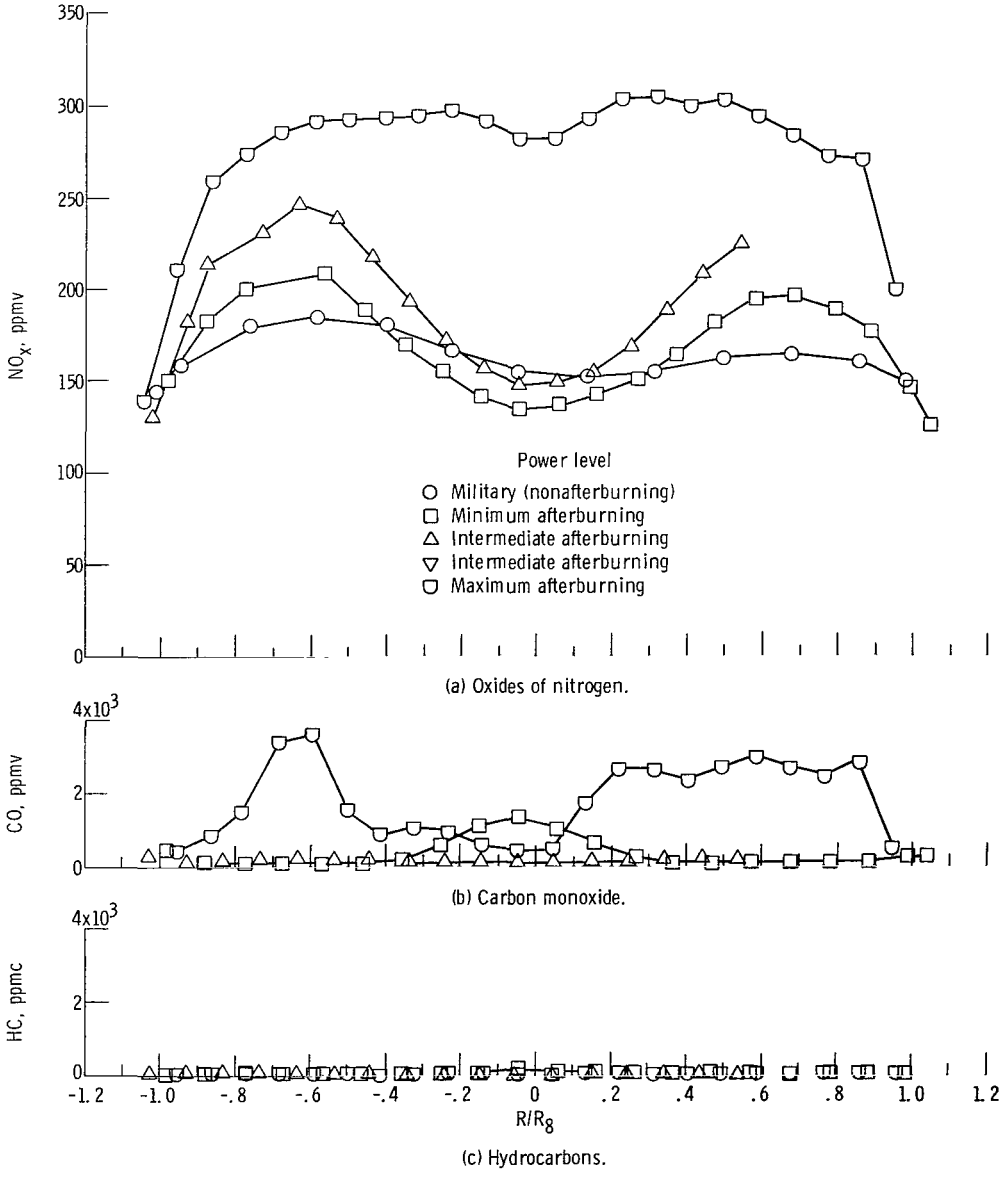

Figure A-8. - Concentration profiles for condition 8 (Mach 3.0, 19.8 km); engine B.

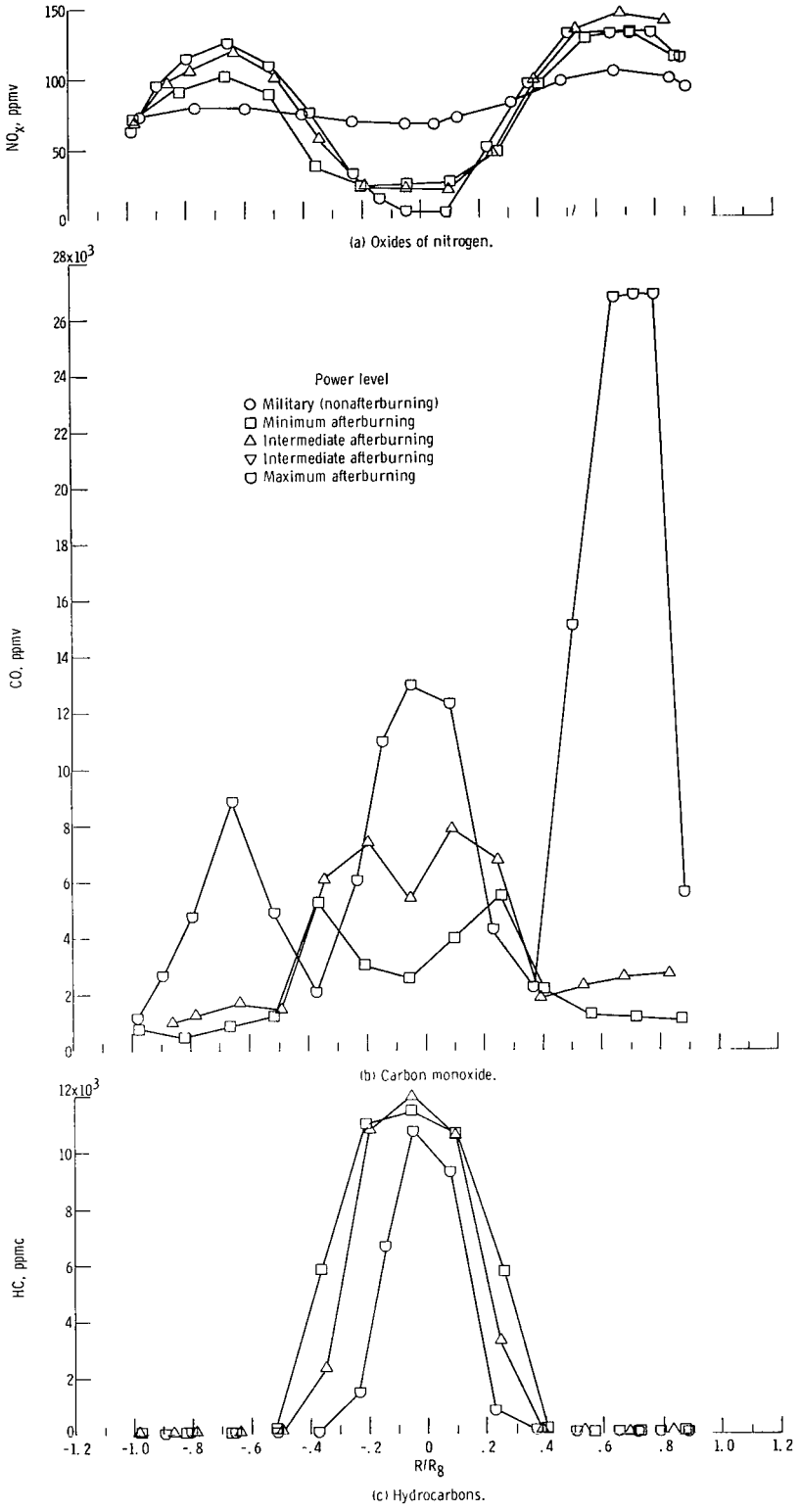

Figure A-9. - Concentration profiles for condition 3 (Mach 2.0, 19.8 km); engine A.

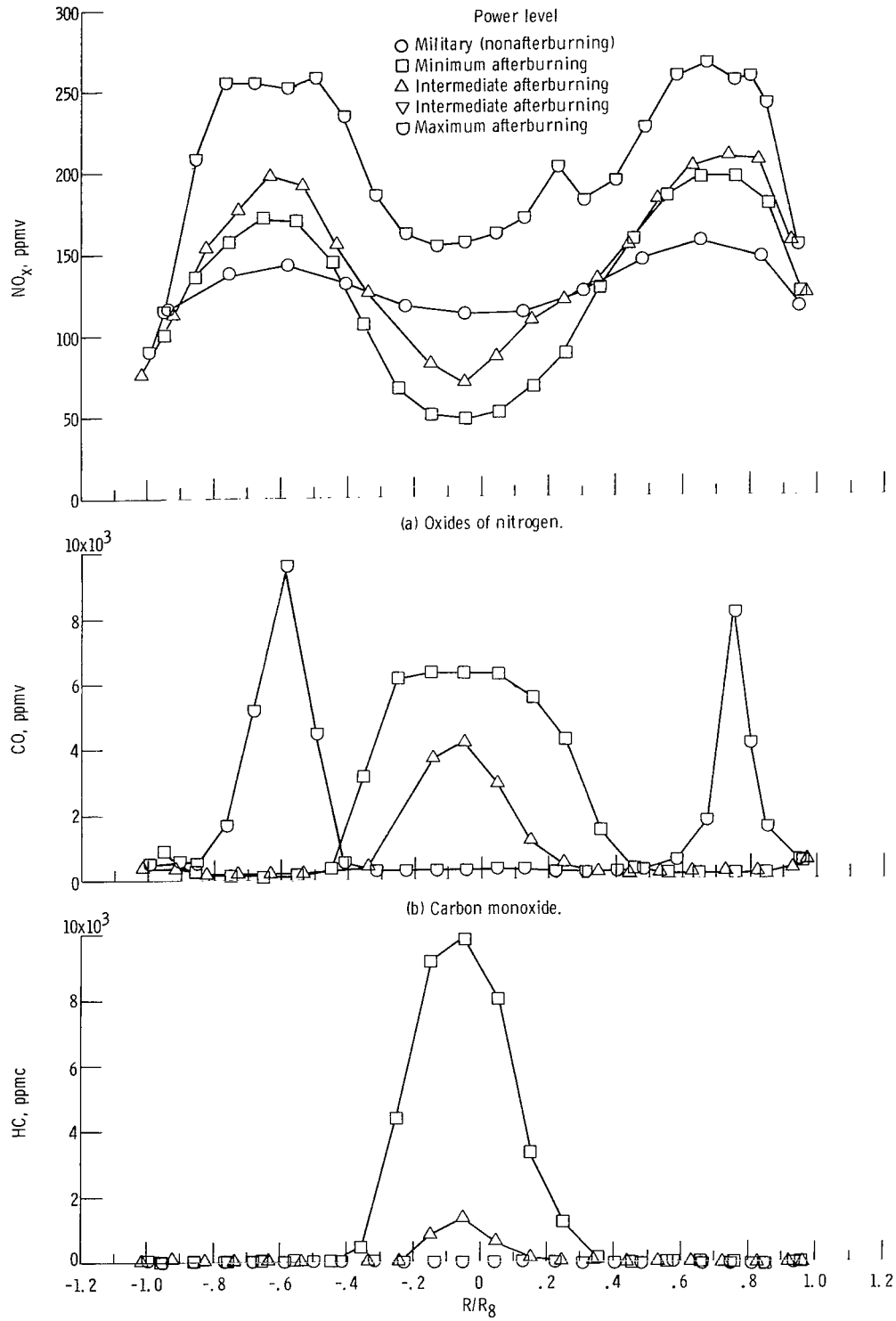

Figure A-10. - Concentration profiles for condition 5 (Mach 2.8, 19.8 km); engine A.

APPENDIX B

EXPERIMENTAL DATA

The engine-inlet conditions, the exhaust profile data, and the average exhaust parameters for all flight conditions and power levels tested for both J-58 engines are given in tables B-I to B-XI in this appendix. Symbols used in the tables are defined in the nomenclature below.

COPPM	carbon monoxide concentration, ppmv
CO2PPM	carbon dioxide concentration, ppmv
EI	emission index, g pollutant/kg fuel
EI FAHI	emission index based on metered fuel-air ratio
EI FAR8	emission index based on integrated average gas-sample fuel-air ratio
FAHI	ratio of metered fuel flow to engine-inlet air flow
FAR8	fuel-air ratio calculated from gas sample
H	inlet-air humidity, g H_2O/g dry air
HCPPM	hydrocarbon concentration, ppmC
NOPPM	nitric oxide concentration, ppmv
NOXPPM	oxides of nitrogen ($NO + NO_2$) concentration, ppmv
PT2	engine inlet air pressure, N/cm^2
PT8	exhaust total pressure, N/cm^2
R	radius
R8	exhaust nozzle radius
TT2	engine-inlet air temperature, K
TT8	exhaust total temperature, K

TABLE B-I. - ENGINE INLET TEST CONDITIONS AND EXHAUST PROFILE DATA

FOR CONDITION 1 (MACH 2.0, 16.0 km) ENGINE B

(a) Military (nonafterburning) power; TT2, 388 K; PT2, 7.42 N/cm^2; FAHI, 0.0162; H, 0.0022 g H_2O/g dry air

R/R8	COPPM	CO2PPM	HCPPM	NOPPM	NOXPPM	FAR8	TT8,K	PT8,N/CM2
-1.021	18.	34647.	2.	98.	99.	.0171	982.	11.52
-.959	23.	35903.	2.	102.	103.	.0177	992.	12.03
-.779	16.	36681.	2.	104.	105.	.0181	1014.	12.25
-.595	18.	35832.	2.	103.	105.	.0177	1012.	12.19
-.416	24.	33145.	2.	95.	99.	.0163	990.	12.28
-.233	21.	30262.	2.	87.	90.	.0149	965.	12.15
-.051	22.	28521.	2.	83.	84.	.0140	949.	11.97
.132	15.	28587.	2.	83.	84.	.0140	952.	11.97
.312	19.	30515.	2.	88.	89.	.0150	968.	11.97
.498	16.	33017.	2.	95.	97.	.0163	991.	12.17
.678	18.	35629.	2.	102.	103.	.0176	1014.	12.18
.861	23.	36347.	2.	102.	103.	.0179	1008.	12.40
.987	25.	35462.	2.	99.	99.	.0175	987.	12.04
AVERAGE	20.	34664.	2.	99.	100.	.0171	997.	12.14
EI FAR8	1.15	3136.	.06	9.36	9.47			
EI FAHI	1.21	3305.	.07	9.86	9.99			

(b) Minimum afterburning power; TT2, 387 K; PT2, 7.42 N/cm^2; FAHI, 0.0360; H, 0.0022 g H_2O/g dry air

R/R8	COPPM	CO2PPM	HCPPM	NOPPM	NOXPPM	FAR8	TT8,K	PT8,N/CM2
-1.061	128.	31011.	5.	52.	57.	.0153	650.	6.10
-.963	93.	65931.	3.	91.	94.	.0331	1461.	11.34
-.861	67.	80280.	7.	111.	115.	.0405	1680.	11.72
-.759	99.	84637.	7.	116.	121.	.0428	1743.	11.70
-.658	117.	86740.	6.	117.	122.	.0440	1770.	11.56
-.558	117.	84092.	6.	110.	117.	.0426	1755.	11.58
-.456	243.	75921.	16.	92.	100.	.0383	1690.	11.59
-.354	1407.	67159.	219.	54.	72.	.0345	1595.	11.43
-.253	4165.	59099.	1580.	14.	25.	.0325	1493.	11.41
-.152	5921.	52403.	3868.	9.	13.	.0312	1413.	11.30
-.051	6160.	49849.	5005.	9.	12.	.0306	1397.	11.27
.052	5755.	53046.	3359.	9.	14.	.0312	1421.	11.22
.152	4306.	59712.	1580.	14.	23.	.0329	1501.	11.16
.254	3308.	65237.	1066.	22.	35.	.0350	1583.	11.29
.354	475.	74567.	63.	78.	83.	.0378	1673.	11.35
.458	163.	82571.	17.	98.	101.	.0418	1753.	11.56
.559	193.	88273.	10.	112.	116.	.0448	1802.	11.64
.660	193.	88196.	9.	117.	121.	.0448	1786.	11.60
.760	157.	86596.	7.	116.	121.	.0439	1771.	11.75
.862	143.	83292.	6.	110.	116.	.0422	1742.	11.62
.963	174.	61244.	5.	87.	95.	.0307	1511.	11.58
1.015	184.	47216.	6.	78.	85.	.0235	1312.	10.74
AVERAGE	605.	76514.	219.	94.	100.	.0390	1660.	11.23
EI FAR8	15.63	3104.	2.83	4.00	4.25			
EI FAHI	16.83	3341.	3.05	4.30	4.57			

TABLE B-I. - Continued.

(c) Intermediate afterburning power; TT2, 386 K; PT2, 7.37 N/cm^2; FAHI, 0.0406; H, 0.0028 g H_2O/g dry air

R/R8	COPPM	CO2PPM	HCPPM	NOPPM	NOXPPM	FAR8	TT8,K	PT8,N/CM2
-1.042	175.	48714.	4.	80.	80.	.0243	1154.	10.30
-.944	169.	77250.	5.	106.	113.	.0390	1651.	11.42
-.845	206.	89834.	6.	122.	128.	.0457	1833.	11.55
-.746	239.	93368.	6.	126.	136.	.0476	1882.	11.63
-.646	252.	94811.	8.	128.	137.	.0483	1909.	11.59
-.546	229.	91123.	14.	115.	123.	.0464	1878.	11.58
-.447	194.	82636.	27.	97.	104.	.0419	1804.	11.52
-.347	486.	76307.	86.	75.	82.	.0387	1723.	11.20
-.247	1795.	71075.	478.	37.	50.	.0369	1655.	11.12
-.149	4386.	64708.	2040.	11.	22.	.0358	1588.	10.92
-.050	5387.	60094.	3785.	8.	17.	.0349	1537.	10.86
.048	5553.	59867.	4066.	8.	16.	.0350	1537.	10.85
.150	4261.	66673.	1825.	11.	21.	.0367	1619.	10.83
.249	1084.	75966.	160.	56.	73.	.0389	1735.	11.00
.348	243.	82823.	7.	90	102.	.0420	1815.	11.08
.447	190.	89540.	3.	106.	119.	.0455	1884.	11.31
.545	250.	96000.	4.	123.	136.	.0490	1930.	11.52
.644	275.	96509.	4.	129.	142.	.0493	1922.	11.58
.744	254.	95357.	4.	129.	142.	.0486	1923.	11.57
.842	240.	94397.	4.	126.	137.	.0481	1896.	11.45
.940	210.	74656.	3.	103.	115.	.0377	1724.	11.35
1.043	169.	42120.	10.	76.	84.	.0209	1016.	10.95
AVERAGE	457.	83313.	119.	105.	114.	.0424	1763.	11.12
EI FAR8	10.88	3116.	1.42	4.11	4.47			
EI FAHI	11.33	3247.	1.48	4.28	4.66			

(d) Intermediate afterburning power; TT2, 386 K; PT2, 7.38 N/cm^2; FAHI, 0.0442; H, 0.0022 g H_2O/g dry air

R/R8	COPPM	CO2PPM	HCPPM	NOPPM	NOXPPM	FAR8	TT8,K	PT8,N/CM2
-1.027	194.	58312.	3.	86.	0.	.0292	1340.	10.56
-.929	262.	88168.	3.	116.	0.	.0448	1807.	11.43
-.831	281.	99041.	3.	129.	0.	.0506	1947.	11.34
-.731	316.	102074.	3.	134.	0.	.0523	1989.	11.36
-.634	328.	103676.	3.	135.	0.	.0531	2001.	11.37
-.537	277.	98847.	3.	123.	0.	.0505	1972.	11.38
-.440	202.	90892.	2.	102.	0.	.0462	1892.	11.34
-.342	247.	84988.	5.	85.	0.	.0431	1842.	11.11
-.245	605.	80958.	51.	68.	0.	.0412	1786.	10.82
-.147	1582.	77369.	308.	42.	0.	.0400	1732.	10.60
-.051	2561.	74342.	754.	24.	0.	.0392	1697.	10.65
.047	3515.	73949.	922.	21.	0.	.0396	1677.	10.67
.144	1966.	77904.	439.	35.	0.	.0406	1726.	10.69
.244	604.	84658.	59.	71.	0.	.0432	1831.	10.72
.341	246.	90773.	12.	94.	0.	.0462	1908.	10.82
.440	259.	97781.	7.	113.	0.	.0499	1984.	11.19
.535	311.	102805.	6.	129.	0.	.0527	2020.	11.29
.633	365.	104272.	6.	137.	0.	.0535	2021.	11.50
.730	367.	103800.	5.	137.	0.	.0532	2008.	11.52
.827	353.	103273.	4.	138.	0.	.0529	2018.	11.42
.926	344.	87445.	3.	116.	0.	.0445	1902.	11.38
.974	284.	66967.	3.	92.	0.	.0337	1680.	10.97
AVERAGE	381.	93224.	26.	115.	115.	.0476	1897.	11.23
EI FAR8	8.13	3124.	.27	4.03	4.03			
EI FAHI	8.72	3349.	.29	4.32	4.32			

TABLE B-I. - Concluded.

(e) Maximum afterburning power; TT2, 387 K; PT2, 7.39 N/cm^2; FAHI, 0.0570; H, 0.0109 g H_2O/g dry air

R/R8	COPPM	CO2PPM	HCPPM	NOPPM	NOXPPM	FAR8	TT8,K	PT8,N/CM2
-1.033	767.	63066.	4.	82.	101.	.0319	1431.	9.93
-.986	983.	89309.	4.	105.	127.	.0458	1838.	10.40
-.891	25861.	107689.	5.	121.	131.	.0703	2122.	10.84
-.799	26483.	105788.	5.	118.	118.	.0696	2147.	11.10
-.704	17737.	111382.	4.	133.	133.	.0675	2173.	11.00
-.612	9119.	115578.	4.	150.	153.	.0647	2144.	11.15
-.519	1447.	114689.	4.	140.	154.	.0597	2186.	11.03
-.423	489.	103112.	3.	119.	139.	.0529	2098.	11.22
-.331	380.	99950.	3.	112.	130.	.0512	2053.	11.10
-.236	496.	105549.	3.	127.	147.	.0542	2119.	11.22
-.145	563.	107342.	4.	133.	154.	.0552	2147.	11.23
-.048	411.	97661.	3.	112.	132.	.0499	2059.	11.00
.043	274.	89724.	3.	92.	111.	.0456	1955.	11.02
.137	265.	88420.	3.	86.	104.	.0449	1953.	11.03
.230	417.	96726.	3.	97.	118.	.0494	2043.	10.84
.326	980.	111260.	4.	126.	146.	.0576	2145.	10.84
.420	10291.	114471.	4.	149.	161.	.0648	2235.	10.98
.512	24340.	108023.	5.	121.	121.	.0695	2174.	11.21
.606	26478.	105956.	8.	117.	117.	.0697	2171.	11.05
.698	24667.	108207.	5.	123.	123.	.0698	2153.	10.96
.794	15369.	112614.	3.	138.	138.	.0667	2160.	10.97
.887	2221.	114685.	3.	144.	158.	.0602	2210.	10.89
.979	695.	71029.	3.	91.	110.	.0360	1767.	10.84
1.026	518.	47689.	7.	75.	91.	.0239	1347.	9.86
AVERAGE	11371.	102625.	4.	122.	132.	.0589	2068.	10.84
EI FAR8	199.19	2825.	.04	3.50	3.79			
EI FAHI	203.87	2891.	.04	3.59	3.88			

TABLE B-II. - ENGINE INLET TEST CONDITIONS AND EXHAUST PROFILE DATA FOR CONDITION 2 (MACH 2.0, 17.9 km), ENGINE B

(a) Military (nonafterburning) power; TT2, 387 K; PT2, 5.57 N/cm^2; FAHI, 0.0164; H, 0.0028 g H_2O/g dry air

R/R8	COPPM	CO2PPM	HCPPM	NOPPM	NOXPPM	FAR8	TT8,K	PT8,N/CM2
-1.020	29.	30230.	7.	71.	73.	.0149	958.	8.10
-.960	33.	31950.	6.	76.	78.	.0157	961.	8.63
-.779	37.	33575.	6.	81.	82.	.0166	981.	8.87
-.593	34.	33030.	6.	79.	82.	.0163	985.	8.93
-.413	33.	30878.	5.	75.	78.	.0152	965.	8.94
-.231	29.	28374.	6.	69.	73.	.0140	940.	8.69
-.051	27.	26379.	6.	64.	68.	.0130	928.	8.69
.132	41.	26363.	5.	64.	67.	.0130	929.	8.69
.314	37.	28166.	5.	67.	70.	.0139	942.	8.68
.496	31.	30889.	5.	73.	77.	.0152	967.	8.77
.674	33.	33399.	5.	78.	84.	.0165	985.	8.85
.858	40.	33810.	5.	78.	83.	.0167	982.	8.99
.983	41.	32324.	5.	74.	78.	.0159	957.	8.71
AVERAGE	35.	31934.	6.	76.	79.	.0157	969.	8.77
EI FAR8	2.17	3134.	.17	7.77	8.11			
EI FAHI	2.08	3003.	.17	7.44	7.77			

TABLE B-II. - Continued.

(b) Minimum afterburning power; TT2, 386 K; PT2, 5.52 N/cm^2; FAHI, 0.0346; H, 0.0028 g H_2O/g dry air

R/R8	COPPM	CO2PPM	HCPPM	NOPPM	NOXPPM	FAR8	TT8,K	PT8,N/CM2
-1.035	399.	42323.	21.	58.	68.	.0212	1231.	7.71
-.984	312.	53830.	23.	69.	80.	.0270	1352.	8.21
-.880	202.	64192.	26.	79.	88.	.0322	1496.	8.51
-.776	225.	69048.	32.	82.	90.	.0348	1577.	8.54
-.674	268.	72100.	45.	81.	91.	.0364	1611.	8.52
-.570	349.	70553.	66.	76.	86.	.0356	1593.	8.49
-.465	1056.	61817.	202.	54.	73.	.0316	1516.	8.40
-.360	3427.	52731.	1315.	18.	52.	.0287	1409.	8.35
-.259	5493.	41984.	4787.	7.	37.	.0261	1286.	8.25
-.155	4871.	34682.	5936.	7.	32.	.0227	1195.	8.17
-.050	3337.	30031.	6108.	7.	30.	.0196	1130.	8.17
.053	3163.	31236.	6119.	7.	31.	.0201	1126.	8.23
.156	4170.	36758.	5280.	8.	34.	.0230	1234.	8.29
.261	3764.	49478.	2109.	13.	48.	.0276	1403.	8.28
.365	1181.	64740.	137.	51.	74.	.0331	1559.	8.17
.468	431.	77919.	9.	78.	92.	.0395	1693.	8.37
.572	453.	84127.	7.	89.	104.	.0428	1748.	8.42
.676	419.	83415.	7.	90.	104.	.0424	1725.	8.35
.778	318.	78603.	7.	85.	100.	.0398	1678.	8.42
.886	239.	70630.	7.	79.	90.	.0356	1624.	8.35
.986	205.	48950.	7.	59.	69.	.0244	1427.	8.26
1.038	182.	36413.	8.	50.	56.	.0181	1269.	7.70
AVERAGE	883.	63989.	524.	66.	81.	.0328	1525.	8.29
EI FAR8	26.97	3070.	8.02	3.33	4.05			
EI FAHI	25.54	2908.	7.60	3.15	3.83			

(c) Intermediate afterburning power; TT2, 385 K; PT2, 5.52 N/cm^2; FAHI, 0.0410: H, 0.0028 g H_2O/g dry air

R/R8	COPPM	CO2PPM	HCPPM	NOPPM	NOXPPM	FAR8	TT8,K	PT8,N/CM2
-1.051	211.	39340.	17.	52.	58.	.0195	1234.	7.38
-.952	253.	66000.	15.	76.	84.	.0332	1580.	8.44
-.851	342.	78035.	15.	86.	94.	.0395	1705.	8.51
-.750	469.	83512.	15.	89.	98.	.0425	1773.	8.31
-.648	529.	88172.	14.	93.	103.	.0450	1820.	8.38
-.551	468.	84103.	14.	85.	97.	.0428	1783.	8.41
-.450	418.	75935.	16.	73.	85.	.0385	1692.	8.44
-.350	856.	69069.	69.	54.	69.	.0351	1627.	8.17
-.248	3112.	62505.	864.	21.	47.	.0334	1560.	8.13
-.150	5430.	52786.	3528.	8.	36.	.0310	1473.	8.09
-.051	6207.	42860.	5620.	7.	29.	.0274	1350.	8.06
.049	6220.	39246.	5995.	6.	29.	.0257	1299.	8.05
.150	6054.	46386.	5095.	7.	34.	.0288	1417.	8.04
.251	3328.	62049.	1301.	18.	50.	.0335	1580.	8.08
.350	950.	75912.	159.	61.	74.	.0388	1730.	8.17
.451	656.	88445.	70.	86.	95.	.0452	1862.	8.25
.550	829.	99271.	50.	107.	115.	.0511	1940.	8.20
.650	807.	100290.	37.	110.	118.	.0516	1940.	8.31
.751	681.	96605.	31.	105.	114.	.0495	1892.	8.33
.852	557.	89858.	26.	95.	103.	.0459	1857.	8.41
.948	441.	72255.	23.	79.	88.	.0365	1699.	8.39
1.050	258.	42259.	22.	56.	63.	.0210	1288.	8.07
AVERAGE	852.	76598.	267.	78.	88.	.0392	1701.	8.22
EI FAR8	21.88	3093.	3.44	3.28	3.73			
EI FAHI	20.91	2955.	3.28	3.13	3.56			

TABLE B-II. - Concluded.

(d) Intermediate afterburning power; TT2, 385 K; PT2, 5.54 N/cm^2; FAHI, 0.0443; H, 0.0028 g H_2O/g dry air

R/R8	COPPM	CO2PPM	HCPPM	NOPPM	NOXPPM	FAR8	TT8,K	PT8,N/CM2
-.969	337.	64471.	19.	72.	81.	.0324	1589.	7.89
-.822	507.	84818.	23.	89.	98.	.0432	1847.	8.18
-.630	711.	94265.	34.	98.	105.	.0483	1958.	8.26
-.484	526.	83103.	51.	79.	89.	.0423	1860.	8.34
-.339	786.	73510.	102.	56.	68.	.0374	1752.	8.01
-.243	2439.	67296.	683.	26.	53.	.0354	1699.	7.97
-.147	5247.	58329.	2862.	8.	39.	.0334	1603.	7.89
-.049	6875.	49089.	5064.	6.	33.	.0307	1492.	7.76
.045	7107.	47131.	5475.	7.	28.	.0300	1438.	7.89
.142	5982.	56115.	3628.	8.	38.	.0331	1559.	8.00
.240	2390.	71615.	466.	33.	57.	.0375	1729.	7.91
.337	765.	85561.	22.	74.	85.	.0437	1875.	7.98
.432	857.	98039.	14.	98.	105.	.0504	1997.	8.14
.531	1192.	106330.	15.	115.	122.	.0551	2080.	8.18
.627	1193.	105820.	16.	115.	123.	.0548	2056.	8.21
.723	987.	102180.	16.	110.	118.	.0527	2015.	8.29
.819	793.	96318.	16.	102.	109.	.0494	1987.	8.19
.917	679.	78522.	16.	82.	92.	.0399	1876.	8.13
1.014	326.	40661.	17.	51.	57.	.0203	1449.	8.10
AVERAGE	1011.	84168.	209.	83.	93.	.0432	1857.	8.09
EI FAR8	23.64	3093.	2.44	3.19	3.58			
EI FAHI	23.04	3015.	2.38	3.11	3.49			

(e) Maximum afterburning power; TT2, 384 K; PT2, 5.52 N/cm^2; FAHI, 0.0572; H, 0.0028 g H_2O/g dry air

R/R8	COPPM	CO2PPM	HCPPM	NOPPM	NOXPPM	FAR8	TT8,K	PT8,N/CM2
-1.020	877.	52832.	16.	55.	62.	.0267	1565.	7.03
-.972	1316.	72687.	16.	71.	81.	.0372	1894.	7.33
-.880	4340.	106160.	16.	108.	109.	.0568	2189.	7.92
-.788	6813.	109340.	15.	113.	113.	.0599	2174.	8.07
-.695	7911.	109230.	14.	114.	114.	.0605	2160.	8.00
-.603	7972.	109370.	15.	114.	115.	.0606	2149.	8.03
-.509	3089.	109320.	14.	110.	113.	.0578	2126.	8.16
-.420	1189.	99377.	12.	96.	105.	.0513	2084.	8.26
-.327	827.	94472.	11.	89.	100.	.0485	2043.	8.15
-.235	909.	97643.	11.	94.	107.	.0502	2085.	8.26
-.142	1006.	100150.	10.	97.	110.	.0516	2098.	8.03
-.051	777.	92940.	10.	85.	97.	.0476	2037.	8.05
.042	629.	88420.	10.	77.	90.	.0451	1990.	8.01
.135	852.	95237.	10.	84.	98.	.0489	2096.	7.98
.228	1345.	103780.	10.	99.	111.	.0538	2174.	8.03
.322	3218.	110390.	10.	111.	117.	.0584	2181.	7.96
.412	10279.	110040.	10.	121.	122.	.0623	2190.	8.00
.504	18589.	107440.	10.	102.	102.	.0658	2188.	8.04
.596	21564.	105790.	10.	97.	97.	.0666	2178.	8.10
.689	16684.	108510.	9.	108.	108.	.0652	2145.	8.13
.778	7964.	110930.	9.	116.	116.	.0615	2189.	7.97
.872	3027.	107340.	10.	108.	113.	.0567	2171.	7.90
.966	1445.	72255.	9.	75.	86.	.0371	1849.	7.99
AVERAGE	6751.	101554.	12.	102.	106.	.0557	2110.	7.93
EI FAR8	124.46	2942.	.11	3.09	3.21			
EI FAHI	120.72	2853.	.11	3.00	3.12			

TABLE B-III. - ENGINE INLET TEST CONDITIONS AND EXHAUST PROFILE DATA FOR CONDITION 3 (MACH 2.0, 19.8 km), ENGINE B

(a) Military (nonafterburning) power; TT2, 388 K; PT2, 4.16 N/cm^2; FAHI, 0.0166; H, 0.0034 g H_2O/g dry air

R/R8	COPPM	CO2PPM	HCPPM	NOPPM	NOXPPM	FAR8	TT8,K	PT8,N/CM2
-1.016	48.	34704.	3.	79.	83.	.0171	948.	6.21
-.957	45.	35357.	3.	80.	84.	.0175	951.	6.33
-.776	55.	36236.	3.	84.	87.	.0179	974.	6.49
-.595	53.	35737.	3.	83.	87.	.0176	977.	6.51
-.413	42.	33127.	3.	77.	83.	.0163	959.	6.57
-.232	45.	30168.	3.	71.	76.	.0149	933.	6.33
-.049	40.	28853.	3.	67.	73.	.0142	922.	6.40
.131	44.	29262.	3.	69.	74.	.0144	931.	6.38
.316	52.	31222.	3.	74.	80.	.0154	951.	6.31
.493	48.	33581.	3.	79.	84.	.0166	967.	6.38
.674	53.	35847.	3.	83.	88.	.0177	977.	6.35
.859	44.	36222.	3.	82.	88.	.0179	976.	6.53
.947	49.	35608.	3.	81.	86.	.0176	962.	6.48
AVERAGE	49.	34632.	3.	80.	85.	.0171	964.	6.43
EI FAR8	2.81	3133.	.09	7.57	8.01			
EI FAHI	2.90	3232.	.10	7.81	8.26			

(b) Minimum afterburning power; TT2, 386 K; PT2, 4.17 N/cm^2; FAHI, 0.0360; H, 0.0034 g H_2O/g dry air

R/R8	COPPM	CO2PPM	HCPPM	NOPPM	NOXPPM	FAR8	TT8,K	PT8,N/CM2
-.969	447.	65921.	3.	71.	81.	.0332	1442.	6.18
-.867	539.	79102.	3.	80.	90.	.0402	1615.	6.23
-.766	697.	83669.	3.	83.	93.	.0427	1662.	6.30
-.664	832.	85513.	4.	82.	93.	.0437	1680.	6.11
-.561	813.	83776.	6.	78.	88.	.0428	1665.	6.08
-.459	1178.	75248.	59.	61.	75.	.0385	1602.	6.28
-.357	4556.	61101.	1185.	12.	27.	.0336	1479.	6.15
-.254	7371.	48890.	5659.	6.	6.	.0311	1370.	6.01
-.150	6854.	39360.	8594.	7.	7.	.0275	1241.	6.11
-.049	5195.	34042.	9191.	7.	7.	.0242	1182.	5.98
.050	6569.	37718.	9341.	7.	7.	.0269	1219.	5.99
.157	7301.	51856.	6556.	7.	7.	.0331	1398.	5.99
.256	3924.	65682.	2643.	18.	29.	.0364	1525.	5.93
.359	980.	75668.	1378.	58.	65.	.0394	1614.	5.99
.461	765.	83833.	908.	73.	77.	.0433	1705.	6.14
.564	941.	89114.	676.	82.	87.	.0461	1744.	6.09
.664	817.	86999.	453.	84.	89.	.0447	1707.	6.20
.767	637.	83684.	307.	83.	88.	.0428	1650.	6.03
.870	480.	80363.	178.	80.	87.	.0409	1629.	6.04
.972	389.	61935.	69.	66.	77.	.0312	1441.	6.25
AVERAGE	1447.	76366.	904.	67.	75.	.0397	1598.	6.13
EI FAR8	36.71	3044.	11.48	2.80	3.14			
EI FAHI	40.26	3339.	12.59	3.07	3.44			

TABLE B-III. - Continued.

(c) Intermediate afterburning power; TT2, 387 K; PT2, 4.16 N/cm^2; FAHI, 0.0461; H, 0.0034 g H_2O/g dry air

R/R8	COPPM	CO2PPM	HCPPM	NOPPM	NOXPPM	FAR8	TT8,K	PT8,N/CM2
-1.024	773.	62178.	256.	63.	73.	.0316	1416.	5.73
-.927	1449.	89954.	224.	85.	95.	.0465	1823.	6.07
-.828	2031.	97667.	186.	92.	100.	.0510	1922.	6.14
-.732	2364.	101244.	182.	95.	104.	.0531	1939.	6.00
-.634	2230.	101674.	241.	96.	105.	.0533	1936.	6.09
-.537	2030.	100340.	242.	92.	102.	.0524	1939.	6.00
-.438	1704.	94408.	229.	79.	91.	.0491	1899.	5.95
-.342	2160.	83334.	282.	50.	66.	.0434	1776.	5.84
-.246	5056.	73652.	1135.	14.	35.	.0404	1674.	5.89
-.149	8141.	66614.	3664.	6.	9.	.0398	1601.	5.80
-.050	10496.	56064.	7042.	6.	6.	.0373	1538.	5.64
.048	9713.	59253.	6472.	6.	6.	.0383	1542.	5.68
.147	6984.	72002.	3100.	8.	23.	.0417	1675.	5.72
.240	2877.	85253.	1095.	40.	64.	.0453	1791.	5.79
.341	1558.	91975.	727.	67.	85.	.0480	1866.	5.70
.435	1914.	99773.	591.	88.	101.	.0523	1949.	6.04
.536	2594.	105602.	407.	102.	114.	.0557	1999.	6.19
.631	2467.	103995.	309.	101.	113.	.0547	1963.	6.06
.730	1916.	100271.	286.	98.	111.	.0524	1914.	6.00
.827	1922.	100568.	220.	99.	112.	.0525	1936.	6.19
.923	1769.	94557.	216.	90.	103.	.0492	1895.	6.05
1.022	862.	56443.	172.	64.	79.	.0287	1401.	6.00
AVERAGE	2208.	92034.	466.	82.	94.	.0482	1844.	5.98
EI FAR8	46.55	3049.	4.92	2.83	3.25			
EI FAHI	48.41	3171.	5.11	2.94	3.38			

(d) Intermediate afterburning power; TT2, 386 K; PT2, 4.16 N/cm^2; FAHI, 0.0520; H, 0.0034 g H_2O/g dry air

R/R8	COPPM	CO2PPM	HCPPM	NOPPM	NOXPPM	FAR8	TT8,K	PT8,N/CM2
-1.046	809.	51800.	159.	58.	71.	.0263	1208.	5.36
-.997	1276.	73741.	151.	68.	83.	.0378	1613.	5.83
-.903	2702.	103573.	125.	95.	105.	.0545	2021.	6.10
-.808	3386.	109083.	123.	100.	109.	.0579	2070.	6.03
-.713	3962.	111603.	94.	103.	112.	.0596	2061.	6.03
-.618	4841.	114358.	81.	107.	115.	.0616	2079.	5.91
-.525	4512.	113224.	74.	104.	111.	.0608	2080.	5.95
-.429	2471.	104607.	64.	87.	99.	.0549	2032.	5.88
-.335	2029.	95896.	76.	68.	83.	.0499	1943.	5.93
-.241	3008.	90130.	218.	44.	64.	.0475	1878.	5.69
-.145	5403.	84834.	934.	18.	41.	.0464	1795.	5.58
-.050	8625.	77091.	2976.	8.	14.	.0452	1724.	5.61
.046	9655.	76109.	3773.	8.	9.	.0457	1685.	5.57
.140	5850.	83660.	1287.	18.	39.	.0462	1809.	5.53
.236	2913.	94416.	315.	52.	73.	.0498	1926.	5.71
.329	2495.	101543.	165.	75.	91.	.0533	2018.	5.72
.423	3097.	108485.	127.	95.	106.	.0574	2068.	5.74
.519	3986.	113688.	137.	110.	120.	.0607	2105.	6.01
.614	4184.	113727.	118.	113.	124.	.0609	2088.	6.00
.754	3497.	110804.	70.	106.	117.	.0588	2052.	6.00
.898	3380.	108494.	97.	101.	113.	.0575	2066.	6.03
AVERAGE	3346.	102758.	178.	90.	102.	.0545	1977.	5.93
EI FAR8	62.86	3034.	1.68	2.79	3.15			
EI FAHI	65.42	3157.	1.75	2.90	3.28			

TABLE B-III. - Concluded.

(e) Maximum afterburning power; TT2, 389 K; PT2, 4.11 N/cm^2; FAHI, 0.0570; H, 0.0023 g H_2O/g dry air

R/RP	COPPM	CO2PPM	HCPPM	NOPPM	NOXPPM	FAR8	TT8,K	PT8,N/CM2
-1.031	974.	48962.	21.	66.	80.	.0248	1428.	5.38
-.982	3291.	93609.	5.	85.	98.	.0494	1881.	5.64
-.887	15657.	110373.	6.	113.	121.	.0657	2116.	5.81
-.796	23624.	106735.	7.	107.	114.	.0684	2110.	5.78
-.701	25621.	105954.	6.	105.	107.	.0691	2117.	5.81
-.609	24750.	106342.	6.	105.	107.	.0688	2116.	5.95
-.518	10382.	112159.	4.	107.	110.	.0636	2110.	5.94
-.422	3682.	107464.	4.	92.	99.	.0571	2092.	5.84
-.331	2620.	100133.	4.	83.	94.	.0525	2031.	5.92
-.237	2356.	98662.	4.	79.	93.	.0516	2001.	5.85
-.145	2166.	96416.	3.	77.	91.	.0503	1982.	5.79
-.051	1625.	88954.	3.	69.	84.	.0460	1889.	5.73
.045	1350.	81813.	5.	61.	75.	.0420	1804.	5.76
.136	1597.	84173.	4.	60.	76.	.0434	1844.	5.79
.231	2705.	96647.	3.	73.	87.	.0507	1980.	5.69
.325	5372.	110134.	3.	91.	100.	.0595	2092.	5.69
.415	26045.	105469.	4.	98.	106.	.0691	2128.	5.76
.510	27178.	95128.	13.	86.	110.	.0640	2122.	5.85
.603	27209.	94083.	32.	86.	110.	.0635	2107.	5.91
.697	27074.	98571.	29.	87.	109.	.0659	2096.	5.86
.789	26746.	105601.	5.	97.	108.	.0696	2103.	5.79
.882	5967.	111733.	3.	102.	110.	.0607	2126.	5.89
.929	3336.	97459.	3.	84.	100.	.0515	2017.	5.94
.978	1966.	72184.	3.	64.	82.	.0373	1720.	5.71
AVERAGE	15278.	100817.	9.	93.	105.	.0602	2048.	5.81
EI FAR8	262.78	2725.	.07	2.63	2.96			
EI FAHI	273.92	2840.	.08	2.74	3.08			

TABLE B-IV. - ENGINE INLET TEST CONDITIONS AND EXHAUST PROFILE DATA FOR CONDITION 4 (MACH 2.4, 19.8 km), ENGINE B

(a) Military (nonafterburning) power; TT2, 462 K; PT2, 7.45 N/cm^2; FAHI, 0.0142; H, 0.0014 g H_2O/g dry air

R/RP	COPPM	CO2PPM	HCPPM	NOPPM	NOXPPM	FAR8	TT8,K	PT8,N/CM2
-1.010	24.	30047.	4.	100.	0.	.0148	952.	9.15
-.949	33.	31560.	3.	104.	0.	.0155	968.	9.45
-.770	24.	32931.	3.	111.	0.	.0162	995.	9.78
-.591	26.	32676.	2.	109.	0.	.0161	1001.	9.71
-.411	27.	30757.	2.	104.	0.	.0151	996.	9.64
-.230	27.	28391.	2.	94.	0.	.0140	970.	9.59
-.050	26.	27014.	2.	90.	0.	.0133	963.	9.37
.129	22.	27314.	2.	89.	0.	.0134	965.	9.40
.310	26.	29055.	2.	95.	0.	.0143	981.	9.46
.489	30.	30979.	2.	101.	0.	.0153	989.	9.56
.670	29.	32642.	2.	105.	0.	.0161	1003.	9.70
.850	19.	33245.	2.	105.	0.	.0164	992.	9.86
.970	21.	31887.	2.	98.	0.	.0157	967.	9.63
AVERAGE	26.	31646.	2.	104.	104.	.0156	987.	9.64
EI FAR8	1.64	3135.	.07	10.75	10.75			
EI FAHI	1.79	3429.	.08	11.76	11.76			

TABLE B-IV. - Continued.

(b) Minimum afterburning power; TT2, 463 K; PT2, 7.43 N/cm^2; FAHI, 0.0318; H, 0.0014 g H_2O/g dry air

R/R8	COPPM	CO2PPM	HCPPM	NOPPM	NOXPPM	FAR8	TT8,K	PT8,N/CM2
-.969	421.	53277.	4.	85.	0.	.0267	1349.	8.92
-.868	145.	65147.	5.	98.	0.	.0327	1520.	9.47
-.766	181.	76999.	10.	109.	0.	.0389	1682.	9.22
-.765	146.	69193.	10.	108.	0.	.0348	1576.	9.30
-.664	136.	69994.	3.	106.	0.	.0352	1590.	9.44
-.664	137.	70092.	3.	106.	0.	.0352	1590.	9.39
-.561	224.	67534.	5.	101.	0.	.0340	1567.	9.25
-.460	964.	61208.	54.	81.	0.	.0311	1508.	9.37
-.356	2100.	60736.	293.	65.	0.	.0316	1516.	9.23
-.152	6243.	43596.	7447.	9.	0.	.0288	1345.	9.09
-.050	6396.	39146.	9855.	6.	0.	.0278	1290.	9.00
.052	4920.	35328.	10479.	6.	0.	.0254	1234.	9.04
.155	5430.	44203.	6026.	6.	0.	.0279	1361.	9.08
.257	3042.	59240.	826.	29.	0.	.0316	1534.	9.07
.359	614.	72814.	30.	84.	0.	.0369	1686.	9.14
.461	304.	83541.	3.	104.	0.	.0424	1805.	9.26
.563	350.	88323.	2.	116.	0.	.0449	1842.	9.14
.665	335.	86472.	2.	116.	0.	.0439	1801.	9.14
.767	282.	83277.	2.	111.	0.	.0422	1746.	9.15
.869	215.	76220.	2.	100.	0.	.0385	1690.	9.25
.973	253.	51492.	2.	77.	0.	.0257	1424.	9.12
1.022	251.	40727.	3.	72.	0.	.0203	1250.	8.39
AVERAGE	808.	68182.	507.	90.	90.	.0349	1588.	9.14
EI FAR8	23.21	3078.	7.30	4.24	4.24			
EI FAHI	25.32	3358.	7.96	4.63	4.63			

(c) Intermediate afterburning power; TT2, 463 K; PT2, 7.50 N/cm^2; FAHI, 0.0375; H, 0.0030 g H_2O/g dry air

R/R8	COPPM	CO2PPM	HCPPM	NOPPM	NOXPPM	FAR8	TT8,K	PT8,N/CM2
-1.039	290.	42861.	9.	69.	69.	.0214	1165.	8.27
-.940	233.	68472.	10.	89.	102.	.0345	1581.	9.13
-.840	298.	80026.	9.	105.	118.	.0405	1769.	9.35
-.740	399.	86403.	9.	111.	125.	.0439	1867.	9.23
-.642	444.	90225.	9.	118.	136.	.0460	1913.	9.17
-.544	386.	87473.	8.	110.	126.	.0445	1891.	9.27
-.444	288.	80474.	8.	95.	110.	.0408	1809.	9.22
-.346	439.	74648.	13.	81.	96.	.0378	1735.	9.12
-.247	1482.	69960.	167.	57.	84.	.0360	1676.	8.84
-.147	3528.	64718.	1018.	24.	63.	.0348	1608.	8.73
-.049	5617.	58966.	2955.	12.	43.	.0340	1554.	8.78
.049	6708.	56328.	4401.	11.	30.	.0340	1513.	8.85
.148	5623.	61097.	2634.	13.	39.	.0349	1572.	8.92
.247	2410.	70991.	393.	47.	77.	.0372	1695.	8.85
.345	520.	79250.	46.	85.	102.	.0403	1794.	8.93
.445	405.	87678.	22.	104.	121.	.0446	1887.	9.26
.543	479.	92403.	18.	117.	135.	.0472	1946.	9.32
.641	505.	93096.	16.	121.	137.	.0476	1928.	9.33
.740	483.	91607.	15.	120.	136.	.0468	1913.	9.35
.840	455.	90657.	14.	116.	133.	.0462	1910.	9.31
.938	405.	68509.	13.	87.	104.	.0346	1725.	9.29
1.035	295.	39966.	16.	65.	80.	.0199	1143.	8.69
AVERAGE	633.	77683.	113.	96.	112.	.0395	1744.	9.04
EI FAR8	16.13	3108.	1.45	4.00	4.66			
EI FAHI	16.95	3266.	1.52	4.20	4.90			

TABLE B-IV. - Concluded.

(d) Intermediate afterburning power; TT2, 463 K; PT2, 7.48 N/cm^2; FAHI, 0.0409; H, 0.0030 g H_2O/g dry air

R/R8	COPPM	CO2PPM	HCPPM	NOPPM	NOXPPM	FAR8	TT8,K	PT8,N/CM2
-1.019	306.	51293.	19.	78.	89.	.0257	1301.	8.35
-.923	355.	77121.	16.	105.	117.	.0390	1719.	9.14
-.824	436.	87152.	14.	122.	136.	.0444	1888.	9.24
-.730	540.	93035.	14.	130.	143.	.0475	1965.	9.34
-.437	347.	83702.	13.	104.	114.	.0425	1856.	9.15
-.339	418.	79124.	15.	91.	100.	.0401	1788.	8.95
-.245	651.	80238.	36.	81.	95.	.0408	1811.	8.81
-.147	1458.	76843.	167.	61.	85.	.0396	1758.	8.72
-.050	2522.	74141.	393.	45.	74.	.0389	1728.	8.73
.047	2933.	72563.	606.	37.	68.	.0384	1702.	8.76
.144	2332.	75364.	302.	49.	78.	.0393	1742.	8.79
.242	904.	81020.	50.	80.	97.	.0414	1823.	8.84
.338	442.	88152.	17.	103.	116.	.0449	1904.	8.90
.436	490.	95739.	14.	123.	139.	.0490	1995.	9.13
.531	564.	101201.	14.	140.	155.	.0519	2041.	9.15
.628	671.	101270.	15.	141.	158.	.0520	2023.	9.41
.726	662.	100283.	16.	139.	153.	.0515	2006.	9.04
.821	658.	100155.	17.	136.	149.	.0514	2016.	9.01
.919	602.	83320.	18.	109.	124.	.0424	1894.	8.98
1.017	356.	45005.	21.	75.	83.	.0225	1396.	8.67
AVERAGE	567.	85276.	28.	112.	126.	.0435	1853.	8.99
EI FAR8	13.19	3116.	.32	4.29	4.81			
EI FAHI	13.97	3300.	.34	4.55	5.09			

(e) Maximum afterburning power; TT2, 462 K; PT2, 7.44 N/cm^2; FAHI, 0.0526; H, 0.0030 g H_2O/g dry air

R/R8	COPPM	CO2PPM	HCPPM	NOPPM	NOXPPM	FAR8	TT8,K	PT8,N/CM2
-1.018	809.	60081.	34.	81.	93.	.0304	1445.	8.18
-.971	979.	79028.	34.	99.	113.	.0404	1776.	8.44
-.880	1292.	107967.	30.	141.	148.	.0560	2114.	8.87
-.788	1289.	111384.	26.	150.	159.	.0579	2150.	9.08
-.696	1467.	113663.	21.	155.	164.	.0592	2165.	9.07
-.512	1414.	113333.	18.	159.	172.	.0590	2162.	9.07
-.420	1078.	110292.	19.	146.	157.	.0571	2155.	8.82
-.327	957.	105459.	20.	126.	140.	.0545	2142.	8.59
-.232	899.	102906.	20.	114.	128.	.0530	2119.	8.35
-.142	938.	100930.	21.	105.	119.	.0520	2092.	8.12
-.050	951.	100045.	24.	99.	115.	.0515	2090.	8.22
.042	1005.	100305.	25.	99.	116.	.0517	2106.	8.16
.134	1065.	104357.	25.	113.	127.	.0539	2144.	8.11
.228	1182.	109320.	22.	134.	151.	.0567	2202.	8.37
.320	1477.	113997.	21.	156.	170.	.0594	2228.	8.62
.411	2148.	116707.	16.	172.	182.	.0613	2227.	8.67
.503	3259.	116894.	13.	182.	198.	.0620	2212.	9.01
.596	4635.	119754.	8.	164.	173.	.0644	2206.	9.17
.688	3890.	119943.	8.	162.	166.	.0640	2182.	8.92
.778	4004.	120289.	10.	178.	178.	.0643	2186.	8.86
.872	2060.	116230.	10.	172.	172.	.0609	2183.	8.77
AVERAGE	2011.	109266.	20.	148.	158.	.0571	2118.	8.82
EI FAR8	36.09	3080.	.18	4.38	4.66			
EI FAHI	38.90	3321.	.19	4.72	5.02			

TABLE B-V. - ENGINE INLET TEST CONDITIONS AND EXHAUST PROFILE DATA FOR

CONDITION 5 (MACH 2.8, 19.8 km), ENGINE B

(a) Military (nonafterburning) power; TT2, 557 K; PT2, 13.30 N/cm^2; FAHI, 0.0121; H, 0.0036 g H_2O/g dry air

R/R8	COPPM	CO2PPM	HCPPM	NOPPM	NOXPPM	FAR8	TT8,K	PT8,N/CM2
-.997	20.	24761.	5.	133.	134.	.0122	959.	12.93
-.936	19.	26592.	4.	145.	145.	.0131	982.	13.52
-.761	31.	28627.	4.	159.	159.	.0141	1011.	13.88
-.582	33.	28865.	4.	164.	164.	.0142	1021.	13.87
-.403	29.	27620.	4.	158.	158.	.0136	1022.	13.76
-.227	33.	25618.	4.	146.	146.	.0126	1007.	13.64
-.050	30.	24230.	4.	137.	137.	.0119	996.	13.55
.128	33.	24548.	4.	137.	137.	.0121	999.	13.56
.305	30.	25935.	4.	141.	141.	.0127	1006.	13.56
.482	33.	27402.	4.	146.	146.	.0135	1009.	13.64
.663	32.	28578.	3.	148.	148.	.0141	1014.	13.85
.839	38.	28787.	3.	146.	146.	.0142	1007.	13.58
.957	41.	27129.	3.	136.	136.	.0133	974.	13.53
AVERAGE	31.	27619.	4.	149.	149.	.0136	1005.	13.65
EI FAR8	2.26	3134.	.14	17.72	17.73			
EI FAHI	2.53	3510.	.16	19.85	19.85			

(b) Minimum afterburning power; TT2, 555 K; PT2, 13.31 N/cm^2; FAHI, 0.0292; H, 0.0036 g H_2O/g dry air

R/R8	COPPM	CO2PPM	HCPPM	NOPPM	NOXPPM	FAR8	TT8,K	PT8,N/CM2
-1.011	503.	38020.	6.	99.	116.	.0190	1230.	12.01
-.959	332.	49300.	6.	123.	136.	.0246	1380.	12.93
-.858	103.	63457.	7.	156.	168.	.0318	1585.	13.28
-.758	94.	69787.	7.	169.	184.	.0351	1681.	13.43
-.654	97.	74213.	8.	178.	189.	.0374	1745.	13.25
-.556	93.	73561.	9.	175.	188.	.0370	1745.	13.33
-.454	117.	67858.	10.	160.	171.	.0341	1692.	13.22
-.351	359.	60925.	17.	135.	153.	.0306	1603.	13.31
-.251	1286.	55996.	125.	102.	136.	.0286	1529.	12.77
-.151	3061.	51138.	596.	62.	109.	.0273	1473.	12.80
-.053	4072.	47737.	1009.	47.	96.	.0263	1430.	12.75
.050	4120.	47358.	960.	49.	95.	.0261	1408.	12.79
.153	3123.	50379.	390.	74.	108.	.0269	1468.	12.84
.254	1080.	57017.	70.	111.	133.	.0290	1556.	12.86
.352	263.	64091.	7.	135.	146.	.0322	1644.	12.90
.453	97.	71879.	5.	154.	164.	.0362	1741.	13.13
.556	103.	77531.	6.	169.	175.	.0391	1814.	13.08
.658	106.	77705.	6.	174.	180.	.0392	1813.	13.14
.758	97.	75777.	6.	171.	176.	.0382	1764.	13.48
.859	82.	69895.	6.	160.	166.	.0351	1696.	12.96
.959	190.	50063.	5.	118.	127.	.0250	1447.	13.12
1.008	236.	38434.	5.	101.	109.	.0191	1298.	12.25
AVERAGE	344.	64545.	38.	147.	159.	.0325	1625.	13.04
EI FAR8	10.59	3119.	.58	7.42	8.05			
EI FAHI	11.71	3450.	.64	8.21	8.91			

TABLE B-V. - Continued.

(c) Intermediate afterburning power; TT2, 554 K; PT2, 13.37 N/cm^2; FAHI, 0.0357; H, 0.0036 g H_2O/g dry air

F/R8	COPPM	CO2PPM	HCPPM	NOPPM	NOXPPM	FAR8	TT8,K	PT8,N/CM2
-1.018	220.	43290.	6.	109.	116.	.0215	1276.	11.67
-.920	132.	69746.	6.	151.	158.	.0351	1672.	13.02
-.821	141.	80893.	6.	179.	188.	.0409	1877.	13.07
-.728	172.	85871.	6.	195.	207.	.0435	1969.	13.16
-.631	179.	89828.	6.	208.	220.	.0456	2024.	13.14
-.533	159.	87695.	6.	198.	203.	.0445	1995.	13.20
-.436	106.	77039.	5.	170.	177.	.0389	1846.	13.10
-.340	124.	71660.	5.	145.	154.	.0361	1772.	12.93
-.243	235.	68689.	6.	123.	141.	.0346	1735.	12.67
-.147	609.	66322.	36.	81.	128.	.0336	1691.	12.40
-.050	1248.	63738.	115.	41.	119.	.0326	1646.	12.35
.047	1576.	63224.	193.	26.	115.	.0326	1630.	12.30
.144	1094.	66433.	105.	49.	128.	.0339	1680.	12.25
.239	334.	71784.	21.	111.	145.	.0362	1779.	12.43
.335	135.	78217.	9.	145.	160.	.0395	1854.	12.66
.432	135.	83993.	8.	169.	185.	.0425	1932.	12.85
.528	158.	89468.	7.	191.	205.	.0454	2002.	13.06
.530	160.	89359.	7.	192.	204.	.0454	1998.	13.16
.626	176.	89849.	6.	200.	212.	.0456	1998.	13.08
.722	169.	88563.	6.	197.	209.	.0450	1960.	13.02
.819	158.	86700.	6.	190.	203.	.0440	1935.	12.94
.917	168.	70340.	5.	151.	168.	.0354	1775.	12.94
1.013	190.	39404.	6.	102.	117.	.0196	1530.	12.42
AVERAGE	196.	76837.	10.	164.	178.	.0388	1831.	12.81
EI FAR8	5.08	3129.	.12	7.00	7.59			
EI FAHI	5.49	3387.	.13	7.58	8.22			

(d) Intermediate afterburning power; TT2, 552 K; PT2, 13.35 N/cm^2; FAHI, 0.0393; H, 0.0036 g H_2O/g dry air

F/R8	COPPM	CO2PPM	HCPPM	NOPPM	NOXPPM	FAR8	TT8,K	PT8,N/CM2
-.999	221.	52731.	7.	119.	127.	.0263	1422.	11.74
-.905	181.	79588.	7.	165.	178.	.0402	1840.	12.95
-.811	193.	88702.	6.	189.	204.	.0450	1993.	13.14
-.716	210.	92409.	6.	203.	218.	.0470	2065.	13.13
-.620	226.	95149.	6.	214.	228.	.0485	2111.	13.15
-.524	188.	92297.	5.	199.	217.	.0470	2062.	13.05
-.429	148.	86163.	5.	174.	193.	.0437	1991.	12.97
-.337	133.	80632.	5.	148.	166.	.0408	1932.	12.86
-.239	152.	77548.	5.	132.	149.	.0391	1898.	12.43
-.146	191.	75274.	5.	121.	139.	.0380	1854.	12.37
-.049	243.	73841.	8.	116.	132.	.0373	1826.	12.18
.043	303.	72867.	10.	115.	131.	.0368	1814.	12.18
.138	274.	75056.	9.	119.	137.	.0379	1843.	12.19
.140	122.	76273.	3.	135.	146.	.0385	1900.	12.25
.234	148.	82268.	3.	150.	160.	.0416	1967.	12.56
.426	178.	90365.	3.	190.	203.	.0459	2061.	12.84
.519	209.	92401.	3.	204.	221.	.0470	2084.	13.15
.615	221.	92850.	3.	213.	228.	.0473	2077.	13.10
.710	217.	92032.	3.	211.	228.	.0468	2041.	13.08
AVERAGE	192.	85407.	5.	180.	194.	.0433	1964.	12.92
EI FAR8	4.49	3131.	.06	6.90	7.45			
EI FAHI	4.92	3433.	.07	7.56	8.17			

TABLE B-V. - Concluded.

(e) Maximum afterburning power; TT2, 555 K; PT2, 13.32 N/cm^2; FAHI, 0.0513; H, 0.0033 g H_2O/g dry air

R/R8	COPPM	CO2PPM	HCPPM	NOPPM	NOXPPM	FAR8	TT8,K	PT8,N/CM2
-1.036	480.	45163.	5.	87.	98.	.0226	1292.	10.60
-.946	483.	86053.	6.	139.	148.	.0438	1955.	11.64
-.857	674.	107936.	6.	181.	194.	.0556	2179.	12.12
-.767	1035.	112839.	6.	194.	207.	.0585	2211.	12.32
-.677	1761.	115722.	5.	206.	217.	.0605	2244.	12.32
-.585	2122.	116694.	4.	214.	221.	.0612	2247.	12.32
-.498	945.	113084.	4.	202.	211.	.0586	2198.	12.43
-.409	549.	108984.	4.	196.	210.	.0561	2206.	12.54
-.317	596.	109798.	3.	196.	213.	.0566	2208.	12.57
-.228	785.	112069.	3.	210.	223.	.0579	2237.	12.46
-.139	612.	109064.	3.	200.	212.	.0562	2196.	12.51
-.048	366.	102007.	3.	184.	195.	.0523	2165.	12.27
.040	274.	97199.	3.	166.	180.	.0496	2129.	12.43
.130	356.	101984.	3.	172.	185.	.0522	2171.	12.56
.219	601.	109230.	3.	186.	202.	.0563	2223.	12.43
.308	1220.	114814.	3.	198.	210.	.0597	2234.	12.44
.398	2251.	117352.	3.	212.	220.	.0617	2250.	12.34
.487	3378.	118259.	3.	220.	220.	.0628	2259.	12.37
.577	4659.	118015.	3.	254.	254.	.0634	2240.	12.39
.668	3971.	117265.	3.	247.	247.	.0626	2232.	12.36
.757	3229.	117992.	3.	238.	247.	.0626	2247.	12.17
.845	2566.	117538.	2.	231.	237.	.0620	2283.	12.20
.934	653.	84434.	3.	154.	168.	.0430	2056.	12.08
.980	623.	59233.	3.	117.	128.	.0299	1760.	11.05
AVERAGE	1695.	105577.	4.	195.	204.	.0549	2140.	12.05
EI FAR8	31.55	3088.	.04	5.96	6.24			
EI FAHI	33.60	3288.	.04	6.34	6.65			

TABLE B-VI. - ENGINE INLET TEST CONDITIONS AND EXHAUST PROFILE DATA FOR CONDITION 6 (MACH 2.8, 22.0 km), ENGINE B

(a) Military (nonafterburning) power: TT2, 560 K; PT2, 9.52 N/cm^2; FAHI, 0.0121; H, 0.0109 g H_2O/g dry air

R/R8	COPPM	CO2PPM	HCPPM	NOPPM	NOXPPM	FAR8	TT8,K	PT8,N/CM2
-.998	18.	26346.	8.	116.	116.	.0129	933.	9.15
-.938	18.	26522.	7.	124.	124.	.0130	956.	9.52
-.762	15.	28493.	6.	137.	137.	.0140	988.	9.73
-.583	12.	28953.	6.	143.	143.	.0142	1009.	9.62
-.404	32.	27660.	6.	139.	139.	.0136	1008.	9.62
-.228	17.	25659.	5.	129.	129.	.0126	994.	9.62
-.052	17.	24306.	5.	120.	120.	.0119	984.	9.35
.127	23.	24651.	5.	120.	120.	.0121	988.	9.37
.305	17.	26239.	5.	125.	125.	.0129	996.	9.42
.485	25.	27638.	5.	131.	131.	.0136	999.	9.70
.662	23.	28318.	5.	130.	130.	.0139	999.	9.99
.842	24.	28754.	5.	127.	128.	.0141	993.	9.81
.958	29.	27122.	5.	118.	121.	.0133	964.	9.82
AVERAGE	21.	27663.	5.	130.	131.	.0136	989.	9.68
EI FAR8	1.49	3135.	.20	15.46	15.49			
EI FAHI	1.66	3501.	.22	17.26	17.30			

TABLE B-VI. - Continued.

(b) Minimum afterburning power; TT2, 555 K; PT2, 9.52 N/cm^2; FAHI, 0.0295; H, 0.0109 g H_2O/g dry air

R/R8	COPPM	CO2PPM	HCPPM	NOPPM	NOXPPM	FAR8	TT8,K	PT8,N/CM2
-1.022	2702.	34645.	212.	54.	91.	.0186	1152.	8.71
-.969	1755.	45027.	41.	87.	112.	.0232	1277.	9.22
-.867	289.	58227.	12.	121.	136.	.0292	1453.	9.50
-.768	150.	64414.	14.	133.	146.	.0323	1546.	9.57
-.665	122.	68095.	17.	139.	154.	.0342	1591.	9.38
-.561	127.	67235.	20.	138.	152.	.0338	1588.	9.34
-.460	254.	62353.	31.	124.	141.	.0313	1544.	9.42
-.357	996.	57109.	113.	99.	123.	.0290	1491.	9.39
-.254	3137.	52080.	720.	49.	90.	.0279	1434.	9.05
-.154	5276.	44804.	3342.	23.	74.	.0267	1343.	9.07
-.052	5908.	35835.	9242.	17.	61.	.0255	1261.	9.13
.051	5155.	31776.	11504.	16.	56.	.0242	1209.	9.13
.152	5487.	37629.	7081.	19.	66.	.0251	1289.	9.13
.255	3464.	52020.	1016.	46.	90.	.0282	1455.	9.15
.360	668.	66581.	36.	109.	132.	.0337	1602.	9.29
.462	210.	77681.	5.	136.	154.	.0392	1729.	9.44
.561	234.	83637.	5.	147.	166.	.0424	1790.	9.45
.665	244.	83046.	5.	149.	165.	.0421	1772.	9.38
.768	217.	80344.	5.	143.	158.	.0406	1730.	9.36
.869	180.	74831.	5.	132.	145.	.0377	1675.	9.29
.973	218.	51205.	5.	99.	110.	.0256	1443.	9.31
1.025	218.	37936.	6.	87.	95.	.0188	1280.	8.75
AVERAGE	823.	63064.	355.	114.	134.	.0322	1540.	9.27
EI FAR8	25.59	3080.	5.53	5.83	6.82			
EI FAHI	27.82	3349.	6.01	6.34	7.42			

(c) Intermediate afterburning power; TT2, 553 K; PT2, 9.43 N/cm^2; FAHI, 0.0351; H, 0.0109 g H_2O/g dry air

R/R8	COPPM	CO2PPM	HCPPM	NOPPM	NOXPPM	FAR8	TT8,K	PT8,N/CM2
-1.036	721.	35909.	14.	95.	101.	.0181	1177.	8.46
-.938	297.	58546.	10.	120.	135.	.0294	1495.	9.41
-.839	207.	70643.	9.	141.	158.	.0356	1656.	9.37
-.739	246.	77791.	9.	152.	170.	.0393	1755.	9.43
-.642	260.	81526.	8.	156.	177.	.0413	1805.	9.47
-.542	223.	79640.	8.	149.	169.	.0403	1786.	9.39
-.444	183.	74690.	7.	135.	154.	.0377	1725.	9.17
-.345	262.	69977.	7.	118.	138.	.0353	1674.	8.92
-.247	660.	67237.	29.	99.	124.	.0341	1639.	8.78
-.150	2097.	62835.	323.	64.	101.	.0327	1589.	8.88
-.051	4870.	54073.	2154.	25.	74.	.0306	1490.	8.93
.047	6775.	46511.	4986.	18.	62.	.0292	1408.	9.02
.147	5764.	50237.	3106.	22.	74.	.0296	1465.	9.11
.246	2263.	63323.	375.	68.	110.	.0331	1621.	9.13
.344	430.	76799.	38.	126.	150.	.0389	1773.	9.13
.443	349.	88261.	23.	154.	178.	.0449	1907.	9.35
.542	409.	94730.	17.	173.	195.	.0484	1980.	9.47
.639	457.	95007.	14.	172.	196.	.0486	1969.	9.49
.737	439.	92512.	13.	167.	191.	.0472	1930.	9.37
.836	435.	89791.	11.	156.	181.	.0458	1912.	8.99
.935	386.	71560.	9.	122.	146.	.0361	1760.	8.83
1.032	268.	38370.	8.	85.	105.	.0191	1316.	8.64
AVERAGE	560.	73378.	109.	133.	154.	.0372	1710.	9.10
EI FAR8	15.10	3109.	1.47	5.89	6.84			
EI FAHI	15.98	3291.	1.55	6.24	7.24			

TABLE B-VI. - Concluded.

(d) Intermediate afterburning power; TT2, 553 K; PT2, 9.48 N/cm^2; FAHI, 0.0351; H, 0.0109 g H_2O/g dry air

R/R8	COPPM	CO2PPM	HCPPM	NOPPM	NOXPPM	FAR8	TT8,K	PT8,N/CM2
-1.059	341.	30247.	8.	72.	90.	.0150	972.	7.15
-1.010	414.	46137.	7.	89.	110.	.0231	1334.	8.47
-.914	234.	69214.	8.	120.	141.	.0348	1672.	9.29
-.819	295.	78945.	8.	138.	159.	.0400	1824.	9.17
-.721	363.	85695.	9.	151.	173.	.0436	1911.	9.29
-.626	374.	89520.	10.	156.	177.	.0456	1942.	9.27
-.531	311.	86169.	11.	148.	170.	.0438	1910.	9.31
-.434	240.	81007.	11.	131.	151.	.0410	1850.	9.13
-.340	258.	77128.	14.	116.	136.	.0390	1802.	9.06
-.243	437.	74911.	24.	102.	123.	.0379	1783.	8.81
-.146	1191.	71532.	139.	81.	112.	.0366	1735.	8.59
-.049	3133.	63943.	785.	46.	90.	.0341	1656.	8.73
.045	5104.	57779.	1951.	25.	76.	.0326	1574.	8.75
.143	4284.	60476.	1203.	34.	82.	.0331	1610.	8.77
.238	1229.	72929.	100.	91.	122.	.0374	1766.	8.75
.333	452.	85251.	7.	134.	159.	.0434	1913.	9.01
.431	501.	96798.	6.	166.	191.	.0495	2042.	9.02
.524	599.	102572.	7.	187.	212.	.0527	2107.	9.13
.621	632.	103775.	8.	187.	209.	.0534	2094.	9.28
.719	586.	100643.	9.	179.	200.	.0516	2058.	9.28
.815	557.	98572.	10.	175.	192.	.0505	2047.	9.13
.909	588.	86007.	9.	149.	163.	.0438	1941.	9.20
1.007	380.	46620.	10.	102.	107.	.0233	1482.	8.92
AVERAGE	538.	80268.	42.	138.	159.	.0408	1825.	9.01
EI FAR8	13.28	3115.	.52	5.59	6.44			
EI FAHI	13.88	3256.	.54	5.84	6.73			

(e) Maximum afterburning power; TT2, 552 K; PT2, 9.50 N/cm^2; FAHI, 0.0516; H, 0.0109 g H_2O/g dry air

R/R8	COPPM	CO2PPM	HCPPM	NOPPM	NOXPPM	FAR8	TT8,K	PT8,N/CM2
-1.055	420.	32854.	8.	77.	85.	.0164	1120.	7.64
-.965	711.	74270.	6.	119.	135.	.0377	1776.	8.48
-.873	828.	100405.	6.	162.	179.	.0517	2117.	8.99
-.781	898.	104879.	6.	171.	191.	.0541	2162.	8.90
-.690	1021.	107456.	6.	177.	197.	.0556	2213.	9.02
-.599	848.	105245.	7.	180.	197.	.0543	2179.	9.02
-.507	587.	97309.	6.	163.	183.	.0499	2104.	9.23
-.413	426.	91041.	5.	150.	171.	.0464	2053.	9.21
-.325	453.	93173.	5.	151.	171.	.0476	2073.	9.21
-.231	611.	100799.	5.	168.	190.	.0517	2146.	9.26
-.141	674.	103046.	5.	171.	193.	.0530	2168.	9.19
-.050	527.	95433.	5.	150.	172.	.0488	2108.	8.96
.043	405.	88992.	4.	133.	153.	.0453	2038.	9.01
.132	536.	95088.	4.	142.	163.	.0486	2113.	9.04
.223	789.	104568.	5.	164.	188.	.0539	2198.	9.00
.317	2314.	115424.	5.	192.	213.	.0606	2277.	9.03
.405	8227.	116289.	5.	206.	219.	.0646	2259.	9.11
.497	12033.	114542.	4.	205.	215.	.0658	2266.	9.12
.590	12248.	114442.	4.	197.	203.	.0659	2266.	9.26
.682	8760.	115666.	4.	192.	201.	.0645	2263.	9.16
.773	8248.	115331.	4.	187.	197.	.0641	2272.	8.93
.864	7550.	115283.	4.	182.	194.	.0636	2266.	8.95
.956	1223.	82745.	4.	122.	144.	.0425	1988.	8.77
1.000	886.	54847.	4.	92.	113.	.0278	1625.	8.13
AVERAGE	3559.	98260.	5.	163.	178.	.0521	2082.	8.85
EI FAR8	69.79	3028.	.05	5.24	5.75			
EI FAHI	70.06	3039.	.05	5.26	5.77			

TABLE B-VII. - ENGINE INLET TEST CONDITIONS AND EXHAUST PROFILE DATA FOR CONDITION 7 (MACH 2.8, 23.5 km), ENGINE B

(a) Military (nonafterburning) power; TT2, 554 K; PT2, 7.50 N/cm^2; FAHI, 0.0125; H, 0.0091 g H_2O/g dry air

R/R8	COPPM	CO2PPM	HCPPM	NOPPM	NOXPPM	FAR8	TT8,K	PT8,N/CM2
-1.009	45.	24635.	6.	104.	104.	.0121	928.	7.40
-.948	47.	26401.	6.	112.	112.	.0130	946.	7.71
-.768	55.	28482.	6.	124.	124.	.0140	977.	7.86
-.587	57.	28861.	6.	128.	128.	.0142	994.	7.78
-.407	56.	27869.	6.	125.	125.	.0137	995.	7.84
-.228	60.	26118.	5.	116.	116.	.0128	985.	7.71
-.051	54.	24764.	5.	109.	109.	.0122	974.	7.59
.129	59.	24846.	5.	107.	107.	.0122	976.	7.56
.309	58.	26533.	5.	112.	112.	.0131	986.	7.49
.489	63.	27850.	5.	117.	117.	.0137	994.	7.66
.669	67.	28559.	5.	117.	117.	.0141	987.	7.65
.847	67.	28553.	5.	113.	113.	.0141	977.	7.68
.967	69.	27151.	5.	106.	106.	.0134	954.	7.81
AVERAGE	59.	27672.	5.	117.	117.	.0136	977.	7.73
EI FAR8	4.24	3130.	.20	13.86	13.86			
EI FAHI	4.62	3413.	.22	15.11	15.11			

(b) Minimum afterburning power; TT2, 553 K; PT2, 7.48 N/cm^2; FAHI, 0.0296; H, 0.0091 g H_2O/g dry air

R/R8	COPPM	CO2PPM	HCPPM	NOPPM	NOXPPM	FAR8	TT8,K	PT8,N/CM2
-1.015	1694.	38116.	25.	70.	88.	.0197	1189.	6.80
-.964	1077.	48968.	8.	87.	103.	.0249	1323.	7.20
-.862	324.	62596.	7.	108.	120.	.0315	1516.	7.37
-.762	339.	70303.	7.	120.	130.	.0355	1608.	7.47
-.661	375.	75819.	8.	127.	139.	.0384	1655.	7.43
-.559	371.	75225.	9.	126.	136.	.0381	1661.	7.37
-.456	377.	69125.	10.	114.	125.	.0349	1623.	7.39
-.355	783.	61760.	23.	97.	113.	.0313	1554.	7.28
-.254	1849.	56057.	104.	75.	97.	.0290	1485.	7.32
-.153	2636.	53323.	229.	60.	86.	.0280	1448.	7.08
-.051	2811.	51049.	256.	59.	82.	.0270	1417.	7.11
.052	2538.	50328.	202.	63.	85.	.0264	1409.	7.18
.152	1362.	53528.	58.	77.	93.	.0274	1452.	7.26
.254	478.	61068.	10.	94.	105.	.0308	1545.	7.18
.355	298.	70608.	6.	109.	119.	.0356	1651.	7.33
.458	402.	81395.	6.	126.	136.	.0413	1766.	7.45
.559	497.	85642.	6.	135.	145.	.0436	1794.	7.46
.660	427.	82661.	6.	132.	139.	.0420	1727.	7.34
.764	333.	77274.	6.	125.	132.	.0391	1651.	7.45
.865	250.	71199.	6.	113.	120.	.0359	1579.	7.39
.965	332.	53523.	6.	90.	95.	.0268	1391.	7.30
1.018	385.	40496.	6.	80.	82.	.0202	1245.	6.92
AVERAGE	576.	66841.	17.	109.	120.	.0338	1562.	7.30
EI FAR8	17.06	3110.	.25	5.30	5.83			
EI FAHI	19.35	3527.	.29	6.01	6.61			

TABLE B-VII. - Continued.

(c) Intermediate afterburning power; TT2, 552 K; PT2, 7.50 N/cm^2; FAHI, 0.0356; H, 0.0091 g H_2O/g dry air

R/R8	COPPM	CO2PPM	HCPPM	NOPPM	NOXPPM	FAR8	TT8,K	PT8,N/CM2
-1.028	580.	39483.	5.	85.	85.	.0198	1190.	6.70
-.931	377.	63434.	4.	105.	114.	.0319	1547.	7.27
-.834	486.	76652.	4.	123.	136.	.0389	1720.	7.27
-.735	689.	84975.	4.	135.	150.	.0433	1810.	7.28
-.638	828.	90735.	4.	144.	161.	.0465	1871.	7.24
-.540	754.	88501.	4.	140.	159.	.0453	1871.	7.24
-.442	491.	80379.	4.	124.	142.	.0408	1813.	7.28
-.345	318.	73427.	4.	109.	125.	.0371	1747.	7.30
-.247	246.	69522.	4.	98.	114.	.0350	1695.	7.27
-.147	214.	66806.	4.	90.	105.	.0336	1663.	7.15
-.048	189.	64133.	4.	86.	101.	.0322	1621.	7.18
.048	202.	62144.	4.	85.	100.	.0312	1599.	7.13
.147	225.	64561.	4.	90.	106.	.0324	1632.	7.08
.243	331.	72266.	4.	104.	120.	.0365	1726.	7.27
.341	589.	82741.	4.	121.	141.	.0421	1833.	7.25
.441	924.	93909.	4.	144.	164.	.0482	1958.	7.39
.538	1122.	99432.	5.	159.	181.	.0513	2002.	7.23
.636	1037.	96987.	4.	155.	179.	.0499	1963.	7.23
.731	832.	90905.	4.	143.	164.	.0466	1889.	7.22
.832	655.	85831.	4.	129.	149.	.0438	1836.	7.23
.929	545.	71306.	4.	104.	125.	.0361	1694.	7.33
1.028	435.	38805.	4.	74.	88.	.0194	1294.	7.07
AVERAGE	621.	77224.	4.	121.	138.	.0392	1737.	7.18
EI FAR8	15.93	3113.	.05	5.12	5.81			
EI FAHI	17.45	3411.	.06	5.61	6.37			

(d) Intermediate afterburning power; TT2, 554 K; PT2, 7.49 N/cm^2; FAHI, 0.0389; H, 0.0091 g H_2O/g dry air

R/R8	COPPM	CO2PPM	HCPPM	NOPPM	NOXPPM	FAR8	TT8,K	PT8,N/CM2
-1.055	1316.	29875.	6.	64.	79.	.0154	908.	5.44
-1.006	544.	46393.	4.	79.	97.	.0233	1337.	6.63
-.911	490.	70800.	3.	106.	127.	.0358	1718.	7.19
-.814	728.	83457.	4.	123.	148.	.0426	1911.	7.33
-.718	995.	92375.	4.	138.	163.	.0474	2025.	7.27
-.622	1147.	97385.	4.	150.	173.	.0502	2078.	7.30
-.528	978.	95491.	4.	145.	169.	.0491	2056.	7.22
-.434	660.	86956.	3.	126.	147.	.0444	1970.	7.36
-.336	453.	78976.	3.	111.	129.	.0401	1902.	7.31
-.241	359.	70809.	3.	93.	121.	.0357	1846.	7.33
-.145	328.	74665.	3.	94.	111.	.0377	1811.	7.25
-.051	273.	71030.	3.	89.	106.	.0358	1771.	7.03
.045	239.	68238.	3.	86.	104.	.0343	1733.	7.13
.141	278.	70727.	3.	93.	109.	.0356	1767.	7.22
.235	460.	77366.	3.	109.	129.	.0392	1857.	7.09
.333	825.	89427.	3.	131.	152.	.0458	1992.	7.16
.427	1229.	102432.	3.	156.	176.	.0530	2135.	7.21
.523	1537.	106770.	4.	171.	190.	.0555	2194.	7.36
.619	1352.	103999.	4.	163.	188.	.0539	2121.	7.34
.715	1069.	97513.	4.	149.	171.	.0502	2009.	7.35
.809	893.	93210.	3.	137.	157.	.0478	1960.	7.28
.906	756.	80160.	3.	113.	131.	.0408	1839.	7.27
1.001	503.	44330.	3.	77.	91.	.0222	1398.	7.04
AVERAGE	836.	82034.	4.	124.	144.	.0419	1862.	7.12
EI FAR8	20.14	3106.	.04	4.89	5.71			
EI FAHI	21.56	3324.	.05	5.23	6.11			

TABLE B-VII. - Concluded.

(e) Maximum afterburning power; TT2, 547 K; PT2, 7.48 N/cm^2; FAHI, 0.0511; H, 0.0091 g H_2O/g dry air

F/RP	COPPM	CO2PPM	HCPPM	NOPPM	NOXPPM	FAR8	TT8,K	PT8,N/CM2
-1.046	649.	31700.	8.	74.	88.	.0159	1091.	5.84
-.867	2129.	105452.	4.	144.	166.	.0551	2247.	6.99
-.776	2607.	109146.	4.	151.	171.	.0574	2235.	7.10
-.684	3342.	110781.	4.	158.	181.	.0587	2270.	7.07
-.595	3771.	111762.	4.	162.	187.	.0595	2281.	7.03
-.503	2590.	107369.	4.	154.	183.	.0564	2218.	7.10
-.413	1344.	97342.	3.	137.	165.	.0503	2171.	7.27
-.323	1058.	91721.	3.	126.	154.	.0471	2128.	7.30
-.231	1207.	96032.	3.	134.	160.	.0495	2162.	7.33
-.140	1355.	98899.	3.	141.	166.	.0511	2174.	7.09
-.050	1105.	93368.	3.	126.	152.	.0480	2115.	7.13
.041	818.	87061.	3.	109.	134.	.0445	2047.	7.13
.131	754.	88468.	3.	117.	128.	.0452	2064.	7.13
.222	1137.	96063.	3.	129.	146.	.0495	2155.	7.10
.311	2047.	106645.	3.	152.	172.	.0557	2207.	7.05
.402	12040.	113241.	3.	169.	178.	.0651	2252.	7.22
.494	26618.	103889.	3.	129.	133.	.0686	2346.	7.22
.585	26552.	106122.	3.	138.	141.	.0698	2320.	7.14
.675	8355.	114114.	2.	168.	176.	.0634	2264.	7.04
.765	4774.	114158.	2.	162.	179.	.0614	2260.	7.08
.856	5016.	113585.	3.	158.	173.	.0612	2308.	7.00
.949	1787.	77019.	2.	100.	121.	.0398	1972.	7.06
.992	1234.	52393.	3.	78.	97.	.0267	1618.	6.49
AVERAGE	5350.	96950.	4.	138.	156.	.0524	2106.	6.93
EI FARP	104.43	2974.	.03	4.41	5.00			
EI FAHI	106.37	3029.	.04	4.50	5.09			

TABLE B-VIII. - ENGINE INLET TEST CONDITIONS AND EXHAUST PROFILE DATA FOR CONDITION 8 (MACH 3.0, 19.8 km), ENGINE B

(a) Military (nonafterburning) power; TT2, 598 K; PT2, 16.23 N/cm^2; FAHI, 0.0118; H, 0.0039 g H_2O/g dry air

F/RP	COPPM	CO2PPM	HCPPM	NOPPM	NOXPPM	FAR8	TT8,K	PT8,N/CM2
-1.017	16.	22730.	3.	145.	145.	.0111	955.	14.19
-.955	11.	24691.	3.	159.	159.	.0121	984.	14.97
-.774	20.	27261.	3.	180.	180.	.0134	1011.	15.61
-.591	18.	27768.	3.	184.	185.	.0136	1025.	15.39
-.410	17.	26570.	3.	180.	180.	.0130	1025.	15.14
-.232	7.	24846.	3.	166.	166.	.0122	1018.	15.09
-.049	13.	23608.	3.	156.	158.	.0116	1006.	14.66
.129	14.	23450.	3.	153.	154.	.0115	1006.	14.73
.311	11.	24778.	3.	155.	156.	.0122	1012.	14.91
.493	9.	26260.	3.	164.	164.	.0129	1017.	15.08
.676	12.	26814.	3.	165.	165.	.0132	1015.	15.20
.856	16.	27018.	3.	161.	162.	.0133	1008.	15.21
.977	13.	25643.	3.	151.	152.	.0126	985.	15.14
AVERAGE	14.	26199.	3.	167.	167.	.0129	1008.	15.17
EI FAR8	1.10	3136.	.11	20.86	20.92			
EI FAHI	1.19	3407.	.12	22.67	22.73			

TABLE B-VIII. - Continued.

(b) Minimum afterburning power; TT2, 602 K; PT2, 16.25 N/cm^2; FAHI, 0.0294; H, 0.0039 g H_2O/g dry air

R/R8	COPPM	CO2PPM	HCPPM	NOPPM	NOXPPM	FAR8	TT8,K	PT8,N/CM2
-1.091	626.	27329.	10.	92.	102.	.0137	990.	12.23
-.985	420.	48352.	5.	137.	150.	.0242	1356.	14.00
-.882	116.	61534.	6.	179.	183.	.0308	1547.	14.44
-.777	91.	68484.	7.	196.	201.	.0344	1561.	14.39
-.675	92.	73448.	6.	206.	211.	.0370	1698.	14.44
-.571	86.	73949.	5.	201.	209.	.0372	1720.	14.44
-.464	87.	69191.	4.	182.	190.	.0347	1677.	14.32
-.361	181.	62404.	6.	160.	170.	.0313	1614.	14.25
-.256	535.	57809.	22.	140.	155.	.0291	1550.	13.90
-.153	1110.	54118.	85.	122.	141.	.0276	1504.	13.81
-.048	1324.	52733.	111.	115.	136.	.0270	1481.	13.52
.055	1057.	54130.	69.	117.	138.	.0275	1490.	13.50
.157	624.	57600.	27.	126.	143.	.0291	1538.	13.48
.262	249.	61315.	6.	139.	156.	.0308	1594.	13.85
.368	88.	66156.	3.	156.	165.	.0332	1635.	14.01
.471	64.	71583.	3.	172.	183.	.0360	1684.	14.17
.574	83.	76028.	4.	184.	195.	.0383	1712.	14.45
.679	88.	75612.	4.	186.	198.	.0381	1650.	14.40
.783	91.	72959.	4.	182.	190.	.0367	1535.	14.36
.886	82.	67110.	3.	170.	179.	.0337	1483.	14.34
.992	202.	48923.	3.	134.	144.	.0244	1461.	14.07
1.041	277.	38559.	3.	112.	124.	.0192	1355.	14.26
AVERAGE	210.	62450.	7.	165.	174.	.0313	1533.	14.13
EI FAR8	6.70	3127.	.12	8.61	9.10			
EI FAHI	7.12	3322.	.13	9.15	9.67			

(c) Intermediate afterburning power, TT2, 601 K; PT2, 16.30 N/cm^2; FAHI, 0.0362; H, 0.0039 g H_2O/g dry air

R/R8	COPPM	CO2PPM	HCPPM	NOPPM	NOXPPM	FAR8	TT8,K	PT8,N/CM2
-1.030	265.	42152.	3.	116.	129.	.0210	1229.	12.39
-.931	139.	67249.	2.	169.	181.	.0338	1657.	13.96
-.832	140.	78892.	2.	198.	212.	.0398	1930.	14.09
-.735	171.	83995.	2.	215.	231.	.0425	2029.	14.08
-.637	185.	87523.	2.	225.	246.	.0444	2091.	14.24
-.537	167.	86865.	2.	222.	238.	.0441	2082.	14.12
-.442	141.	81537.	2.	203.	217.	.0412	2021.	14.21
-.342	98.	75905.	2.	177.	193.	.0383	1937.	14.12
-.246	82.	71236.	2.	158.	172.	.0358	1861.	13.87
-.147	77.	67474.	2.	144.	157.	.0339	1797.	13.80
-.053	72.	65266.	2.	137.	148.	.0327	1771.	13.69
.048	77.	66661.	2.	138.	150.	.0334	1782.	13.70
.146	106.	71619.	2.	142.	155.	.0360	1854.	13.71
.246	106.	75408.	2.	155.	169.	.0380	1884.	13.61
.342	118.	79039.	2.	173.	189.	.0399	1900.	13.87
.440	142.	83456.	2.	193.	209.	.0422	1936.	14.12
.539	175.	87426.	2.	211.	225.	.0444	1949.	14.28
AVERAGE	151.	75858.	2.	186.	200.	.0383	1866.	13.96
EI FAR8	3.97	3131.	.03	8.01	8.65			
EI FAHI	4.17	3295.	.03	8.43	9.10			

TABLE B-VIII. - Concluded.

(d) Maximum afterburning power; TT2, 601 K; PT2, 16.23 N/cm^2; FAHI, 0.0535; H, 0.0039 g H_2O/g dry air

R/RS	COPPM	CO2PPM	HCPPM	NOPPM	NOXPPM	FAR8	TT8,K	PT8,N/CM2
-1.048	470.	48042.	3.	117.	138.	.0241	1203.	11.50
-.957	413.	90521.	2.	191.	210.	.0461	1606.	12.76
-.868	857.	110160.	2.	242.	258.	.0569	2352.	13.24
-.777	1462.	114024.	2.	260.	274.	.0594	2286.	13.25
-.687	3389.	116483.	2.	279.	285.	.0618	2285.	13.47
-.595	3569.	117233.	2.	292.	292.	.0624	2162.	13.58
-.503	1254.	115012.	2.	283.	292.	.0598	2276.	13.71
-.413	866.	112556.	2.	277.	293.	.0582	2343.	13.90
-.323	1043.	113623.	2.	285.	295.	.0590	2346.	13.75
-.232	930.	113470.	2.	290.	297.	.0588	2381.	13.77
-.141	591.	108631.	2.	275.	291.	.0560	2378.	13.79
-.050	417.	104132.	3.	268.	282.	.0534	2323.	13.49
.043	481.	106517.	3.	273.	283.	.0547	2306.	13.61
.131	1708.	114323.	3.	296.	296.	.0597	2319.	13.72
.223	2640.	116555.	3.	305.	305.	.0615	2402.	13.74
.313	2568.	116795.	3.	305.	305.	.0615	2297.	13.69
.402	2316.	116183.	3.	302.	302.	.0611	2378.	13.72
.492	2659.	116807.	3.	308.	308.	.0616	2345.	13.84
.585	2970.	116385.	3.	298.	298.	.0616	2261.	13.79
.677	2662.	116003.	3.	279.	284.	.0612	2223.	13.57
.767	2460.	115942.	3.	269.	272.	.0610	2254.	13.40
.857	2810.	116851.	3.	268.	271.	.0617	2330.	13.20
.949	466.	92033.	3.	185.	200.	.0470	2214.	13.10
AVERAGE	1851.	108246.	3.	259.	267.	.0565	2171.	13.28
EI FARP	33.58	3035.	.02	7.71	7.96			
EI FAHI	35.22	3236.	.03	8.08	8.35			

TABLE B-IX. - ENGINE INLET TEST CONDITIONS AND EXHAUST PROFILE DATA FOR CONDITION 3 (MACH 2.0, 19.8 km), ENGINE A

(a) Military (nonafterburning) power; TT2, 386 K; PT2, 4.14 N/cm^2; FAHI, 0.0182; H, 0.0086 g H_2O/g dry air

R/RS	COPPM	CO2PPM	HCPPM	NOPPM	NOXPPM	FAR8	TT8,K	PT8,N/CM2
-.962	43.	31088.	6.	0.	73.	.0153	921.	6.33
-.775	40.	33290.	7.	0.	79.	.0164	974.	6.54
-.593	42.	33290.	7.	0.	79.	.0164	979.	6.54
-.412	52.	30797.	7.	0.	74.	.0152	959.	6.58
-.233	53.	28106.	7.	0.	69.	.0138	940.	6.44
-.050	43.	27207.	7.	0.	67.	.0134	938.	6.39
-.049	40.	27239.	7.	0.	67.	.0134	938.	6.40
-.049	43.	26928.	8.	0.	67.	.0132	934.	6.36
.130	42.	28689.	8.	0.	72.	.0141	955.	6.39
.316	44.	32615.	8.	0.	82.	.0161	996.	6.45
.492	42.	38305.	9.	0.	97.	.0189	1042.	6.49
.670	39.	41896.	10.	0.	103.	.0207	1082.	6.57
.859	36.	40770.	11.	0.	97.	.0202	1052.	6.62
.914	37.	39122.	12.	0.	92.	.0193	1025.	6.46
AVERAGE	42.	34987.	8.	85.	85.	.0173	998.	6.51
EI FARP	2.40	3133.	.23	7.94	7.94			
EI FAHI	2.27	2972.	.22	7.53	7.53			

TABLE B-IX. - Continued.

(b) Minimum afterburning power; TT2, 386 K; PT2, 4.16 N/cm^2; FAHI, 0.0421; H, 0.0086 g H_2O/g dry air

R/R8	COPPM	CO2PPM	HCPPM	NOPPM	NOXPPM	FAR8	TT8,K	PT8,N/CM2
-.974	776.	52070.	24.	0.	72.	.0263	1275.	5.90
-.822	497.	78527.	30.	0.	91.	.0399	1731.	6.29
-.670	820.	88896.	43.	0.	101.	.0455	1814.	6.34
-.516	1221.	79510.	108.	0.	88.	.0408	1740.	6.35
-.361	5262.	46446.	5825.	0.	38.	.0288	1415.	6.32
-.204	3013.	31579.	10974.	0.	23.	.0227	1186.	6.31
-.051	2595.	29839.	11471.	0.	25.	.0219	1134.	6.24
.101	3989.	34431.	10648.	0.	26.	.0245	1231.	6.25
.264	5484.	46857.	5786.	0.	46.	.0292	1358.	6.28
.410	2117.	71276.	157.	0.	95.	.0370	1613.	6.27
.569	1232.	95030.	17.	0.	127.	.0490	1859.	6.36
.721	1198.	98412.	19.	0.	131.	.0508	1935.	6.31
.879	1042.	89420.	23.	0.	113.	.0459	1804.	6.32
AVERAGE	1750.	74124.	1625.	89.	89.	.0391	1650.	6.27
EI FAR8	45.09	3001.	20.97	3.77	3.77			
EI FAHI	41.91	2790.	19.49	3.50	3.50			

(c) Intermediate afterburning power; TT2, 389 K; PT2, 4.15 N/cm^2; FAHI, 0.0498; H, 0.0086 g H_2O/g dry air

R/R8	COPPM	CO2PPM	HCPPM	NOPPM	NOXPPM	FAR8	TT8,K	PT8,N/CM2
-.982	598.	55067.	22.	0.	70.	.0277	1317.	5.60
-.861	982.	89803.	22.	0.	98.	.0461	1827.	6.09
-.787	1253.	95278.	20.	0.	105.	.0491	1916.	6.05
-.636	1670.	102960.	19.	0.	118.	.0535	2032.	6.21
-.492	1430.	92225.	23.	0.	100.	.0476	1929.	6.16
-.344	6028.	61829.	2323.	0.	53.	.0354	1639.	6.13
-.196	7349.	40473.	10781.	0.	22.	.0295	1404.	6.15
-.050	5378.	33154.	12098.	0.	16.	.0254	1262.	5.92
-.049	5826.	34696.	11907.	0.	20.	.0263	1285.	6.05
.094	7867.	44404.	10628.	0.	20.	.0317	1428.	6.03
.249	6757.	58872.	3268.	0.	46.	.0347	1563.	5.99
.392	1828.	81988.	107.	0.	98.	.0425	1790.	6.01
.538	2299.	105755.	52.	0.	133.	.0554	2028.	6.11
.689	2594.	111913.	36.	0.	143.	.0589	2137.	6.12
.837	2693.	112459.	30.	0.	139.	.0593	2166.	6.17
AVERAGE	2624.	87469.	1136.	99.	99.	.0464	1846.	6.08
EI FAR8	57.43	3008.	12.45	3.56	3.56			
EI FAHI	53.51	2803.	11.60	3.31	3.31			

TABLE B-IX. - Concluded.

(d) Maximum afterburning power; TT2, 395 K; PT2, 4.16 N/cm^2; FAHI, 0.0639; H, 0.0086 g H_2O/g dry air

F/RP	COPPM	CO2PPM	HCPPM	NOPPM	NOXPPM	FAR8	TT8,K	PT8,N/CM2
-.984	1128.	56778.	23.	0.	64.	.0289	1355.	5.34
-.895	2631.	103098.	26.	0.	96.	.0541	2026.	5.90
-.795	4768.	115813.	27.	0.	114.	.0623	2160.	5.91
-.655	8826.	116292.	27.	0.	125.	.0649	2192.	5.99
-.517	4898.	114741.	25.	0.	110.	.0618	2168.	5.91
-.375	2095.	91093.	36.	0.	75.	.0474	1993.	5.75
-.235	6013.	78073.	1469.	0.	32.	.0434	1831.	5.63
-.141	10982.	69327.	6626.	0.	14.	.0444	1696.	5.61
-.049	12947.	55657.	10735.	0.	5.	.0405	1590.	5.66
-.047	13107.	56749.	10701.	0.	3.	.0411	1643.	5.68
.088	12209.	63696.	9298.	0.	5.	.0436	1735.	5.68
.229	4287.	83886.	918.	0.	48.	.0452	1919.	5.69
.369	2244.	97710.	123.	0.	95.	.0511	2040.	5.76
.508	15069.	113044.	99.	0.	130.	.0669	2213.	5.95
.652	26729.	100923.	81.	0.	130.	.0670	2272.	6.02
.722	26615.	98040.	51.	0.	130.	.0654	2243.	5.92
.790	26849.	96896.	71.	0.	131.	.0648	2269.	5.89
.887	5580.	109590.	47.	0.	113.	.0594	2169.	5.89
AVERAGE	10087.	100354.	449.	102.	102.	.0572	2077.	5.85
EI FARP	131.66	2840.	4.05	3.02	3.02			
EI FAHI	162.48	2540.	3.62	2.70	2.70			

TABLE B-X. - ENGINE INLET TEST CONDITIONS AND EXHAUST PROFILE DATA FOR CONDITION 4 (MACH 2.4, 19.8 km), ENGINE A

(a) Military (nonafterburning) power; TT2, 469 K; PT2, 7.30 N/cm^2; FAHI, 0.0153; H, 0.0047 g H_2O/g dry air

F/RP	COPPM	CO2PPM	HCPPM	NOPPM	NOXPPM	FAR8	TT8,K	PT8,N/CM2
-.941	27.	28288.	9.	0.	99.	.0139	923.	9.00
-.758	29.	31632.	8.	0.	116.	.0156	989.	9.48
-.585	28.	32495.	7.	0.	122.	.0160	1014.	9.37
-.405	32.	30393.	6.	0.	119.	.0150	999.	9.43
-.405	27.	29145.	11.	0.	106.	.0143	990.	9.51
-.227	18.	27280.	9.	0.	102.	.0134	981.	9.38
-.049	26.	25576.	7.	0.	95.	.0126	969.	9.26
.125	25.	25616.	5.	0.	95.	.0126	969.	9.22
.303	19.	27239.	5.	0.	101.	.0134	984.	9.13
.487	19.	30725.	5.	0.	112.	.0151	1005.	9.33
.661	31.	33348.	5.	0.	119.	.0164	1030.	9.43
.847	19.	32759.	5.	0.	112.	.0161	1013.	9.42
.900	21.	30889.	4.	0.	105.	.0152	986.	9.30
AVERAGE	25.	30773.	7.	111.	111.	.0151	995.	9.35
EI FARP	1.64	3134.	.21	11.87	11.87			
EI FAHI	1.62	3096.	.21	11.73	11.73			

TABLE B-X. - Continued.

(b) Minimum afterburning power; TT2, 467 K; PT2, 7.29 N/cm^2; FAHI, 0.0375; H, 0.0047 g H_2O/g dry air

R/R8	COPPM	CO2PPM	HCPPM	NOPPM	NOXPPM	FAR8	TT8,K	PT8,N/CM2
-.950	893.	45037.	15.	0.	94.	.0228	1284.	8.36
-.850	261.	65919.	9.	0.	120.	.0331	1592.	9.04
-.755	284.	76293.	10.	0.	136.	.0386	1746.	9.08
-.656	393.	85835.	14.	0.	152.	.0436	1872.	9.04
-.556	390.	88057.	20.	0.	155.	.0448	1905.	9.09
-.455	587.	76433.	49.	0.	136.	.0388	1794.	9.16
-.348	3427.	57507.	1039.	0.	96.	.0310	1599.	9.10
-.250	5939.	44352.	6264.	0.	58.	.0284	1452.	9.04
-.150	5881.	37493.	9809.	0.	43.	.0267	1352.	9.01
-.053	5980.	36668.	10354.	0.	41.	.0266	1322.	8.94
-.052	6013.	37752.	9983.	0.	37.	.0270	1349.	8.89
.050	6816.	45403.	8056.	0.	47.	.0303	1437.	8.87
.152	6007.	53623.	3424.	0.	62.	.0317	1534.	8.85
.254	5243.	53137.	1940.	0.	75.	.0302	1520.	8.82
.352	3886.	54233.	792.	0.	91.	.0295	1514.	8.91
.453	1140.	65190.	47.	0.	124.	.0333	1623.	9.07
.552	432.	79236.	6.	0.	149.	.0402	1766.	9.17
.654	400.	86715.	7.	0.	161.	.0441	1841.	9.16
.749	345.	86634.	8.	0.	160.	.0440	1872.	9.09
.855	293.	75633.	10.	0.	139.	.0382	1788.	9.08
.956	735.	46090.	19.	0.	96.	.0232	1433.	8.98
AVERAGE	1305.	69710.	691.	125.	125.	.0360	1680.	8.98
EI FAR8	36.34	3050.	9.64	5.70	5.70			
EI FAHI	34.94	2933.	9.27	5.48	5.48			

(c) Intermediate afterburning power; TT2, 466 K; PT2, 7.28 N/cm^2; FAHI, 0.0451; H, 0.0047 g H_2O/g dry air

R/R8	COPPM	CO2PPM	HCPPM	NOPPM	NOXPPM	FAR8	TT8,K	PT8,N/CM2
-1.015	537.	31006.	14.	0.	74.	.0155	1075.	7.59
-.918	408.	59073.	7.	0.	106.	.0297	1523.	8.62
-.820	358.	81470.	6.	0.	137.	.0413	1836.	8.96
-.725	569.	93999.	4.	0.	161.	.0481	2010.	8.89
-.625	785.	103080.	5.	0.	184.	.0531	2120.	8.93
-.532	720.	101830.	5.	0.	181.	.0524	2108.	8.94
-.434	520.	86242.	4.	0.	148.	.0439	1964.	8.90
-.339	919.	73106.	47.	0.	122.	.0373	1817.	8.83
-.242	3363.	65205.	797.	0.	90.	.0349	1711.	8.66
-.147	6476.	59736.	3230.	0.	57.	.0350	1632.	8.57
-.052	7624.	57980.	5400.	0.	48.	.0359	1613.	8.50
-.052	7773.	56984.	5958.	0.	45.	.0357	1606.	8.48
.045	6777.	62097.	3991.	0.	50.	.0368	1647.	8.49
.142	4322.	69083.	1411.	0.	70.	.0377	1744.	8.49
.238	2316.	71086.	331.	0.	95.	.0371	1763.	8.51
.334	933.	70811.	54.	0.	112.	.0361	1749.	8.61
.434	447.	75096.	13.	0.	129.	.0380	1784.	8.78
.528	560.	87090.	8.	0.	156.	.0444	1923.	8.93
.624	725.	98585.	10.	0.	180.	.0506	2036.	9.02
.719	755.	101666.	7.	0.	191.	.0523	2104.	8.95
.817	716.	100970.	8.	0.	189.	.0519	2157.	8.96
.911	649.	78044.	6.	0.	144.	.0397	1941.	8.87
.961	711.	57718.	5.	0.	113.	.0292	1626.	8.52
AVERAGE	933.	80934.	156.	142.	142.	.0414	1854.	8.75
EI FAR8	22.71	3096.	1.90	5.67	5.67			
EI FAHI	20.90	2849.	1.75	5.22	5.22			

TABLE B-X. - Concluded.

(d) Maximum afterburning power; TT2, 462 K; PT2, 7.49 N/cm^2; FAHI, 0.0588; H, 0.0024 g H_2O/g dry air

R/RR	COPPM	CO2PPM	HCPPM	NOPPM	NOXPPM	FAR8	TT8,K	PT8,N/CM2
-1.017	567.	35558.	4.	60.	0.	.0178	1169.	7.36
-.969	733.	54695.	2.	78.	0.	.0276	1497.	7.91
-.875	918.	96638.	3.	124.	0.	.0497	2097.	9.03
-.784	1779.	117219.	4.	153.	0.	.0613	2240.	8.98
-.693	2715.	121235.	4.	163.	0.	.0641	2251.	9.00
-.692	7391.	120537.	4.	160.	0.	.0664	2267.	8.80
-.599	14298.	117823.	4.	156.	0.	.0690	2309.	9.04
-.506	3353.	121441.	3.	153.	0.	.0646	2274.	9.04
-.418	831.	107584.	3.	124.	0.	.0555	2220.	9.04
-.324	611.	95309.	3.	96.	0.	.0488	2135.	8.81
-.233	720.	91858.	9.	81.	0.	.0470	2096.	8.53
-.141	1228.	92270.	71.	65.	0.	.0476	2073.	8.39
-.052	2784.	88361.	492.	42.	0.	.0466	2006.	8.26
-.052	2907.	87646.	529.	42.	0.	.0463	2000.	8.26
.041	3337.	87943.	671.	41.	0.	.0468	1992.	8.18
.131	1673.	93072.	182.	66.	0.	.0483	2081.	8.12
.223	835.	96240.	37.	89.	0.	.0494	2134.	8.28
.319	665.	97862.	21.	104.	0.	.0502	2135.	8.45
.411	789.	105810.	17.	125.	0.	.0545	2183.	8.73
.501	1465.	116558.	18.	154.	0.	.0608	2245.	8.99
.592	7046.	122247.	10.	164.	0.	.0672	2271.	9.07
.685	20510.	115748.	12.	144.	0.	.0716	2292.	8.93
.774	26679.	111584.	11.	131.	0.	.0730	2252.	8.97
.869	4007.	120151.	8.	149.	0.	.0642	2307.	8.97
.961	1110.	69894.	5.	86.	0.	.0357	1758.	8.77
AVERAGE	5802.	103168.	16.	127.	127.	.0560	2121.	8.75
EI FARR	106.30	2970.	.15	3.82	3.82			
EI FAHI	101.00	2822.	.14	3.63	3.63			

TABLE B-XI. - ENGINE INLET TEST CONDITIONS AND EXHAUST PROFILE DATA FOR CONDITION 5 (MACH 2.8, 19.8 km), ENGINE A

(a) Military (nonafterburning) power; TT2, 557 K; PT2, 13.18 N/cm^2; FAHI, 0.0135; H, 0.0026 g H_2O/g dry air

R/RR	COPPM	CO2PPM	HCPPM	NOPPM	NOXPPM	FAR8	TT8,K	PT8,N/CM2
-.991	16.	21729.	2.	0.	102.	.0106	896.	11.98
-.939	18.	23925.	2.	0.	116.	.0117	925.	13.42
-.759	22.	27983.	2.	0.	137.	.0138	993.	13.73
-.583	15.	28226.	2.	0.	143.	.0139	1010.	13.58
-.406	14.	26218.	2.	0.	131.	.0129	996.	13.60
-.231	11.	23631.	2.	0.	117.	.0116	977.	13.60
-.050	11.	22463.	2.	0.	111.	.0110	968.	13.27
.126	16.	22655.	2.	0.	113.	.0111	973.	13.27
.305	17.	24787.	2.	0.	125.	.0122	990.	13.28
.484	10.	28580.	2.	0.	145.	.0140	1017.	13.39
.656	15.	31517.	2.	0.	156.	.0155	1040.	13.70
.839	13.	30428.	2.	0.	147.	.0150	1021.	13.84
.957	11.	24822.	2.	0.	116.	.0122	954.	13.61
AVERAGE	15.	27314.	2.	135.	135.	.0134	993.	13.55
EI FARR	1.11	3136.	.06	16.14	16.14			
EI FAHI	1.10	3108.	.06	16.00	16.00			

TABLE B-XI. - Continued.

(b) Minimum afterburning power; TT2, 553 K; PT2, 13.25 N/cm^2; FAHI, 0.0332; H, 0.0026 g H_2O/g dry air

R/R8	COPPM	CO2PPM	HCPPM	NOPPM	NOxPPM	FAR8	TT8,K	PT8,N/CM2
-.957	862.	37184.	21.	0.	99.	.0188	1196.	12.22
-.860	219.	57312.	2.	0.	136.	.0287	1496.	13.24
-.759	114.	68463.	2.	0.	157.	.0344	1670.	13.19
-.656	113.	76226.	2.	0.	171.	.0384	1788.	13.24
-.554	127.	77502.	2.	0.	169.	.0391	1816.	13.25
-.449	308.	66978.	4.	0.	144.	.0337	1703.	13.26
-.354	3135.	52836.	491.	0.	106.	.0282	1550.	13.15
-.251	6134.	40205.	4441.	0.	66.	.0254	1421.	13.15
-.153	6293.	34085.	9180.	0.	50.	.0248	1344.	12.97
-.049	6255.	34537.	9884.	0.	48.	.0254	1335.	12.89
.052	6444.	40488.	8023.	0.	51.	.0276	1391.	12.84
.152	5512.	48875.	3371.	0.	67.	.0289	1491.	12.78
.249	4210.	51265.	1255.	0.	87.	.0283	1518.	12.83
.354	1457.	56299.	137.	0.	127.	.0289	1549.	12.93
.454	271.	63869.	19.	0.	157.	.0321	1622.	13.22
.561	130.	73499.	12.	0.	183.	.0370	1745.	13.38
.653	127.	77974.	9.	0.	195.	.0394	1798.	13.34
.756	114.	78264.	8.	0.	194.	.0395	1820.	13.29
.856	113.	72116.	7.	0.	178.	.0363	1775.	13.28
.956	482.	47733.	8.	0.	124.	.0239	1427.	13.24
AVERAGE	954.	63725.	538.	148.	148.	.0327	1632.	13.13
EI FAR8	29.22	3066.	8.26	7.42	7.42			
EI FAHI	28.68	3009.	8.10	7.28	7.28			

(c) Intermediate afterburning power; TT2, 552 K; PT2, 13.22 N/cm^2; FAHI, 0.0395; H, 0.0026 g H_2O/g dry air

R/R8	COPPM	CO2PPM	HCPPM	NOPPM	NOxPPM	FAR8	TT8,K	PT8,N/CM2
-1.021	351.	24248.	13.	0.	75.	.0121	1023.	11.19
-.923	331.	50190.	5.	0.	112.	.0251	1450.	12.50
-.825	127.	73070.	4.	0.	154.	.0368	1768.	13.03
-.731	161.	81537.	4.	0.	176.	.0412	1918.	13.07
-.633	192.	90136.	4.	0.	197.	.0458	2043.	13.14
-.536	182.	90389.	4.	0.	192.	.0459	2030.	13.15
-.437	147.	79430.	4.	0.	155.	.0401	1917.	13.14
-.341	383.	68570.	16.	0.	126.	.0346	1785.	12.99
-.149	3687.	60369.	863.	0.	81.	.0326	1656.	12.46
-.051	4172.	60340.	1350.	0.	70.	.0331	1652.	12.47
.045	2886.	64562.	622.	0.	86.	.0342	1700.	12.42
.147	1106.	69218.	153.	0.	107.	.0354	1764.	12.37
.245	400.	69140.	24.	0.	120.	.0349	1775.	12.46
.342	183.	68400.	8.	0.	132.	.0344	1757.	12.69
.440	111.	71256.	6.	0.	153.	.0358	1790.	12.84
.531	152.	78117.	6.	0.	180.	.0394	1884.	13.15
.630	185.	85087.	5.	0.	201.	.0431	1968.	13.35
.727	181.	87217.	5.	0.	207.	.0443	2016.	13.16
.826	190.	87119.	5.	0.	205.	.0442	2030.	13.14
.924	268.	64600.	4.	0.	155.	.0325	1731.	13.06
.972	490.	49138.	5.	0.	124.	.0246	1442.	12.41
AVERAGE	363.	71801.	42.	156.	156.	.0363	1785.	12.83
EI FAR8	10.05	3120.	.57	7.11	7.11			
EI FAHI	9.25	2870.	.53	6.54	6.54			

TABLE B-XI. - Concluded.

(d) Maximum afterburning power; TT2, 551 K; PT2, 13.22 N/cm^2; FAHI, 0.0567; H, 0.0026 g H_2O/g dry air

R/R8	COPPM	CO2PPM	HCPPM	NOPPM	NOXPPM	FAR8	TT8,K	PT8,N/CM2
-.995	436.	32794.	4.	0.	90.	.0164	1204.	10.82
-.954	509.	50871.	2.	0.	115.	.0255	1534.	11.33
-.856	471.	102086.	3.	0.	208.	.0524	2233.	12.60
-.770	1664.	119697.	3.	0.	255.	.0626	2347.	12.74
-.683	5160.	120382.	3.	0.	255.	.0650	2354.	12.72
-.588	9564.	119329.	4.	0.	252.	.0670	2356.	12.89
-.499	4431.	120920.	3.	0.	257.	.0649	2328.	12.78
-.412	514.	112206.	3.	0.	234.	.0579	2186.	12.75
-.318	292.	99648.	2.	0.	185.	.0509	2179.	12.42
-.229	254.	94205.	2.	0.	161.	.0480	2149.	12.16
-.137	263.	95515.	2.	0.	154.	.0487	2215.	11.69
-.050	291.	97679.	2.	0.	155.	.0499	2230.	11.60
.042	300.	99967.	2.	0.	160.	.0511	2249.	11.52
.130	294.	101989.	2.	0.	170.	.0522	2282.	11.45
.220	219.	94745.	2.	0.	202.	.0483	2194.	11.62
.309	179.	88923.	2.	0.	182.	.0452	2138.	12.78
.399	209.	93239.	2.	0.	193.	.0475	2144.	12.72
.486	267.	101877.	2.	0.	225.	.0521	2170.	12.80
.581	539.	113338.	2.	0.	258.	.0585	2291.	12.86
.672	1762.	119879.	3.	0.	265.	.0628	2357.	12.67
.752	8085.	119992.	2.	0.	254.	.0665	2359.	12.66
.804	4108.	119283.	3.	0.	257.	.0638	2358.	12.48
.851	1558.	116777.	2.	0.	240.	.0609	2353.	12.57
.944	587.	72012.	1.	0.	152.	.0365	1837.	12.45
AVERAGE	2202.	102829.	3.	216.	216.	.0537	2179.	12.43
EI FAR8	41.86	3072.	.02	6.75	6.75			
EI FAHI	39.69	2913.	.02	6.40	6.40			

NATIONAL AERONAUTICS AND SPACE ADMINISTRATION
WASHINGTON, D.C. 20546

OFFICIAL BUSINESS
PENALTY FOR PRIVATE USE $300

SPECIAL FOURTH-CLASS RATE
BOOK

POSTAGE AND FEES PAID
NATIONAL AERONAUTICS AND
SPACE ADMINISTRATION
451

U.S.MAIL

290 001 C1 U A 760206 S00903DS
DEPT OF THE AIR FORCE
AF WEAPONS LABORATORY
ATTN: TECHNICAL LIBRARY (SUL)
KIRTLAND AFB NM 87117

POSTMASTER: If Undeliverable (Section 158 Postal Manual) Do Not Return

"The aeronautical and space activities of the United States shall be conducted so as to contribute . . . to the expansion of human knowledge of phenomena in the atmosphere and space. The Administration shall provide for the widest practicable and appropriate dissemination of information concerning its activities and the results thereof."

—NATIONAL AERONAUTICS AND SPACE ACT OF 1958

NASA SCIENTIFIC AND TECHNICAL PUBLICATIONS

TECHNICAL REPORTS: Scientific and technical information considered important, complete, and a lasting contribution to existing knowledge.

TECHNICAL NOTES: Information less broad in scope but nevertheless of importance as a contribution to existing knowledge.

TECHNICAL MEMORANDUMS: Information receiving limited distribution because of preliminary data, security classification, or other reasons. Also includes conference proceedings with either limited or unlimited distribution.

CONTRACTOR REPORTS: Scientific and technical information generated under a NASA contract or grant and considered an important contribution to existing knowledge.

TECHNICAL TRANSLATIONS: Information published in a foreign language considered to merit NASA distribution in English.

SPECIAL PUBLICATIONS: Information derived from or of value to NASA activities. Publications include final reports of major projects, monographs, data compilations, handbooks, sourcebooks, and special bibliographies.

TECHNOLOGY UTILIZATION PUBLICATIONS: Information on technology used by NASA that may be of particular interest in commercial and other non-aerospace applications. Publications include Tech Briefs, Technology Utilization Reports and Technology Surveys.

Details on the availability of these publications may be obtained from:

SCIENTIFIC AND TECHNICAL INFORMATION OFFICE

NATIONAL AERONAUTICS AND SPACE ADMINISTRATION

Washington, D.C. 20546